

This item was submitted to Loughborough's Institutional Repository (<https://dspace.lboro.ac.uk/>) by the author and is made available under the following Creative Commons Licence conditions.



**CC creative commons**  
COMMONS DEED

**Attribution-NonCommercial-NoDerivs 2.5**

**You are free:**

- to copy, distribute, display, and perform the work

**Under the following conditions:**

**BY:** **Attribution.** You must attribute the work in the manner specified by the author or licensor.

**Noncommercial.** You may not use this work for commercial purposes.

**No Derivative Works.** You may not alter, transform, or build upon this work.

- For any reuse or distribution, you must make clear to others the license terms of this work.
- Any of these conditions can be waived if you get permission from the copyright holder.

**Your fair use and other rights are in no way affected by the above.**

This is a human-readable summary of the [Legal Code \(the full license\)](#).

[Disclaimer](#) 

For the full text of this licence, please go to:  
<http://creativecommons.org/licenses/by-nc-nd/2.5/>

**Environmental Impact of Fluid Catalytic Cracking Unit in a  
Petroleum Refining Complex**

**By**

**Wael Yateem**

*A Doctoral Thesis Submitted as Partial Fulfillment of the Requirement  
For the Award of the Doctor of Philosophy of  
Loughborough University*

*March 2011*

## Abstract

The fluid catalytic cracking (FCC) unit is of great importance in petroleum refining industries as it treats heavy fractions from various process units to produce light ends (valuable products). The FCC unit feedstock consists of heavy hydrocarbon with high sulphur contents and the catalyst in use is zeolite impregnated with rare earth metals i.e. lanthanum and cerium oxides. The catalytic cracking reaction is endothermic and takes place at elevated temperature in a fluidised bed reactor generating sulphur-contaminated coke on the catalyst. In the regenerator, coke is completely burnt producing SO<sub>2</sub>, particulate matter emissions. The impact of the FCC unit is assessed in the immediate neighborhood of the refinery. Emission inventories for years 2008 and 2009 for both SO<sub>2</sub> and PM have been calculated based on real operational data. Comprehensive meteorological data for years 2005 – 2009 are obtained and preprocessed to generate planetary boundary layer parameters using Aermet (Aermod preprocessor). Aermod (US EPA approved dispersion model) is applied to predict ground level concentrations of both pollutants in the selected study area. Model output is validated with the corresponding measured values at discrete receptors. The highest hourly SO<sub>2</sub> predicted concentrations for both years 2008 and 2009 exceeded the corresponding Kuwait EPA ambient air standard, mainly due to elevated emission rates and the prevailing calm and other meteorological conditions. The highest daily SO<sub>2</sub> predicted concentrations also exceeded the Kuwait EPA allowable limit due to high emission rates, while meteorological parameters influence is dampened. Hourly average predicted PM concentrations showed similar variation into SO<sub>2</sub> in different location. The daily average predicted PM concentrations are lower than US EPA specified limit.

An extensive parametric study has been conducted using three scenarios, stack diameter, stack height and emission rates. It is noticed that stack diameter has no effect on ground level concentration, as stack exit velocity is a function of the square of stack diameter. With the increase in stack height, the predicted concentrations decrease showing an inverse relation. The influence of the emission rate is linearly related to the computed ground level concentrations

SO<sub>x</sub> additives are tested for SO<sub>2</sub> emissions reduction. In the year 2008, reduction of SO<sub>2</sub> annual total emission by 43 % results in full compliance with Kuwait EPA hourly specified limit,

using an appropriate amount of additives. Similarly, 57 % reduction of SO<sub>2</sub> annual total emission leads to no exceedance in predicted concentrations for the year 2009.

The application of the state of the art technology, ESP has reduced about 90 % of PM emissions for the year 2009.

## **Acknowledgements**

I would like to express my sincere and deepest gratitude to Prof. Nassehi for his dedicated and excellent supervision, which includes the invaluable advice, discussion, co-operation and guidance throughout this research work.

I would like to show my appreciation and deep thanks to Prof. Nagy who has been supportive and helpful.

I would also like to extend my deepest gratitude to Dr. Khan for his special guidance, support and encouragement during the research work.

I would like to express my special thanks to Dr. Mufreh Alrashidi for his help and guidance during this research work.

I also would like to thank Mr. Aamir Ashfaque for his special help and support during the research work.

Finally, I would like to express my love and deepest gratitude to my wife and son who gave me love, encouragement and support throughout the years of my study.

# TABLE OF CONTENTS

<b>a.</b>	<b>Abstracts</b> .....	<b>i</b>
<b>b.</b>	<b>Acknowledgement</b> .....	<b>iii</b>
<b>1.</b>	<b>INTRODUCTION</b> .....	<b>1</b>
<b>2.</b>	<b>LITERATURE REVIEW</b> .....	<b>5</b>
2.1	Introduction.....	6
2.2	Fluidized Catalytic Cracking Unit / Technology .....	6
2.3	Sulphur Dioxide (SO <sub>2</sub> ) Emissions .....	8
2.4	Particulate Matters (PM) .....	14
2.5	Dispersion Models.....	18
<b>3.</b>	<b>PROCESS DISCRPTION</b> .....	<b>35</b>
3.1	Introduction.....	36
3.2	Fluidized Catalytic Cracking Unit .....	38
3.3	FCC Catalyst.....	39
3.4	Catalyst Components .....	39
3.5	Process Description.....	41
3.5.1	<i>Reactor Fee Preheating Section</i> .....	42
3.5.2	<i>Reactor –Regenerator Section</i> .....	43
3.5.3	<i>Main Fractionator Section</i> .....	44
3.5.4	<i>Gas Concentration Section</i> .....	44
3.5.5	<i>Energy Recovery Section</i> .....	45
<b>4.</b>	<b>AIR DISPERSION MODELS</b> .....	<b>46</b>
4.1	Introduction.....	47
4.2	Objectives of the Dispersion Models .....	48
4.3	Key Features of the Dispersion Models.....	49
4.4	Constrains of the Dispersion Models .....	49
4.5	Gaussian-Plume Models .....	50
4.6	Features of the Gaussian Plume Models.....	54
4.7	Limitations of the Gaussian Plume Models.....	54
4.8	ISCT3 .....	55
4.9	ISC-PRIME.....	55

4.10	CTDMPLUS .....	55
4.11	Aermod .....	56
4.12	Features of Aermod.....	59
4.13	Advantages of Aermod over ISCT3 .....	61
4.14	Applications of Aermod.....	62
4.15	Selection of Dispersion Model.....	62
4.16	Meteorological data Sensitivity .....	63
<b>5.</b>	<b>EMISSION INVENTORIES .....</b>	<b>65</b>
5.1	Introduction.....	66
5.2	Material Balance .....	67
5.3	Emission Inventories for Year 2008 .....	69
5.4	Emission Inventories for Year 2009 .....	76
<b>6.</b>	<b>MODEL APPLICATIONS .....</b>	<b>84</b>
6.1	Introduction.....	85
6.2	Model Input Data .....	85
6.3	Area of Study .....	86
6.4	Meteorological Data.....	88
6.5	Meteorological Effects.....	91
<b>7.</b>	<b>RESULTS AND DISCUSSIONS .....</b>	<b>94</b>
7.1	Introduction.....	95
7.2	Simulation of Concentration for Year 2008.....	95
7.3	Model Results for Year 2008 Emission Data .....	99
7.4	Model Results for Year 2009 Emission Data .....	104
7.5	Parametric Sensitivity Study .....	109
7.6	Mitigation Method of Sulphur Oxides.....	114
7.7	Particulate Emission Control .....	115
<b>8.</b>	<b>CONCLUSION, RECOMENDATIONS AND FUTURE WORK .....</b>	<b>116</b>
8.1	Recommendations and Future Work .....	119
<b>9.</b>	<b>REFERENCES.....</b>	<b>121</b>
<b>10.</b>	<b>APPENDIX.....</b>	<b>130</b>
10.1	Published articles & conference paper.....	

## LIST OF FIGURES

Fig. 3.1: Flow diagram of typical refinery .....	37
Fig. 3.2: Fluid catalytic cracking process .....	38
Fig. 3.3: A schematic flow diagram of FCC Unit used in petroleum refineries .....	42
Fig. 4.1: Overview of the air pollution modeling procedure .....	48
Fig. 4.2: Concentration distribution from a continuous point source of effective height h .....	54
Fig. 4.3: Overview of the Aermoc modeling procedure .....	57
Fig. 4.4: Type of model applied according to the complexity of the problem .....	63
Fig. 5.1: Overall material balance around reactor and regenerator.....	67
Fig 5.2: Regional map of Kuwait.....	69
Fig. 5.3: Hourly maximum, minimum and seasonal average temperatures in Kuwait.....	70
Fig. 5.4: SO <sub>2</sub> emission rates (g/s) for winter season for year 2008 .....	71
Fig. 5.5: SO <sub>2</sub> emission rates (g/s) for spring season for year 2008.....	72
Fig. 5.6: SO <sub>2</sub> emission rates (g/s) for summer season for year 2008.....	72
Fig. 5.7: SO <sub>2</sub> emission rates (g/s) for autumn season for year 2008.....	72
Fig. 5.8: Particulate matter (PM) emission rates (g/s) for winter season for year 2008 .....	74
Fig. 5.9: Particulate matter (PM) emission rates (g/s) for spring season for year 2008 .....	74
Fig. 5.10: Particulate matter (PM) emission rates (g/s) for summer season for year 2008 .....	75
Fig. 5.11: Particulate matter (PM) emission rates (g/s) for autumn season for year 2008 .....	75
Fig. 5.12: SO <sub>2</sub> emission rates (g/s) for winter season for year 2009 .....	77
Fig. 5.13: SO <sub>2</sub> emission rates (g/s) for spring season for year 2009.....	77
Fig. 5.14: SO <sub>2</sub> emission rates (g/s) for summer season for year 2009.....	78
Fig. 5.15: SO <sub>2</sub> emission rates (g/s) for autumn season for year 2009.....	78
Fig. 5.16: Particulate matter (PM) emission rates (g/s) for winter season for year 2009 .....	79
Fig. 5.17: Particulate matter (PM) emission rates (g/s) for spring season for year 2009 .....	80
Fig. 5.18: Particulate matter (PM) emission rates (g/s) for summer season for year 2009 .....	80
Fig. 5.19: Particulate matter (PM) emission rates (g/s) for autumn season for year 2009 .....	81
Fig: 6.1: Map of the refinery and its vicinity .....	86
Fig. 6.2: Percent value Vs. mesh grid .....	87
Fig. 6.3: Wind rose for year 2008 .....	87
Fig. 6.4: Wind class distribution for year 2008 .....	89



Fig. 6.5: Wind rose for years (2005- 2009) .....	90
Fig. 6.6: Wind class distribution for years (2005 – 2009) .....	90
Fig. 6.7: Maximum hourly predicted SO <sub>2</sub> ground level concentration for each month for year 2008.....	91
Fig. 6.7: Predicted SO <sub>2</sub> concentrations Vs. Measured SO <sub>2</sub> concentrations .....	92
Fig. 7.1: Spiral plot shows top 300 hourly ground level concentration of SO <sub>2</sub> for year 2008 emission rate .....	96
Fig. 7.2: Spiral plot shows top 300 daily maximum and average ground level concentration of SO <sub>2</sub> for year 2008 emission rates.....	97
Fig. 7.3: Spiral plot shows top 300 hourly ground level concentration of SO <sub>2</sub> for year 2009 emission rate .....	98
Fig. 7.4: Spiral plot shows top 300 daily maximum and average ground level concentration of SO <sub>2</sub> for year 2009 emission rates.....	99
Fig. 7.5: Isopleths plot of the predicted hourly average ground level concentration of SO <sub>2</sub> for year 2008.....	100
Fig. 7.6: Isopleths plot of the predicted daily average ground level concentration of SO <sub>2</sub> for year 2008.....	101
Fig. 7.7: Isopleths plot of the predicted hourly average ground level concentration of PM for year 2008.....	103
Fig. 7.8: Isopleths plot of the predicted daily average ground level concentration of PM for year 2008.....	104
Fig. 7.9: Isopleths plot of the predicted hourly average ground level concentration of SO <sub>2</sub> for year 2009.....	105
Fig. 7.10: Isopleths plot of the predicted daily average ground level concentration of SO <sub>2</sub> for year 2009.....	106
Fig. 7.11: Isopleths plot of the predicted hourly average ground level concentration of PM for year 2009.....	108
Fig. 7.12: Isopleths plot of the predicted daily average ground level concentration of PM for year 2009.....	109
Fig. 7.13: Hourly and daily predicted ground level concentrations of SO <sub>2</sub> versus stack height .....	111

Fig. 7.14: Hourly and daily predicted SO<sub>2</sub> ground level concentrations versus SO<sub>2</sub> emission rate  
.....112

## LIST OF TABLES

Table 4.1: Comparison of the dispersion model features: AERMOD Vs ISCST3 .....	64
Table 5.1: SO <sub>2</sub> monthly emission factors for year 2008 .....	81
Table 5.2: PM monthly emission factors for year 2008.....	81
Table 5.3: SO <sub>2</sub> monthly emission factors for year 2009 .....	82
Table 5.4: PM monthly emission factors for year 2009.....	82
Table 6.1: Selected discrete receptors information.....	88
Table 7.1: Effective stack heights for different stack radius and plume rise .....	114

**CHAPTER ONE**  
**INTRODUCTION**

## Introduction

Fluid catalytic cracking (FCC) of heavy ends into high value liquid fuels is a key process in the petroleum refining industry. It gained a great importance since 1942 when there was high demand of fuels for military vehicles and equipments during the World War II. After the war, FCC process development took place to increase the yield, which allowed refineries to utilize their crude oil resources more efficiently, to produce more valuable products. This unit converts high boiling petroleum fractions, namely gasoil to high value products i.e. high-octane gasoline (about 45% of all gasoline produced), LPG and heating oil. Its heavy feedstock (vacuum gas oil, coker gas oil, unconverted oil and waxy distillate), coming from vacuum rerun unit, delayed coker unit and crude distillation units respectively is catalytically cracked into lighter products (liquefied petroleum gas, gasoline, diesel and fuel oils).

Environmental concerns about this process have increased, during the last decade due to its great contribution of sulphur oxides and particulate matter emissions, which have adverse impact on the immediate neighborhoods of the refinery. Sulphur oxides emission is mainly depend on the elemental sulphur contents in the feedstock and coke. These emissions are generated as a result of the combustion of coke during the spent catalyst reactivation process. Particulate matter emissions are produced due to the attrition of the catalyst resulted from particle erosion and fracture during the process and the thermal shock of the fresh makeup catalyst addition, forming fines, Whitcombe et al., (2003).

In the present work, comprehensive emission inventories from FCC unit in an oil refinery have been prepared based on real operational data. These inventories are calculated based on complete combustion of sulphur and coke impregnated on the catalyst in the regenerator. Mainly for both SO<sub>2</sub> and particulate matter (PM), emission rates are calculated accurately using material balance for years 2008 and 2009, considering seasonal variations in the operation of the process unit. These results reflect the variation of sulphur in feedstock that comes from various refinery units. These emission inventories are used in dispersion model to assess their impact on the immediate surroundings of the refinery.

The US Environmental Protection Agency (US EPA) most advanced dispersion model AERMOD has been selected for prediction of ground level concentration of SO<sub>2</sub> and PM. The selection is based on the accurate calculation of the planetary boundary layer parameters through both surface and mixed layer scaling. AERMOD is capable to construct vertical profiles of required meteorological variables based on measurements and extrapolations of those measurements using similarity (scaling) relationships. It also applies Gaussian plume treatment horizontally and vertically for stable conditions and non-Gaussian probability density function for unstable conditions. AERMOD provides reliable predicted concentrations if turbulent wind velocity measurements are used to estimate plume dispersion, Venkatram et al., (2004).

The meteorological data for years 2005 -2009 are obtained and used in preprocessor AERMET to generate planetary boundary layer parameters. These generated data are used in AERMOD for years 2008 and 2009 emissions. AERMOD is used to predict daily SO<sub>2</sub> ground level concentration and the output is compared with the corresponding recorded values from Kuwait Environmental Public Authority (K-EPA) monitoring stations for the model validation process.

AERMOD is applied using year 2008 and 2009 emissions inventories to predict SO<sub>2</sub> and PM ground level concentrations, considering the monthly emission variations (emission factors). Sensitivity study is conducted to investigate the influence of grid size, stack height, stack diameter and emission rates.

Mitigation methods are tested using AERMOD for both years 2008 and 2009. SO<sub>2</sub> emissions are controlled by the addition of SO<sub>x</sub> transfer additives. PM emissions are minimised by the installation of electrostatic precipitator, (ESP). Both methods have shown high reduction in both pollutants' emission rates. Consequently, the predicted ground level concentrations of these pollutants have substantially decreased.

Chapter one describes detailed introduction of fluid catalytic cracking, (FCC) process in petroleum refining industries and the associated environmental aspects and its impact on the surroundings of refinery with mitigation methods.

Chapter two illustrates comprehensive views of previous research work conducted on fluid catalytic cracking process, emissions mainly SO<sub>2</sub> and PM. Application of air dispersion models for assessing the environmental impact of different emission's sources and pollution abating methodologies have been extensively reviewed.

Chapter three describes the process details of FCC unit in typical petroleum refining complex, feedstock components, chemical catalytic reactions, catalyst characteristics and FCC process operational parameters.

Chapter four compares various air dispersion models, their theories, applications, advantages and limitations. US EPA approved dispersion model, Aermom is selected for the present work. In chapter five, and emission inventories calculations for years 2008 and 2009 are presented. Material balance over the FCC unit is applied using real operational data.

Chapter five presents monthly emission inventories and their calculations methods for both years 2008 and 2009. Monthly emission factors for both years are also computed in this chapter.

Chapter six describes the application of Aermom and its preprocessor, Aermom with all required input parameters including meteorological data for years 2005 – 2009 and source characteristics.

Chapter seven discusses the model output for various practical scenarios, year 2008 emission rate for SO<sub>2</sub> and PM, year 2009 emission rate both pollutants, sensitivity study of stack height and diameter and different emission rates.

Chapter eight summarises all the work the contribution and salient conclusions with the recommendations and future research ideas.

**CHAPTER TWO**  
**LITERATURE REVIEW**



## 2.1 Introduction

A literature review is an account of what has been published on a topic by accredited fluidized catalytic cracking unit under different aspects. Occasionally it is divided into three different segments, i) Generally about FCC unit, ii) SO<sub>2</sub> emissions and iii) PM emissions. The purpose is to convey knowledge and ideas have been established and illuminate the strength of FCC unit.

With respect to the growing environmental concerns, legislators are aiming at stern regulations in order to curtail the pollution levels. This can be considered as the sole entity that has driven industrialists and researchers alike into drawing up novel ideas in order to design FCC process satisfying the prevailing norms. The attempts include innovative design, improved operation, catalyst development, selective operating conditions, feedstock conditions, additives to reduce emissions, etc. There are several publications that elaborate the different endeavors.

## 2.2 Fluidized Catalytic Cracking Unit / Technology

Kikkinides et al., (2002) examined the problem of FCC catalyst reaction-deactivation, which is treated using a direct approach, and with the modification of the structural properties of the FCC catalysts to achieve better process performance. In the present study an attempt is made to relate the FCC process performance with the structural properties of the catalyst pellet. It is done through the development of 3D stochastic network models employed to represent the porous structure by matching N<sub>2</sub> adsorption–desorption isotherms at 77 K. A comparison between experimental and simulation isotherms during catalyst deactivation showed excellent agreement between model and experiment. It is observed that with continuous deposition of coke on the pore surface, the morphology of the pore space is continuously modified, giving rise to a deviation in the diffusion path of the reactants in these spaces. Catalysts with high accessibility maximize the cracking of large molecule and minimizing secondary reactions like gasoline over-cracking.

Whitcombe et al., (2003) showed the formation of fines in a fluidized catalytic cracker unit (FCCU) due to catalyst attrition and fracture as a major source of catalyst loss. The petroleum industry employs fluid catalytic cracking units (FCCUs) as the major tool to produce gasoline from crude oil. At the centre of this unit is regenerator which is used to burn coke from the surface of the spent catalyst. As the regeneration process is very turbulent, a large amount of catalyst material is discharge to the atmosphere. In addition to the fine particles present in the catalyst, the turbulent conditions inside the FCC alter the particle size distribution of the catalyst generating fine particles and significant amount of aerosols, which has been identified in the stack emission of FCCUs

Chen (2006) described the recent scientific progress in fluid catalytic cracking (FCC) process by bridging the gap between process science and innovation in engineering practices. About 45% of worldwide gasoline production comes either directly from FCC units or indirectly from combination with downstream units, such as alkylation. Modern FCC units can take a wide variety of feedstock and can adjust operating conditions to maximize production of gasoline, middle distillate (LCO) or light olefins to meet different market demands. The new regulations also require reduction in  $SO_x$  and  $NO_x$  emissions, which can be accomplished by the use of catalyst additives and selective catalytic reduction processes. The engineering innovations include shorter reaction time achieved with the help of highly active zeolite FCC catalyst, increased regenerator temperature to ensure complete catalyst regeneration, and control of thermal cracking by a modified feed injection system which cools off the lower riser quicker by fast mixing and vaporization of the feed. As the recent environmental regulations became more stringent, further reduction of the particulates emission is required, and can be achieved by viable technologies including the use of electrostatic precipitator (ESP), wet scrubber and new cyclonic technology.

McMillan et al., (2007) described some industrial applications, to control the size distribution of the particles in a fluidized bed, which is extremely important in order to avoid poor fluidization. One method to control the size of the particles in the bed is to use attrition nozzles, which inject high velocity gas jets into the bed creating high shear regions and grinding particles together. The objective of this study is to test different high velocity attrition nozzles and

operating conditions in order to determine the effects of fluidisation velocity, nozzle size and geometry, bed material and attrition gas properties on the grinding efficiency. Therefore different high velocity attrition nozzles are tested. An empirical correlation is developed for nozzles operating at sonic conditions and is able to accurately predict the grinding efficiencies using experimental data. It is analysed that larger the diameter of the nozzles with an expansion region at the tip, operating at high flow rates using lower density gases with higher equivalent speeds of sound, resulted in the highest grinding efficiencies. Moreover gas properties such as speed of sound and density had a significant impact on the grinding efficiency.

Zhu et al., (2008) reported to improve the understanding of the complex hydrodynamic characteristics in the bottom region of catalyst fluidised bed (CFB) riser over a wide range of operating conditions. The results included radial solids concentrations correspondence to the radial profiles of standard deviation, particle velocity profiles and probability density distributions. Comparisons are made between the flow structures in the riser bottom region, bubbling and turbulent fluidized beds. According to the cross-sectional average solids concentration ( $\epsilon_s$ ), two kinds of the riser bottom regions are identified: dilute bottom region with  $\epsilon_s < 0.1$  (non-S-shaped axial solids concentration profile) and dense bottom region with  $\epsilon_s > 0.1$  (S-shaped axial solids concentration profile). For the dilute bottom region, the flow structure belongs to homogenous dilute phase flow. For the dense bottom region, a core–annulus flow structure with a uniform dilute core region surrounded by a dense-annular zone appears. However, the average down flowing particle velocity changes little with radial positions, suggesting that in the bottom region, the downward movement of particles is dominated by particle–particle interactions.

### **2.3 Sulphur Dioxide (SO<sub>2</sub>) Emissions**

Palomares et al., (1999) discussed the recent findings where metals containing hydrotalcites used as promoter for SO<sub>x</sub> and NO<sub>x</sub> removal. The metal oxides display redox properties; Cobalt (Co) in this case, helps in the reduction of NO, while the addition of an oxidant like cerium oxide is imperative for the removal of SO<sub>2</sub>. The results showed that Co-Al-Mg oxides derived from hydrotalcites are catalysts with high surface area than the Cu-Mg-Al catalyst. The copper catalyst

is observed to perform better with respect to SO<sub>2</sub> oxidation as compared to the cobalt catalyst and its regeneration is also better than that of the cobalt catalyst. It is noticed that the addition of cerium oxide has no significant impact on overall conversion in case of copper impregnated catalyst.

Abdul Wahab et al., (2002) studied the impact of SO<sub>2</sub> emissions from a petroleum refinery on the ambient air quality in Mina Al-Fahal, Oman. Dispersion model ISCST is used to predict SO<sub>2</sub> ground level concentration. The study is performed over a period of 21 days. Computed SO<sub>2</sub> concentrations are compared with the measured values of SO<sub>2</sub> for maximum hourly average concentration, maximum daily concentration and total period average concentration. It is noted that the model output under-predicted the SO<sub>2</sub> concentration for all the three cases due to unavailability of background concentrations and the presence of more dominant sources. Based on the maximum daily average concentration and the total period maximum concentration, the model under-predicted the average measured concentration by 31.77 % and 41.8 % respectively. The model performed slightly better based on maximum hourly average concentration and under-predicted by 10.5 %.

Vallaa et al., (2004) investigated the effects of various types of fluid catalytic cracking (FCC) feed-stocks (VGO, FCC gasoline and FCC gasoline cuts) on sulphur compounds distribution in the gasoline produced from FCC process. Hydrogen transfer reactions played an important role on gasoline sulphur and cracking temperature, it could effects gasoline sulphur removal. The cracking of various FCC gasoline cuts enriched specific sulphur compounds that used to indicate reaction networks through which these compounds can de-sulphurised in the FCC environment. It is suggested that this occurs due to the refractory nature of the sulphur compounds in hydro-treated feeds to be decomposed for the saturated hydrocarbon environment of hydro-treated feeds which enforces the hydrogen transfer reactions and the reduced catalyst to oil ratio needed to achieve the desired conversion.

Yescas et al., (2004) discussed the importance of fluidised-bed catalytic cracking (FCC) unit in the oil refining industry. During the last 60-year , fluid catalytic cracking (FCC) is considered to be one of the most important refining processes, involving the conversion of heavy oil

feedstock into gasoline and other valuable products such as gasoline and C<sub>3</sub>–C<sub>4</sub> olefins. In this process pollutant compounds, such as sulphur in feedstock, are redistributed into products and emissions. In this study, sulfur balance is performed around an industrial FCC unit considering riser and regenerator as coupled reactors. Also kinetic model is used that is tuned using industrial data and solved to predict operating regions of the industrial units at different conditions. It also considers explicitly the formation of hydrogen sulfide during the catalytic cracking of the feedstock. Simulation results indicate the portion of sulfur in the feedstock that goes to fuels and the portion that is lost as emissions from the processes. It is also observed that the sour gas production is directly proportional to the catalyst to oil ratio. Finally in the end it is noted that the operation at middle catalyst to oil ratios yields to gasoline with lowest sulfur levels and leads to maximum profit.

Barth et al., (2004) studied the use of materials containing mixed oxides MCM-36 mixed with alkaline earth aluminium oxide pillars, which are highly active additives for the reduction of NO with CO under reaction conditions similar to the oxygen depleted zone of the FCC regenerator. The high-temperature flue gas stream at the exit of a regenerator contains O<sub>2</sub>, N<sub>2</sub>, CO, CO<sub>2</sub>, H<sub>2</sub>O, SO<sub>x</sub>, and NO<sub>x</sub>. The NO<sub>x</sub> emissions from the regenerator of a FCC can contribute up to 50% of the total NO<sub>x</sub> emissions in a refinery and consist mainly of NO, which is formed in the regenerator, while NO<sub>2</sub> is formed only after NO is being released to the air. N<sub>2</sub> and N<sub>2</sub>O are formed by the reaction of isocyanates with NO. The reduction of NO by CO over MCM-36-type materials is explained by involving a two-step process as the formation of nitrous oxide as an intermediate. The additives show a reduction of NO<sub>x</sub> emissions simulating during the regeneration of industrial coked FCC catalysts in a fluidized-bed reactor but lower the concentration of NO<sub>x</sub> released in the flue gases. It is noted that high NO conversions yields N<sub>2</sub>, under oxygen deficient conditions and the performance of these pillared materials are greater than the non-pillared ones.

Yassaa et al., (2005) determined the absolute contents and relative distributions of organic aerosols (n-alkanes, n-alkanoic and n-alkenoic acids, n-alkan-2-ones and polycyclic aromatic hydrocarbons (PAH)) in flare gases emitted during the crude oil extraction and in the free atmosphere of the Hassi-Messaoud city (Algeria). PAH are usually present at low concentrations

in the emission and the relative PAH, seemed to be unable to be driven over long distances through the atmosphere, before being decomposed. The pattern of the non-polar fraction released by the torches at Hassi-Messaoud presented sets of branched alkanes and a strong predominance along the whole carbon number range ( $C_{16}$ – $C_{34}$ ) versus odd homologues. It is found that n-Alkanes also abundant both in the direct emission (from 460 to 632  $ng\ m^{-3}$ ) and city atmosphere (0.462  $\mu g\ m^{-3}$ ). Saturated and unsaturated mono-carboxylic acids, accounted for the major fraction of the total particulate organic matter identified both in torch exhaust and atmospheric particulate. The incomplete thermal combustion of torched crude oil is very likely the main source of these particle-bound organic constituents in the city and its surrounding region.

Babich et al., (2005) explained the mechanism of  $NO_x$  formation in the FCC process as an attempt to find ways to reduce it. Nitrogen oxides ( $NO_x$ ) emission during the regeneration of coked fluid catalytic cracking (FCC) catalysts is an environmental problem that's why the reduction of  $NO_x$  levels in the exhaust gases is an essential part of the technology for a green refinery. Through this study it is possible to follow the reaction pathways of N present in FCC feed, as heterocyclic compounds. Presence of Nitrogen in the FCC feed is incorporated as poly-aromatic compounds in the coke deposited on the catalyst during cracking. Decomposition of the coke has been monitored by gas chromatography (GC) and mass spectroscopy (MS) during the catalyst regeneration (temperature programmed oxidation (TPO) and isothermal oxidation. The pyrrolic- and pyridinic-type N specie present more in the outer coke layers, which are oxidized under the conditions when still large amount of C or CO is available from coke to reduced  $NO_x$  formed to  $N_2$ . Quaternary - nitrogen (Q-N) type species are present in the inner layer, strongly adsorbed on the acid sites on the catalyst. Most of the coke is already combusted at this point, lack of reducing agents (C, CO, etc.) results in the presence of  $NO_x$  in the tail gas.

Lopez et al., (2005) assessed the impact of natural gas and fuel oil consumption on the air quality in an Industrial Corridor, Mexico to determine the optimal NG and fuel oil required to reduce  $SO_2$  concentration. Air dispersion model Aermom is used to compute ground level concentration of  $SO_2$ . Model output is then validated against  $SO_2$  field measurements. Different hypothetical emission scenarios are performed to examine the impact of NG and fuel oil mixture. The obtained results in this work indicate that dispersion model Aermom presented good

correlation with the measured concentrations. It is also concluded that increasing 40 % of NG consumption will reduce SO<sub>2</sub> concentration by 90 %.

Long et al., (2005) investigated effects of vanadium on the desulfurization performance of FCC catalysts having different oxidation numbers. Among the existing desulfurization solutions, FCC has greater significance in economical applications; desulfurization catalyst and additives. Molecular modelling studies showed how vanadium with low oxidation number could affect the chemical conversion of sulfur compounds. It is proved with electron paramagnetic resonance (EPR) and temperature programmed reduction (TPR) that vanadium oxidation number decreased when the catalyst is activated. The desulfurization performances of activated equilibrium catalysts are better than that of the un-activated catalysts.

Polato et al., (2005) recent years, many refineries had taken measures to reduce SO<sub>x</sub> emissions. The hydrotalcite-derived Mg, Al-mixed oxides (MO) with variable Mg/Al ratios (3, 1, 1/3), which impregnated with 17 wt % of CeO<sub>2</sub> is use to evaluate SO<sub>x</sub> removal the under conditions of FCC units. Thus, the evolution of SO<sub>2</sub> upon reduction decreases as the importance of the spinel-phase in the mixed oxides increases. The sulphates formed from the spinel-phase are more easily reduced than those from the periclase phase. The growth of the sulphate phase in the early stages of sulphation destroys the small meso-pores of the mixed oxide. Role of ceria (CeO<sub>2</sub>) derived from its basic / redox character enhances the oxidation of SO<sub>2</sub> to SO<sub>3</sub> under FCC regeneration conditions by reacting with SO<sub>2</sub> to get sub stoichiometric cerium oxide, which is re-oxidized with oxygen. Results showed the regeneration of the sulfated additives that the composition of the reductive stream influenced the regeneration profiles, the total quantity of sulfur released, and the reduction products distribution for each sample. These results could be related to the nature of the reducing agent and to the fact that the thermal stability and the reducibility of the sulphates are significantly affected by the metal with redox properties present in the additive.

Siddiqui et al., (2006) showed use of additives to reduce the sulphur compounds in gasoline. Many countries worldwide are introducing regulations to reduce sulphur levels in gasoline to less than 30 ppm within the coming few years. To meet this regulation, refiners are considering various options to reduce sulphur in gasoline. Sulphur in gasoline increases SO<sub>x</sub> emissions in

combustion gases, reduces the activity of vehicle catalytic converters, and promotes corrosion of engine parts. Among the various available options for the reduction of gasoline sulphur in fluid catalytic cracking (FCC), a viable option would be the use of FCC catalyst additives. Alumina supported zinc, titanium and gallium additives are prepared, mixed with Y-zeolite based FCC catalyst. It has been discussed that the sulfur reduction ability of Ga/alumina is better than Zn/alumina and Ti/alumina. The catalyst-additive mixture is evaluated for their sulphur reduction ability in micro-activity test unit (MAT). The Ga/alumina additive is able to reduce sulfur content of FCC gasoline fraction (221°C) by about 31%. It is highlighted that additives slightly reduced catalyst's cracking activity with no change in coke yield namely thiophene, tetrahydrothiophene, alkyl-thiophenes, and benzo-thiophenes are basic in nature, and the additive requires acidic nature.

Centi et al., (2007) observed  $\text{SO}_x$  trap showed enhanced performances with the Cu/Mg/Al ternary (HT) derived materials with respect to binary Cu/Al HT-derived materials. Their performances depend on the feed composition and type of experiments. However, a similar ranking of the  $\text{SO}_x$  trap performances is observed for the different configurations. Cu/Mg/Al = 1:1:2 showed the best performance and also improved hydrothermal stability with respect to Cu/Al binary samples. Therefore, it is an important element to improve the performance of  $\text{SO}_x$  traps using Cu/Mg/Al ternary materials either to protecting  $\text{NO}_x$  traps in auto exhaust uses for FCC applications.

Mizutani et al., (2007) showed automobile exhaust gas can cause serious environmental issues, which are against the regulations, therefore demand for ultra low sulphur gasoline and diesel fuel is increasing in the petroleum refining industry. It is necessary to develop a process that could effectively convert the heavy oil into clean transportation fuels. Atmospheric residue (AR) is now de-sulphurised before fluid catalytic cracking (FCC) to produce low sulphur gasoline. Therefore desulphurisation either before or after FCC needs to be improved by converting the saturate and aromatic fractions in hydro-sulphurised atmospheric residue to the gasoline, regardless of their presence in vacuum gas oil (VGO) and vacuum residue (VR). The gasoline produced from HDS-AR contained tetra-hydrothiophene and  $\text{C}_2$ -thiophene as well as



those in the gasoline from HDS-VGO while the contents of the former species is much larger than those in the gasoline from HDS-VGO.

Polato et al., (2008) noted Mg, Al- mixed oxides derived from hydrotalcite like compounds with an  $M^{3+}/(M^{2+} + M^{3+})$ , which are partially replaced by Cu, Co, Cr or Fe with Mg or Al. They are used as precursors for different mixed oxides (MO): Cu–MO, Co–MO, Cr–MO or Fe - MO. These compounds are more active for  $SO_x$  pick up than the Mg.Al mixed oxide. These materials are evaluated for  $SO_x$  removal under conditions similar to those found in the fluid catalytic cracking (FCC) regenerator. The following order of catalytic activity for  $SO_x$  uptake is observed: Cu–MO > Co–MO > Fe–MO > Cr–MO. The regeneration of the sulphated additives is also studied and the results showed that the composition of the reductive stream influenced the regeneration profiles, the total quantity of sulfur released, and the reduction products distribution, in a specific way. The study of the influence of the composition of the reductive stream on catalytic performance indicated that propane is a less efficient reductive agent than hydrogen, as evidenced by the lower regeneration levels and by the higher temperatures for sulphur release.

## **2.4 Particulate Matter (PM)**

Akeredolu (1989) discussed the air pollution sources in Nigeria. It is found the particulate matter (PM) constitutes the major atmospheric pollution problems. Atmospheric environment problems such as air pollution and thermal stress are growing in many tropical countries partly on account of their rapid rate of industrialization. The potential for air pollution generation has been overlooked and being predicted solely on the basis of indicators of industrialization / urbanization which outpaces the urban planning process. Both anthropogenic and non-anthropogenic sources of particulate matter are found to be important. Particulate matter is shown to constitute the most abundant air pollutants and its impact as well those of gaseous pollutants shown to manifest in measurable urban heat island effects. Biomass/solid waste burning and road surface dust mobilization are the major non-anthropogenic sources of ambient particles. The Harmattan dust haze remobilization resulting from fugitive emissions from open surfaces and biomass burning are the major non-anthropogenic sources of particulate matter to

exist in Nigeria. Also industries generate and emit particulate as well as gaseous pollutants, which have manifested significant negative impact at local levels. Combustion-derived pollution is seen to be increasing. The annual atmospheric particle loading for the country is estimated at  $2.75 \times 10^9$  kg with the following source contributions: bush burning (31.7%), fugitive dust from roads (29.1%), fuel wood burning (21.3%), Harmattan dust (13.8%), solid waste incineration (2.1%), stationary sources (1.6%), automobile exhaust lead (0.2%) and gas flares (0.1%).

Boerefijn et al., (2000) reviewed catalyst particles used for fluid catalytic cracking (FCC) in oil refineries could undergo attrition, and continuous deactivation, which can contribute to the production of fines. Therefore a methodology for evaluation and selection of optimum catalyst and additives for operating FCC units presented. The level of attrition in an FCC unit is a function of particle properties, structure and the hydrodynamic regimes prevailing in the unit. It is necessary to ensure that the catalyst is sufficiently attrition resistant. Thus the performance of the fresh FCC catalyst is not representative by the performance of the circulating catalyst inventory or equilibrated catalyst (e-cat) in FCC unit. Fresh catalyst gives high conversion, coke and gas yields as compared to e-cat. Surface area of the e-cat is typically about 50–60% of the fresh catalyst and the catalyst activity is typically ten units lower compared to fresh catalyst.

The latter depends on the geometry, solids concentration, flow rates and other operating conditions. It also includes the fluidized state as well as dense and lean phase flows and impact of particle flows on stationary surfaces. Attrition of catalyst powder in FCC units can lead to considerable loss of material. Therefore a number of test methods exist, which had proven to be very useful in tackling design issues so that a relative assessment of the attrition propensity of the particles can be made quickly. On the other hand, single-particle impact testing provides an unambiguous method for assessing the attrition propensity of particulate solids. The approach based on single-particle testing, coupled with the hydrodynamic models, is more fundamental and hence generally more reliable.

Bosco et al., (2005) discussed how the refinery and traffic related sources could affect the chemical composition of airborne particulate matter over the town of Gela using pine needles and urban road dust as the means of survey. Factor analysis identified three main sources of

metals: soil, traffic, and industrial emissions. The petrochemical plant appears to be associated with raised levels of As, Mo, Ni, S, Se, V, and Zn. Similarly, enhanced Cu, Pb, Pt, Pd, Sb, and partly Zn concentrations are closely associated with traffic. In addition urban and industrial areas are mainly affected by such emissions e.g. Re-suspension by wind of crustal material and volcanic activity, suspended solid particles are due to coal and oil combustion, motor vehicle exhaust fumes, the construction industry, metal working industries, and other anthropogenic sources, which may present a potential of local hazard to the population. According to the results of this study, a continuous environmental monitoring of the chemical composition of the finest fraction of airborne particulate matter is strongly recommended.

Kulkarni et al. (2007) determined the impact of FCC unit  $PM_{2.5}$  emission events released from a local refinery in the Houston, TX.  $PM_{2.5}$  levels are measured at four different continuous ambient monitoring air-sampling stations. The rare earth elements (REE's) emissions are quantitatively tracked using elemental markers such as lanthanum and lanthanides across the Houston region as they are major constituents of FCC catalyst. REE's including La, Ce, Pr, Nd, Sm, Gd and Dy have adverse impact on human health including central nervous system, liver, kidney and increase of atherosclerosis at the fundus of the eyes. It is noticed that FCC lost catalyst is responsible for elevated  $PM_{2.5}$  emissions i.e. REE's emissions from the refinery. It is observed that during regional haze episode,  $PM_{2.5}$  concentrations are high at the areas located upwind direction from the source i.e. Deer Park and Galveston. FCC catalyst emission represents 12 % of the total  $PM_{2.5}$  at the neighboring downwind site from the refinery. Therefore, it is concluded that  $PM_{2.5}$  in the vicinity of petroleum refineries needs to be measured continuously in order to evaluate the human exposure to REE's emitted mainly from FCC unit and assess the adverse health effect.

Kesarkar et al., (2007) studied the spatial variation of  $PM_{10}$  concentration from various sources over Pune, India. Gaussian air pollutant dispersion model Aermom is used to predict the concentration of  $PM_{10}$ . Weather research and forecasting (WRF) model is used to furnish Aermom with planetary boundary layer and surface layer parameters required for simulation. Emission inventory has been developed and field-monitoring campaign is conducted under Pune air quality management program of the ministry of Environment and Forests. This inventory is

used in AERMOD to predict PM<sub>10</sub>. A comparison between simulated and observed PM<sub>10</sub> concentration showed that the model underestimated the PM<sub>10</sub> concentration over Pune. However, this work is conducted over a short period of time, which is not sufficient to conclude on adequacy of regionally averaged meteorological parameters for driving Gaussian models such as AERMOD.

Pang et al., (2007) studied the modification effects of different chemical elements on ultra stable Y zeolite (USY), the resulting catalysts are evaluated in a micro-activity test unit (MAT) and confined fluidized bed (CFB) reactor. The acidity of catalytically active component, e.g., ultra stable Y zeolite (USY), plays an important role in determining their cracking activity and selectivity. So the relation between the acidity of the zeolite and the conversion of sulphur compounds as well as FCC product distribution are studied. To develop advanced sulfur reduction catalytic cracking catalysts, different type of elements are used to modify USY and the resulting catalysts are evaluated in a confined fluidized bed reactor and a micro-activity testing unit. The assessment results indicated that the USY modified with Cu gave rise to serious coke deposition on the catalyst owing to its high dehydrogenation ability, while the USY zeolites modified with Zn and V only slightly increased coke yield, and the V-modified zeolite reduced the sulfur contents obviously. An optimum catalyst is obtained by the combined rare earth and V modification, over which the sulfur content in FCC gasoline can be decreased and the selectivity for the target products can be improved, with the sulfur content reduced by 30 m% and the selectivity to coke even decreased by 0.20 m% at a comparable conversion level of the base catalyst.

Cerqueira et al., (2008) discussed catalyst deactivation occurred both ways reversibly and irreversibly over the course of the commercial fluid catalytic cracking (FCC). The typical FCC catalyst consists of a mixture of an inert matrix (kaolin), an active matrix (alumina), a binder i.e. (silica or silica–alumina) and Y zeolite. During the FCC process, a significant portion of the feedstock is converted into coke. This coke temporarily deactivates the active sites of the catalyst by poisoning, pore blockage or both resulting in an important activity loss. It happened due to contaminants present in the feedstock or to the de-alumination of the zeolite catalyst component. Aspects related to the various causes of FCC catalysts (and additives) deactivation under

industrial conditions are also recapitulated. The recent advancement in studies related to FCC catalyst additives deactivation proven that this field will continue to deserve attention.

Moreno et al., (2008) derived ambient  $PM_{10}$  and  $PM_{2.5}$  at Puertollano (central Spain) mostly from local industrial emissions (including a refinery and power stations) and mineral (crustal) aerosols from fugitive dusts and African intrusions. Research demonstrate how the concentrations of V and lanthanoid elements in atmospheric PM can be used to identify transient pollution events specifically linked to refinery emissions, even with in areas with high concentrations of other industrial emissions and natural mineral dusts. The total lanthanoid content of PM is controlled primarily by the amount of coarse crustal material present, with the highest values being recorded in  $PM_{10}$  during an African dust intrusion ( $13 \text{ ng m}^{-3}$ ). In contrast La/Ce and La/Sm ratios are controlled by the refinery emissions, rising above natural crustal averages due to the release of La from fluid catalytic converters (FCC). Crustal La/Ce ratios are least common, and La anomalies most common, in  $PM_{2.5}$  measured during local pollution events.

Ravichander et al., (2009) discussed industrial development in the FCC process and the methodology for evaluation and selection of optimum catalyst and additives for operating FCC units. Fluid catalytic cracking (FCC) unit has significant impact on refinery economics producing valuable products like gasoline and light olefins. Mandatory environmental regulations have imposed stringent quality limits on refinery products, especially on gasoline and diesel fuels. The selection of suitable catalysts and additives involve both technical and commercial aspects. The catalyst residence time in the unit is several days depending on the catalyst addition rate and circulating catalyst inventory. Study elaborates the laboratory evaluation methodology adopted; modeling techniques used for making yield predictions and presents case studies of successful catalyst and additive selection and use in a commercial FCC unit.

## **2.5 Dispersion Models**

The changes in the thermal behavior of the regional weather and consequently climate due to urbanization and industrialization are well studied and documented. Air pollution has become a

problem of major concern all over the globe. The continuing expansions of existing industries, the development of new technologies and products with population growth, especially in large urban areas, are introducing a variety of pollutants in large quantities into the atmosphere. Special importance has been given to the possible population risks due to atmospheric dispersion of contaminants from different kinds of hazardous sources (nuclear installations, petrochemical plants, etc.) There are several sources of air pollution, viz., industrial, power generation, transportation, agricultural, and natural sources.

The past ten years has seen the development of several dispersion models that attempt to incorporate current understanding of micrometeorology and dispersion. Regulatory health risk assessment requires estimating pollutant concentrations at source receptor distances of a few metres. This scale is especially important for assessing the risk posed by sources in urban areas such as gasoline stations and dry cleaners, where human receptors may be located within metres from the sources. In principle, several models, such as Aermoc are applicable to such sources because they are designed to treat the effects of buildings on near source dispersion. Moreover the atmosphere is described by similarity scaling relationships using only a single measurement of surface wind speed, direction and temperature to predict vertical profiles of wind speed, direction, temperature, turbulence and temperature gradient. Aermoc can also designed to model particle dispersion and currently only been used to investigate gas phase dispersion.

Degrazia et al., (2000) presented a turbulence parameterization for dispersion models in all stability conditions, excluding the very stable conditions. New sets of turbulence parameterizations can be use in atmospheric dispersion models, with the current knowledge of the planetary boundary layer (PBL) structure and characteristics. The present turbulence parameterisation is based on Taylor's statistical diffusion theory, in which the shear buoyancy PBL spectra are modeled by means of a linear combination of the convective and mechanical turbulent energy. The validation of the present parameterisation applied in a Lagrangian particle model. As a consequence, a parameterisation scheme, able to deal contemporary with neutral and slightly convective condition. Results obtained are quite encouraging. Therefore, the new turbulent parameters may be suitable for applications in regulatory air pollution modelling. In addition, these parameterizations gave continuous values for the PBL at all elevations ( $z_0 \leq z \leq h$ ,

$z_i$ ) and all stability conditions from unstable to stable, where  $h$  and  $z_i$  are the turbulent heights in stable or neutral and convective PBL respectively and is the Monin-Obukhov length. It is the aim of this work to present the general derivations of these expressions to show how they compare to previous results.

Venkatram et al., (2001) suggested an approach for the development of an air quality model designed for regulatory applications. The model is not designed to describe the spatial and temporal distribution of concentrations. Rather, it is designed to meet a more limited objective, which is to simulate concentration frequency distributions observed under a variety of conditions. This approach to model development allows us to neglect model features that might be important in estimating concentrations at specific locations and times. The model is designed to provide estimates of concentration distributions and is thus primarily suitable for regulatory applications. The model assumes that the concentration at a receptor is a combination of concentrations caused by two asymptotic states: the plume remains horizontal and the plume climbs over the hill. The factor that weights the two states is a function of the fractional mass of the plume above the dividing streamline height. The model had been evaluated against data from four complex terrain sites.

Caputo et al., (2003) conducted an inter-comparison between Gaussian, Gaussian segmented plumes and Lagrangian codes. Gaseous emissions are simulated under real meteorological conditions for dispersion models Aermot, HPDM, PCCOSYMA and HYSPLIT. The Aermot and HPDM meteorological preprocessors results are analyzed and the main differences found are in the sensible heat flux (SHTF) and  $u^*$  (friction velocity) computation, which have direct effect on the Monin-Obukhov length and mixing height calculation. Gaussian models (Aermot, HPDM) computed the dispersion parameters by using the similarity relationships, whereas Gaussian segmented model (PCCOSYMA) used P-G stability class to evaluate these parameters. Lagrangian transport model (HYSPLIT) advected the puff and calculated its growth rate with local mixing coefficients. Meteorological parameters have great effect on the performance of air dispersion models. Therefore, Aermot and HPDM have developed effective and sophisticated meteorological parameters preprocessors. It is noticed that HPDM computed the most stable condition and the lowest mixing height. The comparison also showed a significant discrepancy

between HPDM and other Gaussian models. The maximum ground level concentration predicted by Aermot, HPDM and PCCOSYMA are similar.

Sax et al., (2003) established uncertainty analytical approach to elaborate a universal method for the estimation of unpredictability and uncertainty in Gaussian air pollutant dispersion modeling system. Uncertainty is propagated for different components of both models (ISCST3 and Aermot) using Monte Carlo statistical techniques. In this case Aermot predicted a greater range of pollutant concentrations than ISCST3 for low-level sources. Practically uncertainty is very important parameter to record at receptors with highest predicted concentrations that's why indicated results are not 100 % agreed, where the emissions are the dominant source of uncertainty. As Gaussian models are sensitive for the location of emissions release, meteorology, and model parameters, therefore these inputs are well described to minimise uncertainty in the model results. Aermot applications are sufficiently reliable to ensure consistent risk management decisions. If Aermot is to be applied on a regulatory basis in the future, it will be easy to improve to minimize uncertainty within the model parameters by using consistently applied modelling approaches.

Mehdizadeh et al., (2004) showed the emissions from elevated point sources, travel at high altitudes and contribute to regional air pollution. Emissions from industrial stacks are regulated to protect human and environmental health. Thus, industrial facilities are required permits to emit into the atmosphere and to demonstrate their compliance with regulations. That's why emission data is required to evaluate how urban and industrial plumes travelling at high altitudes impact on background plumes. In the process dispersion models are generally used to assess the impact of point source emissions at ground level. So dispersion models, SCREEN and Industrial Source Complex (ISC) are considered to evaluate the importance of individual point source plumes at high altitude. The study mainly considered power plant plumes and developed a general methodology for evaluating their impact on regional air quality.

This study is aimed at determining whether simple dispersion models at high altitudes can be used as a screening tool to evaluate the impact of individual plumes from point sources on regional air quality. The main objective is to determine whether a simplistic approach, using a representative set of meteorological parameters, would accurately predict the prevailing



atmospheric condition. The study also sought to develop a procedure that is less time, data and cost intensive to estimate individual plume impact on air quality. It is noted that crosswind shear effects at high altitudes are not considered in this work. Therefore using the modified ISC model, plumes (mostly for unstable cases) are examined from four power plants, located in eastern Texas. Air quality data collected by the Baylor aircraft from the Baylor Sampling Project are used for calibration and validation. Emissions of SO<sub>2</sub> are considered since SO<sub>2</sub> acts as a non-reactant species in the atmosphere when evaluated over flight times used by the aircraft. User defined meteorological parameters are used instead of the more common annual or probabilistic meteorological data. Results demonstrated that on a typical day, using the most occurring stability class, average wind speed and average mixing height the modified ISC accurately predicted the peak concentrations about 80% of the time. The modified ISC also correctly projected plume width within 70% of the actual spread, at least 60% of the time.

Venkatram et al., (2004) described the evaluation and improvement of dispersion models for estimating ground-level concentrations in the vicinity of small sources located in urban areas. The objective of the study is to identify potential improvements to near-field modeling in urban areas. The models are evaluated with observations from a tracer study conducted at the University of California, Riverside. Experiment simulated a non-buoyant release from the top of a small source in an urban area. Several receptors are located upwind of the dominant westerly wind direction. Model estimates from ISC-PRIME and Aermod-PRIME are evaluated with hourly observed concentrations. These models overestimated the computed highest concentrations. At the same time, the lower range of concentrations is underestimated.

A diagnostic study with a simple Gaussian dispersion model that incorporated site specific meteorology indicated that these problems can be corrected by accounting for wind direction meandering in the vicinity of a source, caused by increased horizontal turbulence in urban areas. While Aermod incorporates lateral meandering, it switches it off in the near field affected by PRIME estimates. However analysis indicates that the PRIME algorithm, which is used to calculate dispersion in the wake cavity, neglects wind meandering and overestimates pollutant concentrations the near field. These concentration estimates might be improved by combining upwind meandering with the PRIME algorithm in Aermod. Because PRIME is designed for

buoyant power plant releases, it might not overestimate concentrations when buoyancy allows the plume to “escape” dispersion in the near field. This study demonstrates that Aermოდ can provide reliable near-field concentration estimates from urban emission sources if turbulent velocity measurements close to a source are used to estimate plume dispersion.

Rama Krishna et al., (2004) examined the assimilative capacity and the dispersion of pollutants resulted from various industrial sources in the Visakhapatnam bowl area, which is situated in coastal Andhra Pradesh, India. Two different air dispersion models (Gaussian plume model, GPM and ISCST-3) are used to predict ground level concentrations of sulphur dioxide and oxides of nitrogen and assimilative capacity of the Visakhapatnam bowl area’s atmosphere for two seasons, namely, summer and winter. The computed 8-hr averaged concentrations of the two pollutants obtained from the GPM and ISCST-3 are compared with those monitored concentrations at different receptors in both seasons and the validation carried out through Q-Q plots. Both models outputs showed similar trend with the observed values from the monitoring stations. The GPM output showed over-prediction, whereas the ISCST-3 showed under-prediction in comparison with the observed concentrations. Terrain features and land/sea breeze influences are not considered in this study, which strongly affected the models outputs.

Venkatram et al., (2004) evaluated dispersion models for estimating ground level concentrations in the vicinity of emission sources in the urban area of university of California, Riverside. Aermოდ-PRIME and ISC-PRIME dispersion models are used to predict SF<sub>6</sub> at different receptors, where SF<sub>6</sub> is used as tracer in a simulated non-buoyant release from a small source in urban area. Both models output are compared with hourly-observed concentrations. The comparison showed that both models overestimate the highest concentrations, whereas lower range of concentrations is underestimated. It is concluded that Aermოდ can predict reliable concentrations if turbulent velocity measurements are used to estimate plume dispersion.

Alrashidi et al., (2005) studied the locations of Kuwait Environmental Public Authority (K-EPA) monitoring station, which measure SO<sub>2</sub> concentrations, emitted from the power stations in the state of Kuwait. The major sources of SO<sub>2</sub> emissions in Kuwait are from west Doha, east Doha, Shuwaikh, Shuaiba, and Az-Zour power stations. Therefore, SO<sub>2</sub> inventory is prepared for

the entire power stations based on fuel consumption as it is highly contaminated with sulphur. The Industrial Source Complex Short Term (ISCST3) dispersion model is used to predict SO<sub>2</sub> ground level concentrations over residential areas. Yearlong meteorological data are obtained from Kuwait International Airport and used in the simulation of the dispersion model. Different discrete receptors in the residential areas are selected.

50 highest predicted and measured daily average concentrations of SO<sub>2</sub> at each monitoring stations are used to carry out the statistical analysis and evaluate the model performance. It is observed that the weather pattern in Kuwait, specially the prevailing wind direction, has strong influence on the ground level concentration of SO<sub>2</sub> in the residential areas located downwind of the both east and west Doha stations. The comparison between the predicted and the measured concentrations of SO<sub>2</sub> from the monitoring stations located at the major populated areas showed that most of these monitoring stations locations are not adequate to measure SO<sub>2</sub> concentrations emitted from the power stations. Therefore, relocation of the monitoring stations is highly recommended to accurately record the highest ground level concentrations of SO<sub>2</sub> emitted from the power stations in Kuwait.

Mandujano et al., (2005) studied extended use of fuels with high sulfur content (fuel oil) in the electric power industry represents one of the biggest concerns on air quality currently in Mexico. The organic sulfur compounds in the fuel oil oxidized as SO<sub>x</sub> during combustion, causing high concentration at the surface level near the releasing point. Shifting towards cleaner energy is crucial, however natural gas (NG) production is currently scarce and substantial investment is required to assure the NG supply to replace the fuel oil. Large investments should be made by the public and private sectors to replace heavy fuel oil use by NG. On the contrary, small increments of the heavy fuel oil cause greater negative effects in the environment. In order to support decision takers, this work assess the air quality impact due to cleaner energy use and determine the optimal NG and fuel oil mixture required to reduce substantially the SO<sub>2</sub> concentration. The dispersion model is applied to compare, against a base case, a set of artificial emissions scenarios based on different fuel oil and NG mixtures. The model is previously validated against SO<sub>2</sub> field measurements performed at an Industrial Corridor, Mexico. The results showed that increasing 40% the NG consumption, the SO<sub>2</sub> concentration in the air is

reduced in 90 % therefore not further NG increasing is needed. The results obtained in this work indicate that the use of the simulation of the dispersion of contaminants with the model Aermoc presents a good correlation between the experimental measurements of the concentration of the sulfur dioxide in different sites, with this inventory of emissions for the sulfur dioxide is well calculated. These results can be quantified the positive effects in the air quality by the use of the NG for different levels of employment in the industry.

Rama Krishna et al., (2005) discussed the Industrial Source Complex Short Term (ISCST-3) model that been used to study the impact of an industrial complex, located at Jeedimetla of Hyderabad city, India, on the ambient air quality. Studies reveal the importance of application of mathematical models for air quality management studies due to different sources in urban areas. The emissions data of 38 elevated point sources and 11 area sources for SO<sub>2</sub> had been considered, along with the meteorological data for 2 months (April and May 2000) representing the summer season and for 1 month (January 2001) representing the winter season have been used for computing the ground level concentrations of SO<sub>2</sub>. The 8 and 24 hour averaged model-predicted concentrations had been compared with corresponding observed concentrations at three receptors in April 2000 and at three receptors in May 2000 where ambient air quality is monitored during the study period. A total of 90 pairs of the predicted and observed concentrations had been used for model validation by computing different statistical errors and through Quantile-Quantile (Q-Q) plot. It is observed that the ISCST-3 model predicted pollutant concentrations are in good agreements with relatively close to those observed values and the model performance are found to be satisfactory.

Abdul Wahab (2006) developed the correlation for the prediction of maximum SO<sub>2</sub> values and their locations around the vicinity of a refinery. The proposed correlations are capable of estimating the hourly maximum SO<sub>2</sub> concentrations from meteorological conditions. Correlation parameters are calculated by multiple regression analysis, using maximum SO<sub>2</sub> concentration as dependent variable and the meteorological parameters as independent variables. The SO<sub>2</sub> data used for the development of these correlations are generated from the industrial source complex short-term (ISCST) model. It is found that wind speed and atmospheric stability class had the most effect on the predicted SO<sub>2</sub> concentration whereas neither mixing height, nor wind

direction, nor temperature had an influence on the maximum SO<sub>2</sub> concentration. Therefore, the suggested correlations require only knowledge of the wind speed and stability class parameters. On the other hand, the developed correlations for estimating the locations of these maximum values of SO<sub>2</sub> concentrations contained only one term that describes the dependence of the locations on wind direction. The derived correlations are shown to be statistically significant.

Holmes et al., (2006) described the detailed review of dispersion modelling packages with reference to the dispersion of particles in the atmosphere. Factors, which are critical to the selection of the model, included the complexity of the environment, the dimensions of the models, nature of the particles sources, the computing power. Finally the time required and accuracy of the desired calculated concentration. Also several major commercial and noncommercial particle dispersion packages are reviewed, which included their advantages and limitations to use for modelling of particle dispersion. Therefore considerable thought has to be given for the choice of the models for each application. The models reviewed included: Box models (AURORA, CPB and PBM), Gaussian models (CALINE4, HIWAY2, CAR-FMI, OSPM, CALPUFF, AEROPOL, AERMOD, UK-ADMS and SCREEN3), Lagrangian / Eulerian Models (GRAL, TAPM, ARIA Regional), CFD models (ARIA Local, MISKAM, MICRO-CALGRID) and models which include aerosol dynamics (GATOR, MONO32, UHMA, CIT, AERO, RPM, AEROFOR2, URM-1ATM, MADRID, CALGRID and UNI-AERO).

Isakov et al., (2007) examined the usefulness of prognostic models output for meteorological observations. These models outputs are used for dispersion applications to construct model inputs. Dispersion model Aermom is used to simulate observed tracer concentrations from Tracer Field Study conducted in Wilmington, California in 2004. Different meteorological observations sources are used i.e. onsite measurements, National Weather Services (NWS), forecast model output from ETA model and readily available and more spatially resolved forecast model from MM5 prognostic model. It is noted that MM5 with higher grid resolution than ETA performed better in describing sea breeze related to flow patterns observed and provided adequate estimates of maximum mixed layer heights observed at the site. It is concluded that MM5 and ETA prognostic models provided reliable meteorological inputs for dispersion models such as Aermom, because wind direction estimates from forecast models are not reliable in coastal areas

and complex terrain. Therefore, comprehensive prognostic meteorological models can replace onsite observations or NWS observations.

Sabatino et al., (2007) described recent urban air quality modelling based on operational models of an integral nature. The use of computational fluid dynamics (CFD) models to address the same problems is increasing rapidly. Operational models e.g. OSPM, Aermot, ADMS-Urban have many comprehensive evaluations in the urban air quality context whereas CFD models do not have such an evaluation record. Applications for both approaches to common problems are studied under the work. Particularly pollutant dispersion from point and line sources (in the simplest neutral atmospheric boundary layer and line sources) are placed within different regular building geometries which are studied in the CFD code FLUENT and then compared with the atmospheric dispersion model ADMS-Urban. Overall CFD simulations with the appropriate choice of coefficients produce similar concentration fields to those predicted by the integral approach. However, some quantitative differences are observed. These differences could be explained by investigating the role of the Schmidt number in the CFD simulations. A further interpretation of the differences between the two approaches is given by quantifying the exchange velocities linked to the mass fluxes between the in-canopy and above-canopy layers.

Kesarkar et al., (2007) discussed the prediction of spatial variation of the concentration of a pollutant governed by various sources and sinks is a complex problem. Gaussian air pollutant dispersion models such as Aermot can be used for this purpose. Aermot requires steady and horizontally homogeneous hourly surface and upper air meteorological observations. However, observations with such frequency are not easily available for most locations in India. To overcome this limitation, a preprocessor is developed for offline coupling of Weather Research and Forecasting (WRF) with Aermot. Using this system, the dispersion of respirable particulate matter (RSPM/PM<sub>10</sub>) over Pune, India has been simulated. Comparison between the simulated and observed temperature and wind fields shows that Weather Research and Forecasting (WRF) is capable of generating reliable meteorological inputs for Aermot. The observed and simulated concentration of PM<sub>10</sub> shows that the model generally underestimates the concentrations over the city.

Stein et al., (2007) illustrated air quality models are useful tools for assessing baseline ambient concentrations, analyzing the relative importance of various emission sources, and testing emission reduction strategies. These assessments typically involve the application of different models depending on program objectives, national, regional, urban, or local scale. Grid models, such as the Community Multi-scale Air Quality model CMAQ, are the best-suited tools to handle the regional features of these chemicals. However, these models are not designed to resolved pollutant concentration on local scales due to technical and computing time limitations. In this study, feasibility of developing an urban hybrid simulation system is tested. Therefore (CMAQ) provides the regional background concentrations, urban-scale photochemistry, and local models such as Hybrid Single Particle Lagrangian Integrated Trajectory model (HYSPLIT) and AMS/EPA Regulatory Model (Aermod) provide the more spatially resolved concentrations due to local emission sources.

In the initial application, the HYSPLIT, Aermod, and CMAQ models are used in combination to calculate high-resolution benzene concentrations in the Houston area. The study period is from 18 August to 4 September of 2000. The Meso-scale Model 5 (MM5) is used to create meteorological fields with a horizontal resolution of  $1 \times 1 \text{ km}^2$ . Finally the ensemble mean concentrations determined by HYSPLIT plus the concentrations estimated by Aermod are added to the CMAQ calculated background to estimate the total mean benzene concentration. These estimated hourly mean concentrations are also compared with available field measurements.

Simpson et al., (2007) demonstrated Aermet model, which is used to estimate hourly mixing heights during the Joint URBAN (2003) experiment in Oklahoma City, Oklahoma. Comparison of observed and estimated mixing heights show that Aermet is able to estimate the daily variations in mixing heights caused by changes in surface temperature, total cloud cover, and the lapse rate above the morning boundary layer. Aermet is the meteorological preprocessor for the Aermod dispersion model. Aermet is a two-dimensional diagnostic model that uses routine meteorological observations and an early morning atmospheric sounding to calculate the convective boundary layer (CBL) height.

Primary goals of Joint URBAN (2003) include measuring meteorological data at several scales of motion and collecting tracer data that resolves dispersion processes within an urban environment. Observed CBL heights are derived from profiler data using a peak signal-to-noise ratio method. Estimated mixing heights using Aermet show good agreement with observations on days of varying temperature and cloud cover whereas CBL heights of over 3000 m are observed in sounding data during the late afternoon.

Touma et al., (2007) introduced the prospect of using prognostic model-generated meteorological output as input to steady-state dispersion model Aermod. An extensive comparison is carried out between the prognostic model generated meteorological output MM5 and National Weather Service (NWS) data obtained from Philadelphia International Airport by using both of these outputs as input to Aermod to estimate hourly and annual average ground level concentrations of benzene over Philadelphia, PA. Aermod is developed by US/EPA to replace Industrial Source Complex (ISC) dispersion model as it is using more advanced representation of planetary boundary layer (PBL). Prognostic models such as MM5 have many advantages. It has an extensive history of use in photochemical grid air quality models. It also provides complete grid-averaged PBL parameters for any region with high grid scale resolution. Aermod is designed to calculate the concentrations of pollutants during calm conditions where wind speed is less than 1 m/s (unlike earlier models, such as ISC), MM5 can furnish Aermod with the unlimited required meteorological data that are not associated with instruments capabilities which NWS depend on. Aermod runs are performed using both MM5 and NWS separately to predict hourly and annual average ground level concentrations of benzene. The comparison between Aermod-MM5 and Aermod-NWS outputs showed that predicted concentrations from Aermod-MM5 are higher than those from Aermod-NWS by factor of 2-3. These results are expected because, dilution velocities estimated from MM5-derived data are lower and consistent with high predicted annual average concentrations, whereas dilution velocities estimated from NWS data generally higher and during calm conditions cannot estimated, leading to under-prediction of benzene concentrations over the area of study.

Princevac et al., (2007) compared the performance of three different methods to estimate the surface friction velocity and the Monin - Obukhov (MO) length in stable conditions. Estimations



from these methods are compared with measurements are made at two urban sites: the Wilmington site located in the middle of an urban area and the VTMX site located on a sloping, smooth area in Salt Lake City. Methods based on measurements of mean winds and temperatures, measured at one or two levels at a non-ideal urban site, can provide adequate estimates of the surface friction velocity and MO length during stable conditions. The methods perform better at the VTMX site than at the Wilmington site. The first method used the mean wind at a single height (Single U or SU), the second used the wind speed at a single level and the temperature difference between two levels (U delta T or UDT), and the third method used to show the two levels of wind speed and temperature (delta U delta T or DUdT). The performance of the SU and UDT methods in estimating surface friction velocity ( $u^*$ ) is comparable. The SU method yielded better estimates of the MO length than the UDT method does. The DUdT method performed poorly in estimating both  $u^*$  and L.

This study shows that a wind speed measured at one level can provides useful estimates of  $u^*$  and L during stable conditions. Supplementing the wind speed with a single temperature difference between two heights does not always improve results; adding information on the difference in wind speeds between two levels can lead to deterioration of the estimates. Thus, the scope of this paper is limited to providing an empirical response to the question: do MO similarity methods that apply to flat terrain provide useful estimates of  $u^*$  and L when the inputs are mean wind speeds and temperatures measured with a 10 m tower located in an urban area.

Isakov (2007) et al., presented currently used dispersion models, such as the AMS/EPA Regulatory Model Aermoc, posses routinely available meteorological observations to construct model inputs. Therefore research examines gridded outputs from comprehensive meteorological models can be used to construct meteorological inputs for dispersion models such as Aermoc. Thus, model estimated concentrations depend upon the availability and quality of meteorological observations, as well as the specification of surface characteristics at the observing site. The values of these meteorological models outputs for air quality modeling is evaluated by first comparing them with onsite measurements made and then using them as inputs to a dispersion model and then comparing their performance to those based on the following inputs from a Tracer Field Study conducted in Wilmington, California in 2004 using four different sources of

inputs: (1) onsite measurements; (2) National Weather Service measurements from a nearby airport; (3) readily available forecast model outputs from the Eta Model; and (4) readily available and more spatially resolved forecast model outputs from the MM5 prognostic model. The comparison of the results from these simulations indicates that comprehensive models, such as MM5 and Eta, have the potential of providing adequate meteorological inputs for currently used short-range dispersion models such as Aermot. The results indicate that these meteorological models have difficulty in estimating wind direction at Wilmington, which is a coastal site. Therefore comprehensive models can simulate mixed layer heights, wind directions and speeds if the model resolution is consistent with the scale of the flow patterns of interest.

Ainslie (2008) et al., developed a source-area model for estimating population exposure to air pollutants at the scale of a neighborhood. The model is based on very simple scaling level analyses of atmospheric dispersion. The model explicitly accounts for the first-order influence of atmospheric dispersion of emissions on surface concentrations with the idea of a source-area, captures the influence of wind speed, wind direction and stability on the dispersion and advection of emissions, with ABL depth in the dilution of pollutants. The source area model is compared against a fixed buffer model that ignores meteorological dispersion. The source area model captures the influence of wind speed, wind direction and stability on the dispersion and advection of emissions and thereby achieves modest improvement of performance over the fixed buffer model. The model is useful for the determination of personal exposures and health effects to local emissions.

Zhang et al., (2008) established GIS (graphical information system) based urban-scale air borne pollution emission inventories of  $\text{SO}_2$ ,  $\text{NO}_x$ , and  $\text{PM}_{10}$  from both fossil energy consumption and industrial production process. Aermot model is used to simulate pollutants concentration in the urban area of Hangzhou a typical Yangtse Delta city in south China. To examine the link between emission inventories and resulting long-term impacts on public health, it is necessary to simulate temporal and spatial distribution of the pollutants' concentration in the southern cities of China. It is come to know that results agreed reasonably by comparing simulated data of  $\text{SO}_2$  /  $\text{NO}_x$  annual average concentrations with observed data at different quality-monitoring stations. Moreover the simulated data of  $\text{PM}_{10}$  annual average concentrations

are much lower than observed data of all monitoring stations because secondary PM<sub>10</sub> data are not included in the simulation. The results are showing that, pollutants concentration is high in well-populated areas therefore the government should improve urban design and plan to separate the two zones to protect public health.

Olvera et al., (2008) performed dispersion simulations of buoyant and neutral plume releases within the recirculation cavity behind a cubical building using a commercially available CFD code and the RNG k- $\epsilon$  turbulence model. Study illustrate that Plume buoyancy could cause considerable flow disturbances inside the wake region, particularly, expanding the velocity defect to greater heights and changing the cavity size, shape and flow direction. Source momentum of a neutral plume release had similar effects on the flow structure and the cavity region to that caused by plume buoyancy. However, the effects of momentum on the concentration profiles are noticeably different from that caused by plume buoyancy. These effects in the downwash algorithms would improve the accuracy of modeling results for far-field concentration distributions and would be mandatory in accident assessments where accurate predictions of short-term are required. The results of this study provide insight into the interaction of plume buoyancy and the near-wake flow structure and concentration distributions.

Britter et al., (2008) presented some mathematical techniques and algorithmic approaches that can make air quality estimate several orders of magnitude faster. In regulatory and public health contexts the long-term average pollutant concentration in the vicinity of a source is frequently of interest. Well-developed Gaussian plume models such as Aermid and ADMS are able to generate time-series air quality estimates of considerable accuracy, applying an up-to-date understanding of atmospheric boundary layer behavior. However, these models acquire a considerable computational cost with runtimes of hours to days. These approaches are often suitable when considering a single industrial complex, but for general policy analyses the computational cost speedily becomes inflexible. It shows that the long-term average concentrations and lateral dispersion need not be accounted for explicitly. It is applied to a simple reference case of a ground-level point source in a neutral boundary layer. A scaling law of exceedance areas is also developed for a particular concentration threshold depends only on the average inverse wind speed, and not on the disturbance of wind directions.

Zeng et al., (2009) illustrated reductions in exposure to urban ambient air pollution that can contribute to significant and measurable improvements in life expectancy. The population exposure modeling system developed in this study indicates that population exposure modeling is more useful than air dispersion modeling. A population exposure modeling system introduced that integrates air dispersion modeling, Geographic Information Systems (GIS) and population exposure techniques to spatially characterize a source-specific exposure to ambient air pollution for an entire urban population at a fine geographical scale. Results based on these models showed that air quality assessments must incorporate more than industrial or vehicle polluting sources-based population exposure values alone, but should consider multiple sources. Also it will help to identifying larger areas of elevated exposure risk; they often don't differentiate the proportion of population exposure attributable towards different polluting sources (e.g. traffic or industrial). The purpose of this research is to develop a modeling system to spatially characterize a source-specific exposure to ambient air pollution across an entire urban population at a fine geographical scale by combining high-resolution air pollution concentration with population distribution.

Zou et al., (2010) evaluated the performance of AERMOD in predicting SO<sub>2</sub> ground level concentration in Dallas and Ellis counties in Texas as these two counties are populous and air pollution has been a concern. Two emission sources are considered in this study i.e. point sources and on-road mobile sources. For the point emission sources, emission rates for 510 sources in Dallas and 76 sources in Ellis are calculated for year 2002. For on-road mobile sources, a method to proportionally allocate mobile emissions to different parts of road segment is used based on the width and the length of the road. Meteorological data are obtained from National Climate Data Center (NCDC). AERMET is used to calculate the hourly planetary boundary layer parameters such as Monin-Obukhov length, convective scale, temperature scale, mixing height and surface heat flux. Air quality observations for these two counties are obtained for year 2002 and three discrete receptors located at the measurement sites are selected. Dispersion model AERMOD is used to simulate SO<sub>2</sub> ground level concentration at different time scale i.e. 1hr, 3hr, 8hr, daily, monthly and annually for both counties separately. The results are validated with the observed concentrations. It is noticed that the 8 hr, daily, monthly and

annually simulated concentrations of SO<sub>2</sub> intervals match with their respective observed concentrations better than the 1 hr and 3 hr simulated concentrations. The results showed that AERMOD performed well at the 8 hr, daily, monthly and annual time scale when combined point and mobile emission sources are used in the simulation as model input. It is also noticed that AERMOD is performed much better in simulating the high end of the spectrum of SO<sub>2</sub> concentrations at monthly scale than at time scales of 1 hr, 3 hr, 8 hr and daily.

Lushi et al., (2010) developed a method for estimation of contaminants short-range emission rates (within 1000 m of the source), using measurements of particulate material deposited at ground level generated from several multiple point sources directed into the atmosphere. Gaussian plume type solution based approach is applied for the advection - diffusion equation with ground level deposition and given emission sources. The results are validated with measured deposition and meteorological data from a large lead - zinc-smelting operation in Trail, British Columbia. Whereas the solution referred to those problems which are incorporated into an inverse algorithm for estimating the emission rates of several contaminants from a smelting operation in British Columbia by means of a linear least squares approach.

**CHAPTER THREE**  
**PROCESS DISCRPTION**

### 3.1 Introduction

An oil refinery is an industrial process plant where crude oil is processed and refined into more useful petroleum products, such as gasoline, diesel fuel, asphalt base, heating oil, kerosene, and liquefied petroleum gas. Oil refineries are typically large industrial complexes with extensive piping running throughout, carrying streams of fluids between large chemical processing units.

Increasing demand on fossil fuel with industrial and economical progression and population growth forced to use the state of the art technologies in refining industries to provide maximum yield with the least environmental impact. This has influence on the refinery processing operations that place a burden on refinery construction in addition to the need to provide increased capacity for refining high sulphur and heavy crude oils. Each refinery has different processing scheme, which is determined by the process equipment available, crude oil characteristics, operating costs and product demand.

Crude oil is having different hydrocarbons, which can be separated on different boiling points through distillation processes. Once these hydrocarbons are separated from contaminants and impurities then purified fuel or lubricant can be sold without any further processing. Smaller molecules such as isobutane and propylene or butylenes can be recombined to meet specific octane requirements through the processes such as alkylation. Octane number of gasoline can also be improved by catalytic reforming process. In this process, hydrogen strips out to produce aromatics, which is having much higher octane ratings. Intermediate products such as gas oils can even be reprocessed to break a heavy, long-chained ends into a lighter short-chained ends, by various types of cracking processes such as fluid catalytic cracking, thermal cracking, and hydrocracking. Figure 3.1 shows typical schematic process flow diagram of an oil refinery.

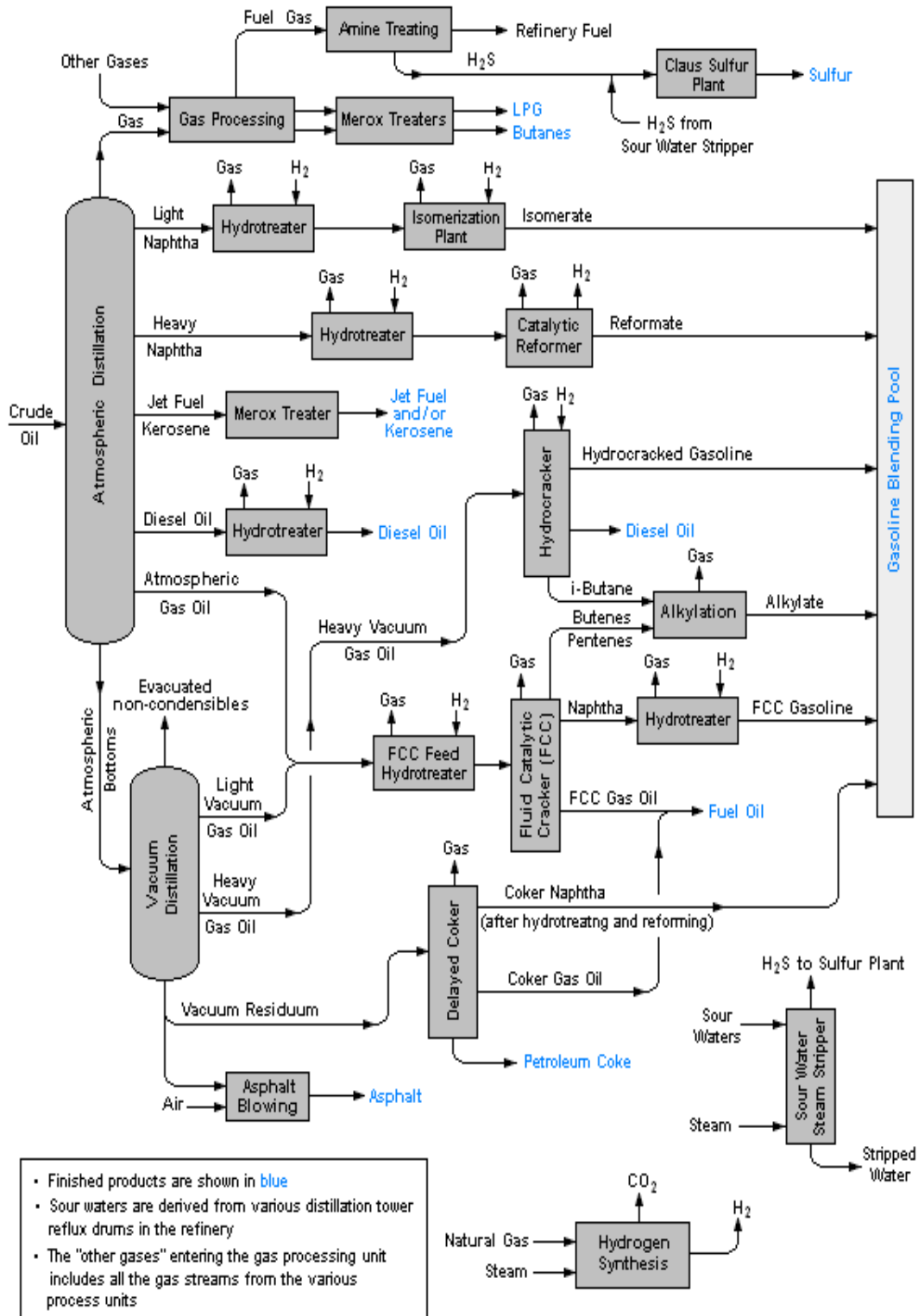


Fig. 3.1: Flow diagram of typical refinery

(Source: [http://en.eikipedia.org/wiki/Process\\_flow\\_diagram](http://en.eikipedia.org/wiki/Process_flow_diagram))



### 3.2 Fluidized Catalytic Cracking Unit (FCC)

Fluid Catalytic Cracking unit (FCC) is one of the topping conversion processes since 1942 where there was high demand of fuels for military vehicles and equipments during the World War II. After the war, FCC process development took place to increase the yield, which allowed refineries to utilise their crude oil resources more efficiently, to produce more valuable products. This unit is often the key to profitability of any refinery. The objective of this unit is to convert high boiling petroleum fractions, namely gas oil to high value products i.e. high-octane gasoline, LPG and heating oil. About 45% of all gasoline produced comes from the FCC and ancillary units, such as the alkylation and MTBE units. Its heavy feedstock (vacuum gas oil, coker gas oil, unconverted oil and waxy distillate), coming from vacuum rerun unit, delayed coker unit and crude distillation units respectively is catalytically cracked into lighter products (liquefied petroleum gas, gasoline, diesel and fuel oils). Environmental concerns about this process have increased, during the last decade due to its great contribution to the sulphur oxides and particulate matter emissions. Currently, FCC operates in constrained regions of medium to high conversion; using synthetic catalysts Fig. 3.2 shows a typical schematic flow diagram of FCC process.

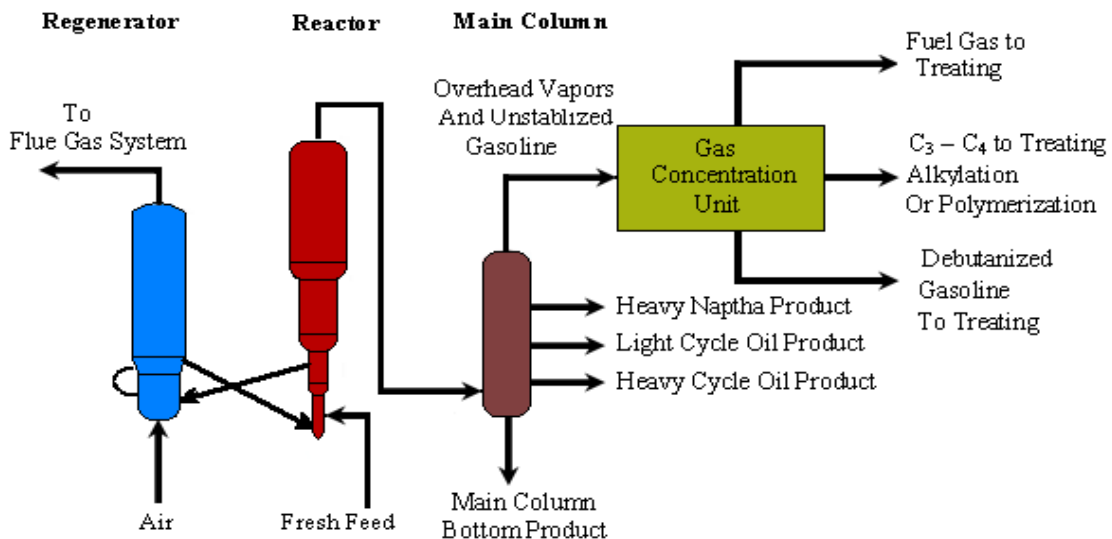


Fig. 3.2: Fluid catalytic cracking process

Fluid catalytic cracking reactions are endothermic and required energy, which is supplied by the regenerated catalyst preheated during re-activation (combustion) process. The operating temperature and pressure are from 725°-745° C and 200 kPa respectively.

### **3.3 FCC Catalyst**

There are various types of catalyst formulations used in FCC unit. The particle size distribution (PSD), the sodium (Na), the rare earth (RE) and the surface area (SA) are some of the important properties of the fresh catalyst that need close consideration. The PSD is an important factor for the fluidized properties of the catalyst. Generally fluidisation improves as the particles fraction increased to 40 µm. The surface area is determined by the amount of nitrogen adsorbed by the catalyst.

Sodium contents always have unfavorable effect on the activity of the catalyst as it deactivates the zeolite and reduces the gasoline octane number. The sodium content is normally expressed as weight percentage of the catalyst. Rare earth metals are usually supplied as a mixture of oxides extracted from ores such as bastnaesite or monazite, which are the generic term for the metallic elements of the lanthanide series. Rare earth elements also improve the catalyst activity and hydrothermal stability.

### **3.4 Catalyst Components**

FCC catalysts are in the form of fine powders with an average particle size diameter of 75 µm. There are four major components in the catalyst.

*D-Zeolite:* It is the important component of the FCC catalyst, with well-defined lattice structure. Silica and alumina tetrahedral are its basic building blocks. Each tetrahedron consists of a silicon or aluminium atom at the center of the tetrahedron with oxygen atoms at the corners. The activity of the zeolite comes from its acid sites. The zeolites uses for the applications of the FCC unit are Type X and Type Y. Presently, all type of the catalysts used in FCC are of Type Y.

The properties of zeolite can play a major role in the overall performance of the catalyst. The reactor / regenerator environment causes significant changes in the chemical and structural composition of the zeolite e.g., in the regenerator; the zeolite is subjected to thermal and hydrothermal treatments. The zeolite retains crystalline structure against feedstock contaminants such as vanadium and sodium. The three important parameters, which govern the behavior of zeolite, are Unit Cell Size, rare earth elements level, Sodium content.

*The Unit Cell Size (UCS):* UCS is a measurement of aluminium sites or the total potential of acidity per unit cell. The negatively charged aluminium atoms are sources of active sites in the zeolite. Silicon atoms do not acquire any activity.

*Rare earth elements:* REE's play an important role to stabilize aluminium atoms in the zeolite structure. When the catalyst is exposed to high temperature steam in the regenerator, rare earth elements protect the aluminium atoms from separating from the zeolite lattice. The rare earth promotes zeolite activity and gasoline selectivity. The insertion of rare earth maintain acid sites, which promotes hydrogen transfer reactions. In addition, rare earth improves thermal and hydrothermal stability in the zeolite.

*Sodium Na:* 'Na' decreases the hydrothermal stability of the zeolite; it originates either from the zeolite or from the feedstock. It also reacts with the zeolite acid sites to reduce catalyst activity. In a de-aluminated zeolite, when the UCS is low, the sodium has an adverse effect on the octane of gasoline. It is attributed to the drop in the number of strong acid sites.

*Matrix:* This refers to the components of the catalyst other than the zeolite. The term active matrix means the component of the catalyst other than the zeolite having catalytic activity. Alumina is the source for an active matrix. The active matrix contributes significantly to the overall performance of the FCC catalyst. The zeolite pores are not suitable for cracking of large hydrocarbon molecules. They are too small to allow diffusion of the large molecules to the cracking sites. An effective matrix must have a porous structure to allow diffusion of hydrocarbons into and out of the catalyst. The active matrix pre-cracks heavy feed molecules for further cracking at the internal zeolite sites. The result is a synergistic interaction between matrix

and zeolite in which the activity attained by their combined effects can be greater than the sum of the individual effects. An active matrix can also serve as a trap to catch some of the vanadium and basic nitrogen. The high boiling fraction of the FCC feed usually contains metals and basic nitrogen that poison the catalyst.

*Filler and binder:* Filler is the type of clay which is incorporated into the catalyst to dilute its activity. Binder does not have catalytic activity. They serve as a glue to hold the zeolite, the matrix and the filler together. The functions of filler and binder are to provide physical integrity, a heat transfer medium and a fluidizing medium in which the more important and expensive zeolite component is incorporated.

### **3.5 Process Description**

The fluid catalytic cracking (FCC) unit is very complex process. Fig 3.3 Shows the FCC unit configuration. In order to explain the unit operation, the process description is broken down into subsections as follows:

- a. Reactor feed preheating section
- b. Reactor-regenerator section
- c. Main fractionator section
- d. Gas concentration section
- e. Power recovery section

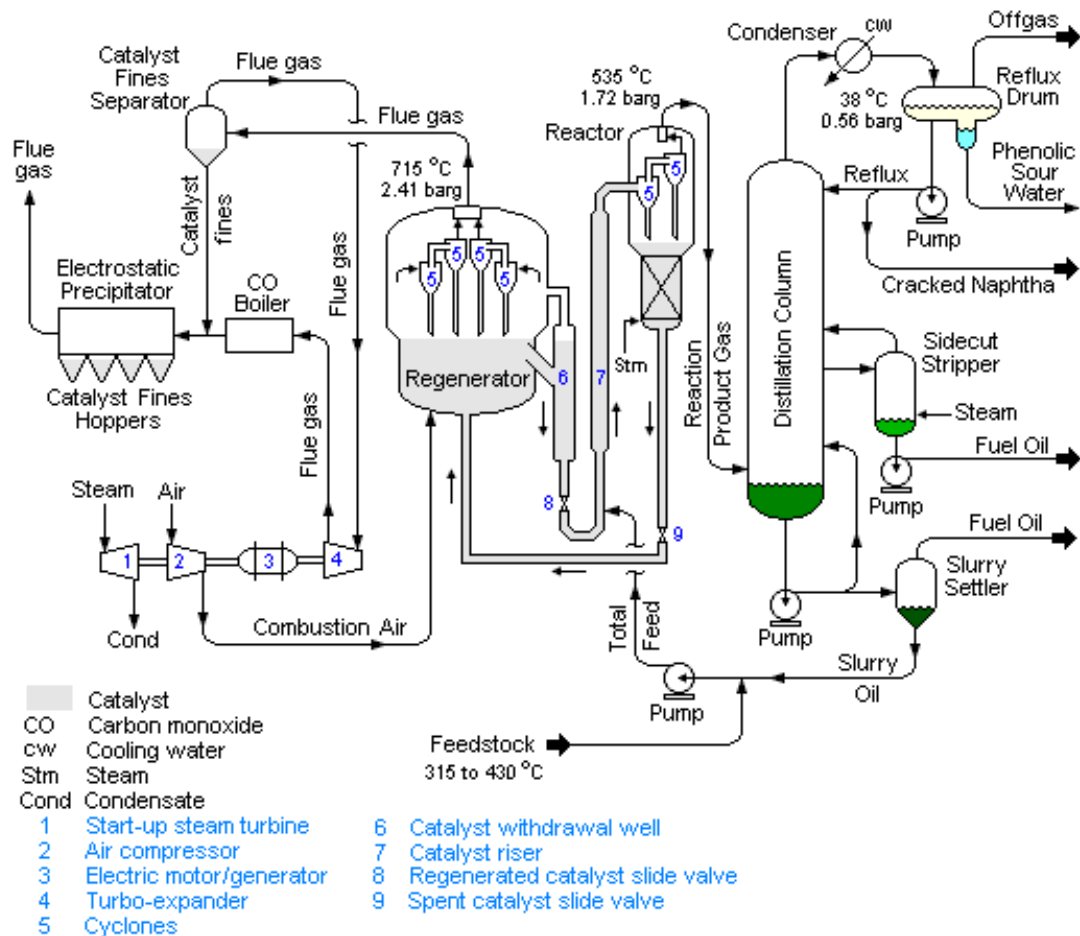


Fig. 3.3: A schematic flow diagram of FCC Unit used in petroleum refineries

(Source: [http://en.wikipedia.org/wiki/fluid\\_catalytic\\_cracking](http://en.wikipedia.org/wiki/fluid_catalytic_cracking))

### 3.5.1 Reactor Feed Preheating Section

In reactor feed preheating section the heavy feed, i.e. raw oil, is brought to the required riser inlet temperature by heating it with the hot material leaving the main column, i.e. pump around and product streams. FCC feedstock is normally gas oil from the vacuum distillation unit. The other supplemental feedstocks are added to the gas oil and the combined material is sent to the surge drum, which provides a steady source of flow to the charge pumps. The material from the surge drum is heated to a temperature of about 230°C to 265°C utilising the heat from the main fractionator bottom and other pump around flows.

### 3.5.2 *Reactor-Regenerator Section*

This is the heart of the FCC unit. In reactor feed reacts in presence of the catalyst and converted it into the products. The catalyst from the reactor, i.e. spent catalyst is regenerated in the regenerator by combustion reaction using about 10 % excess air.

Virtually all of the reactions occur in the riser over a period of 2 to 4 seconds before the catalyst and the products are separated in the reactor. The feed enters the riser at its base where it comes into contact with the regenerated catalyst. The heat absorbed by the catalyst in the regenerator provides the energy to heat the feed to desired reactor temperature (520 – 530 °C). The feed is vapourised on coming into contact with the hot catalyst at a temperature of 730 °C and the cracking reactions start instantaneously.

The ideal riser is like a plug flow reactor where the catalyst and vapour go up the riser with the same velocity and minimum back mixing. As a consequence of the cracking reactions, coke is deposited on the catalyst reducing its activity. The riser exit is connected to the reactor vessel, providing expansion, resulting into velocity drop, where the catalyst is separated from the hydrocarbon vapours and fines are captured by the cyclone assembly. The vapours are then sent through a set of multi-stage cyclones. The cyclones collect the catalyst and return it to the stripper. The product vapours exit the cyclones and flow to the main fractionator for recovery. Extended time of contact between the catalyst and vapours led to re cracking of the desired products. The spent catalyst, along with some hydrocarbons falls into the reactor stripper where steam is used to strip these hydrocarbons off the catalyst. The entire hydrocarbon content of the catalyst is not removed in the stripper and part of it gets carried to the regenerator. This leads to loss of product, loss of throughput and loss of catalyst activity.

The regenerator's main objective is to restore the catalyst activity and supply heat to crack the feed by burning off the coke (containing various contaminants, mainly sulphur) deposited on the spent catalyst. From the regenerator, the catalyst flows down the standpipe, which provides the necessary pressure head for maintaining proper catalyst circulation. SO<sub>2</sub>, NO<sub>x</sub>, CO, CO<sub>2</sub> and PM are emitted from FCC stack as a result of coke combustion process.

### **3.5.3 Main Fractionator Section**

The main purpose of the fractionators is to de-superheat and recover liquid products from the reactor vapor. In main fractionator reactor product vapors are cooled and products such as HCO, LCO, distillate and heavy gasoline are separated. It accomplishes the fractionation by condensing and re-vapourising the hydrocarbon vapors as they flow upwards. The major function of bottom section of the column is to provide a heat transfer zone. The cooled pump also serves to wash down catalyst fines in the vapour. The quench flow is used to control the column bottom temperature and prevent chances of coking. The heat of the bottom circuit is used to preheat feed and steam generation and re-boiling in the gas concentration section. Apart from the bottom product, which is called heavy cycle oil (HCO), the other products from the main column are light cycle oil (LCO), distillate, heavy gasoline and the overhead vapours, which are unstabilised gasoline and lighters. The side refluxes are used to remove heat from the column and to supply heat to the unsaturated gas con section.

### **3.5.4 Gas Concentration Section**

In gas concentration section lighter products from the main fractionator overhead are separated into off-gases, LPG and light gasoline. So the role of the gas plant is to separate the unstabilized gases and light gases to fuel gas, C<sub>3</sub> and C<sub>4</sub> compounds and gasoline. The hydrocarbon vapours are sent to a wet gas compressor. The term “wet gas” refers to the condensable material in the gas at those operating conditions. The compressor is a two-stage steam turbine driven centrifugal compressor. The vapors from the 1st stage are partially condensed and flashed in an inter-stage drum. The second stage discharge is mixed with gas streams from the stripper overhead, the primary absorber bottoms and wash water. They are flashed in the HP separator. The vapors go through the primary absorber and the liquid is sent to the stripper. The absorber recovers the C<sub>3</sub>'s and heavier fractions from the gas against lean oil. The liquid from the HP separator enters the stripper where the light ends are removed by providing an external re-boiler. An external re-boiler provides the heat for the column. The final product streams of heavy gasoline, light gasoline and LPG are further treated in amine treatment or mercox units for removal of H<sub>2</sub>S and mercaptans. The deposited sulfur in the coke leaves the FCC process as flue

gas from the regenerator in the form of SO<sub>2</sub> and SO<sub>3</sub>. SO<sub>2</sub> typically accounts for 80 to 90% of total SO<sub>x</sub> in the FCC flue gases making it the major FCC unit air pollutant.

### ***3.5.5 Energy Recovery Section***

The energy recovery section, where the energy of the flue gases from the regenerator is recovered for the generation of power and steam. The energy recovery section has been provided as an overall efficiency-improving device of the entire unit. The purpose of this section is to utilize the thermal and mechanical energy of the regenerator flue gases. The recovered energy is used generate excess power over and above that required for driving the main air blower and generate high pressure steam. The section consists of the third stage separator, the energy recovery train comprising of the expander turbine, main air blower and motor generator, and the flue gas cooler. The operation of the energy recovery section depends on the condition of the regenerator. Any variation in the operating conditions of the regenerator, i.e. pressure, temperature, flow of air or catalyst content in the flue gas will alter the operation of the energy recovery section.



**CHAPTER FOUR**  
**AIR DISPERSION MODELS**

## 4.1 Introduction

Dispersion modeling is developed in early 1930; it is extensively used to assess the environmental issues. It uses computer simulation that can predict air pollutant concentrations from different types of emission sources. In the last three decades, the strict environmental regulations have lead to massive growth in the use of mathematical models to predict the dispersion of air contaminants and pollutants. Dispersion model simply showed a picture of reality, which is not only containing all the features of the real system but also, contains the features of interest for the modifications of the regulations and their implementation. Dispersion model shows descriptive view of the system where different relationships are utilized using different mathematical equations. The model outputs are presented in the form of graphs and tables.

Gaussian-plume models are the most commonly models used as a steady state dispersion models, based on mathematical approximation of plume and their behavior. They express the fundamental description of the dispersion process with some basic assumptions. These types of model can provide us logical results when used appropriately. The modern dispersion models are user friendly and use sophisticated approach to explain diffusion characteristics and dispersion using the elementary properties of the atmosphere rather than to rely on general mathematical approximation. This approach provides better way to treat more complicated situations e.g. complex terrain and long-distance transport. Figure 4.1 is explaining the execution of various steps with required information for computation of successful runs.

Modern air dispersion models are programs those can compute the pollutants concentration downwind of source using information on:

- i. Pollutant emission rate
- ii. Properties of the emission source.
- iii. Local topography
- iv. Meteorological conditions for the area of interest.
- v. Background concentrations of pollutant.

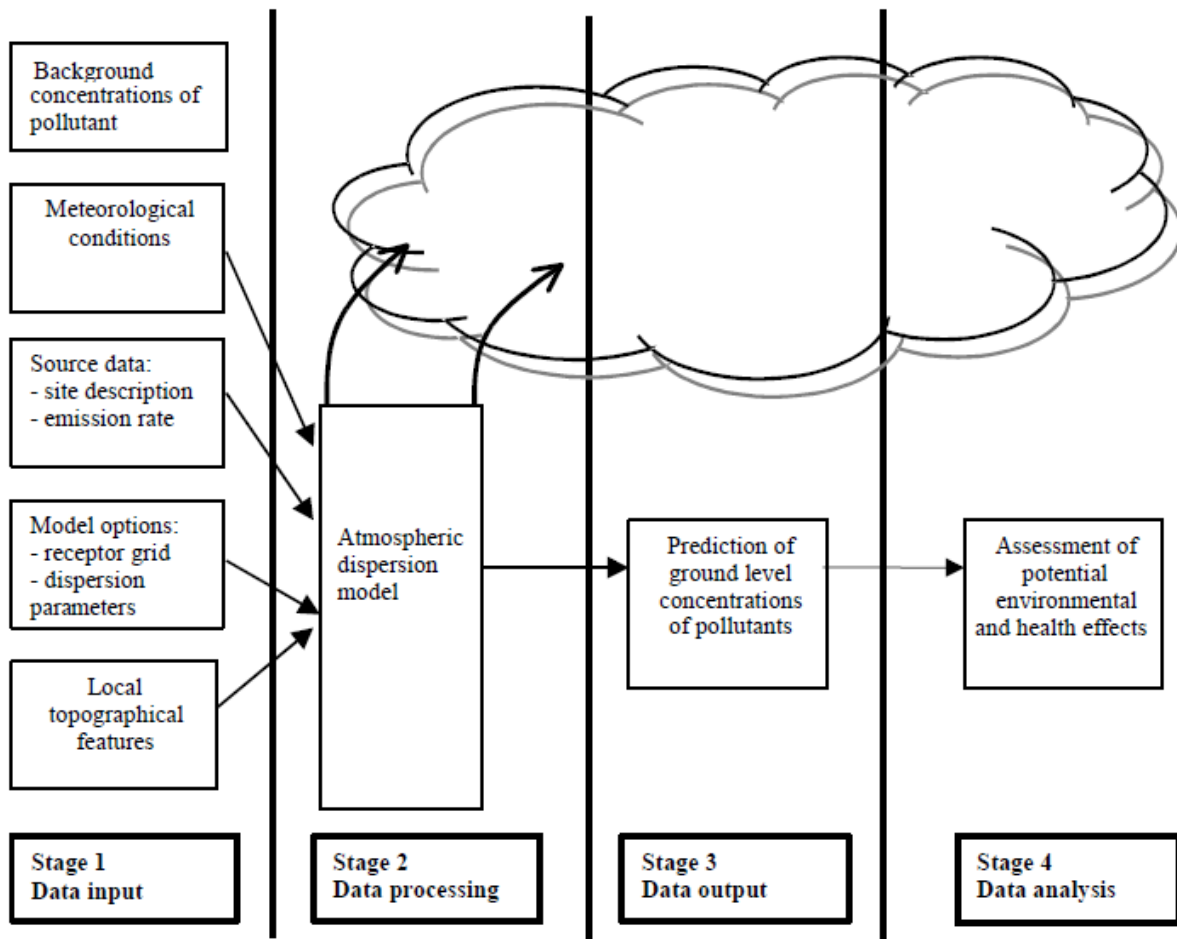


Fig. 4.1: Overview of the air pollution modelling procedure

(US EPA approved Good Practice Guide for Atmospheric Dispersion Modelling)

## 4.2 Objectives of the Dispersion Models

Air quality monitoring is the most important feature of the environmental assessment for both industrial and urban areas. This can be achieved with the dispersion model. The following are the benefits can be attain are:

- i. Stack designs that reflect the engineering perspective.
- ii. A continuous assessment of conformity with standards and guidelines.
- iii. The continuous interpretation to interpret environment impact assessment (EIA).

### **4.3 Key Features of the Dispersion Models**

Dispersion models are favorable to predict downwind concentrations of the contaminants for either long or short term. Particularly they are having unique importance to assess the impacts of emissions from various activities and to estimate changes due to the process modifications. Model results are used to:

- i. Assess compliance of emissions with air quality guidelines, criteria and standards.
- ii. Determine suitable stack heights and design ambient air monitoring networks.
- iii. Identify and control the major contributors to existing air pollution problems.
- iv. Evaluate the policies and mitigation strategies (e.g. the effect of emission standards).
- v. Forecasting pollution episodes and schedule new amenities.
- vi. Apply the risk assessment and planning to manage rare events such as hazardous substance releases accidentally.
- vii. Approximate the influence of geophysical factors on dispersion (e.g. terrain elevation, presence of water bodies and land use).
- viii. To reduce the monitoring cost.

### **4.4 Constrains of Dispersion Models**

It is difficult to locate precise location, magnitude and timing of ground level concentration through most sophisticated atmospheric dispersion model with 100 % accuracy. The adequate (US EPA approved) model is capable of evaluating the process and generate reliable results. However dispersion models having some limitations to assess the effects of specific sources on particular locations are:

- i. Source should be well defined.
- ii. The most sensitive locations should be specified accurate and precise selection of sensitive locations.
- iii. Stringent meteorological condition (calm or unstable).

## 4.5 Gaussian-Plume Models

Gaussian-plume models are widely used for atmospheric dispersion studies in particular for regulatory purpose. They are well understood and easy to apply. They are based on Gaussian distribution of the plume under steady state conditions for both vertical and horizontal directions. These models can calculate uniform concentration across the modelling domain from fixed or variable emission rate and metrological conditions for each hour. The Gaussian-plume dispersion models are not formulated to depend on time, although they do represent an ensemble time average. The meteorological conditions are assumed to be constant during the whole dispersion process from source to receptor. Model calculations in each hour are independent where as emissions and meteorological conditions vary continually. The Gaussian-plume models are those dispersion models that applied under certain conditions, whereas the Gaussian-plume formula provides a better projection for reality if conditions do not change quickly within the studied hour which is being to be modeled.

Gaussian plume equation was developed through the following expression:

The concentration of a pollutant is expressed by simple plume model as:

$$C = \frac{\text{Mass emission rate}}{(\text{wind speed})(\text{area of plume cone disk})} \quad (4.1)$$

Where,

Mass emission rate is in g/s

Wind speed is in m/s

Area of the plume cone disk is in m<sup>2</sup>

Pollutant mass flow is not uniformly distributed within the plume volume. Therefore, Gaussian distribution occurs across the plume due to the change in wind direction over averaging time. In order to describe the distribution of the pollutant mass within the plume, transport of mass within a small control volume is considered. As x-axis is the time-averaged wind direction, y-axis is the crosswind direction and z-axis is vertical direction.

The rate of pollutant molecules transport across the y-axis depends on the concentration difference between the two sides and is equal to  $K \, dC/dx$ , where  $K$  is termed Eddy diffusivity ( $m^2/sec$ ). The magnitude of  $K$  depends on the magnitude of the eddy motions. Transport of mass in x direction depends on the average horizontal wind direction and its magnitude, whereas transport of mass in y and z directions depends on turbulent motions.

The net rate of change in pollutant mass flow in x-direction is expressed as:

Net rate of change of mass flow = mass flow rate in – mass flow rate out

Where:

$$\text{Mass flow rate in} = C \, u \, A_{yz} \quad (4.2)$$

$$\text{Mass flow rate out} = C \, u \, A_{yz} + \frac{\partial}{\partial x} (C \, u \, A_{yz}) \, dx \quad (4.3)$$

$$\text{Net rate of change of mass flow} = - \frac{\partial}{\partial x} (C \, u \, A_{yz}) \, dx = - \frac{\partial}{\partial x} (C \, u) \, V \quad (4.4)$$

$$V = \text{Volume} = A_{yz} \, dx = dy \, dz \, dx$$

$u$  = wind speed in m/s

$$A_{xy} = dx \, dy$$

$$A_{yz} = dy \, dz$$

$$A_{xz} = dx \, dz$$

The net rate of change in pollutant mass flow in z-direction is:

$$\text{Mass flow rate in} = - A_{xy} \frac{\partial}{\partial z} (K_z \, C) \quad (4.5)$$

$$\text{Mass flow rate out} = - \left( A_{xy} \frac{\partial}{\partial z} (K_z \, C) - \frac{\partial}{\partial z} \left[ \frac{\partial}{\partial z} (K_z \, C) \right] V \right)$$

$$\text{Net rate of change} = \frac{\partial}{\partial z} \left[ \frac{\partial}{\partial z} (K_z \, C) \right] V \quad (4.6)$$

Similar result is obtained in the y-direction.

$$\text{Net rate of change in y-direction} = \frac{\partial}{\partial y} \left[ \frac{\partial}{\partial y} (K_y \, C) \right] V$$

Given that the net rate of change in the volume [=  $V \, (dC/dt)$ ] is the change in all three directions.

Advection diffusion equation:

$$\frac{\partial C}{\partial t} = u \frac{\partial C}{\partial x} + \frac{\partial}{\partial y} \left[ K_y \frac{\partial C}{\partial y} \right] + \frac{\partial}{\partial z} \left[ K_z \frac{\partial C}{\partial z} \right] \quad (4.7)$$

Where:

$u \frac{\partial C}{\partial x}$  is the Advection transport by the mean wind speed, u. The change of concentration with respect to y and z directions represents the effect of turbulent “diffusion”, i.e., exchange of polluted air parcel with surrounding air parcels. If the surrounding air is cleaner,  $dC/dz$  &  $dC/dy$  are negative. K is the “eddy diffusivity” and represents the intensity of turbulent motions and varies with stability class.

The Gaussian plume equation is a particular solution under the following assumptions:

The Gaussian plume equation is a particular solution under the following assumptions:

- Steady state conditions  $\frac{\partial C}{\partial t} = 0$
- Constant wind speed with height (u does not depend on z)
- Constant eddy diffusivity (K does not depend on y or z)

$$\sigma_z^2 \text{ is defined as } \frac{2 K_z x}{u} \quad (4.8)$$

$$\sigma_y^2 \text{ is defined as } \frac{2 K_y x}{u} \quad (4.9)$$

Total mass conserved is given as:

$$\int_{-\infty}^{\infty} \int_{-\infty}^{\infty} C \, dx dz = Q \text{ for } x > 0 \quad (4.10)$$

The solution of advection equation at steady state yields Gaussian plume equation:

$$C(x, y, z) = \frac{Q}{2\pi\sigma_y\sigma_z u} \exp\left[-\frac{1}{2}\left(\frac{y}{\sigma_y}\right)^2\right] \left\{ \exp\left[-\frac{1}{2}\left(\frac{z-h}{\sigma_z}\right)^2\right] + \exp\left[-\frac{1}{2}\left(\frac{z+h}{\sigma_z}\right)^2\right] \right\} \quad (4.11)$$

Where:

$C$  = atmospheric concentration of pollutant in  $\text{g/m}^3$

$Q$  = mass emission rate in  $\text{g/s}$

$x$  = downwind distance, relative to the source location in  $\text{m}$

$y$  = crosswind distance, relative to the plume centerline in  $\text{m}$

$z$  = vertical distance, relative to ground in  $\text{m}$

$h$  = effective release height, relative to ground in  $\text{m}$ ,  $h = \text{stack height } (h_s) + \Delta h$

$\sigma_y$  = horizontal dispersion coefficient (function of  $x$ ), representing the standard deviation of the concentration distribution in the crosswind axis direction in metres

$\sigma_z$  = vertical dispersion coefficient (function of  $x$ ), representing the standard deviation of the concentration distribution in the vertical axis direction in metres

$u$  = average wind speed in  $\text{m/s}$

Figure 4.2 shows the concentration distribution from a continuous point source of effective height  $h$  as predicted by the Gaussian plume equation. For unstable conditions (class), non-Gaussian probability density function (Lagrangian) is implemented in dispersion model Aermid to determine concentration distribution from advection equation. The concentration of the pollutant from position  $x', t'$  to new location  $x, t$  can be expressed as:

$$C(x,t) = \int_{-\infty}^{\infty} \int_{-\infty}^{\infty} \int_{-\infty}^{\infty} Q(x, t|x_o, t_o) \langle c(x_o, t_o) \rangle dx_o + \int_{-\infty}^{\infty} \int_{-\infty}^{\infty} \int_{-\infty}^t Q(x, t|x', t') S(x', t') dt' dx' \quad (4.12)$$

This is an additional inherited feature of Aermid over most of the published air dispersion models to provide accurate approximate ground level concentrations for unstable conditions (class).



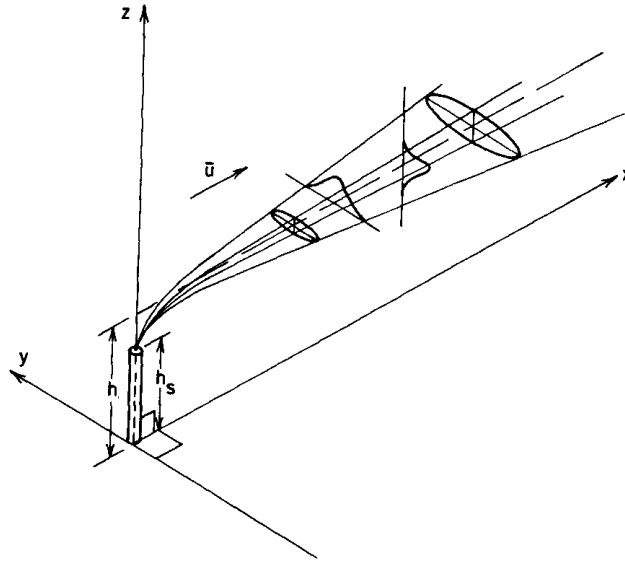


Fig. 4.2: Concentration distribution from a continuous point source of effective height  $h$ .

#### 4.6 Features of Gaussian-Plume Models

Certain characteristics that make of steady-state Gaussian models have following characteristics:

- i. Computer resources, like desktop facilitate the computation of model results in a reasonable time.
- ii. They provide user-friendly graphical interfaces with limited inputs variables.
- iii. The results can easily be comparable.

#### 4.7 Limitations of Gaussian-Plume Models

Gaussian steady-state models assume that the atmosphere is uniform across the entire modeling domain. Existing transportation and dispersion conditions must remain unchanged for the material to reach from the source to the receptor e.g. convective conditions can't be treated with the plume model. Gaussian-plume models over estimate the cases during low wind speed or calm conditions, due to the inverse wind speed that is dependent on the steady-state plume

equation. Moreover Gaussian-plume models consider that the pollutants are transported in a straight line directly to receptors. In moderate terrain, these models overestimate the terrain impingement effects during stable conditions.

## **4.8 ISCST3**

The Industrial Source Complex Short Term (ISCST3) model was developed in 1970, it is the one of the US EPA's approved regulatory model. The ISCST3 model is a steady-state Gaussian plume algorithm. It is applicable for estimating ground level concentration from point, area, and volume sources up to a distance of about 50 kilometers from the source. There are number of options available in this model, which includes the use of stack-tip downwash, buoyancy-induced dispersion and final plume rise.

## **4.9 ISC-PRIME**

ISC-PRIME is an improved version of ISCST3, which uses the Plume Rise Model Enhancements (PRIME) model, it integrates two important features of building downwash - enhanced plume dispersion coefficients that is due to turbulent wake and it could reduced plume rise. Other algorithms are similar to ISCST3 except the building effects.

## **4.10 CTDMPLUS**

CTDMPLUS is one of the advanced forms of the Gaussian plume dispersion model. This model is designed to estimate hourly concentrations of a pollutant from elevated point sources to the receptors on or near to the isolated terrain. This model is able to assess stable and neutral atmospheric conditions as well as all those condition, which are unstable in daytime. It utilises the meteorological data and terrain information in a different ways from other regular models. During stable and neutral feature CTDMPLUS applies to a critical dividing-streamline height. This feature is used to separate the flow in the vicinity of a hill into the two separate layers. In

unstable or convective conditions the model relies on a probability density function (PDF), which describes the vertical velocities to estimate the vertical distribution of pollutants.

## 4.11 AERMOD

AERMIC (the American Meteorological Society / Environmental Protection Agency Regulatory Model Improvement Committee) is founded to introduce the concept of state-of-the-art modeling. AERMIC's focus is on a new period for regulatory steady-state plume modelling. This platform uses air dispersion fundamentals, which are based on planetary boundary layer turbulence structure and scaling concepts. AERMOD can treat both surface and elevated sources in simple and complex terrain.

Primarily AERMOD was developed in 1995 and formally proposed by the US EPA as a replacement for ISCST3. It is equipped with a new simplistic approach following the current concepts about flow and dispersion in complex terrain. AERMOD defines all the parameters of complex terrain that's to be handled in a consistent and continuous manner.

US EPA describes this new model as an advanced dispersion model that incorporates state-of-the-art boundary layer parameterisation technique, convective dispersion, plume rise formulations, plume interactions in a complex terrain. It applies boundary-layer similarity theory to define turbulence and dispersion coefficients as a continuum rather than discrete set of stability classes. It is designed to run with a minimum of observed meteorological parameters.

AERMOD modeling system consists of two preprocessors. The AERMOD mapping program (AERMAP) is a terrain pre-processor, which is used to characterize terrain and generate receptor grids for AERMOD. The other meteorological preprocessor (AERMET) provides planetary boundary layer parameters over a high altitude to yield accurate predicted concentration values for a given meteorological conditions. Meteorological preprocessor (AERMET) also provides all the information required to characterise the state of the surface, mixed layer and the vertical structure of the PBL. Figure 4.3, illustrates successive steps in computation of AERMOD model.

# MODELING SYSTEM STRUCTURE

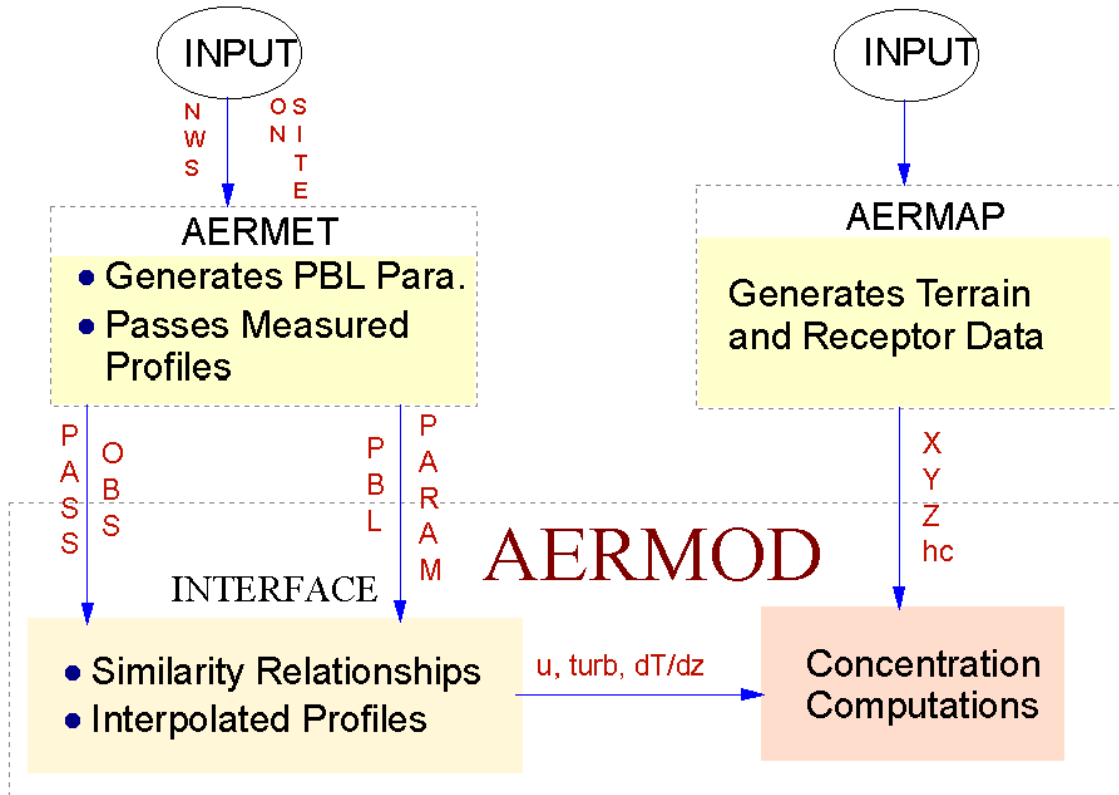


Fig. 4.3: Overview of the AERMOD modeling procedure  
(US EPA approved Good Practice Guide for Atmospheric Dispersion Modeling)

Aermod contains advanced and improved algorithms for:

- (1) Dispersion in both the convective and stable boundary layers.
- (2) Plume rise and buoyancy.
- (3) Estimation of vertical profiles of wind, turbulence, and temperature.
- (4) Treatment of receptors on all types of terrain (complex and flat).
- (5) Treatment of building wake effects.
- (6) Characterisation of the boundary layer parameters.

Aermod is a steady state Gaussian plume model. It assumes the pollutant concentrations at all distances from the source during a modeled hour are controlled by the averaged meteorology. Aermod uses Gaussian distribution for stable conditions and non-Gaussian probability density function for unstable conditions. In the stable boundary layer, the dispersion process is governed mainly by the averaged hourly meteorology. The crosswind and vertical distributions (dispersion coefficients in y and z direction) are assumed to follow Gaussian distribution.

In the convective boundary layer (unstable conditions), the crosswind distribution is also assumed to follow Gaussian distribution, but due to the presence of the vertical mixing resulted from the turbulence in this layer, the vertical dispersion distribution is positively skewed and results in a non-Gaussian vertical concentration distribution described as a non-Gaussian probability density function. The positive skewness is consistent with higher frequency of the occurrence of downdrafts than updrafts; for an elevated non-buoyant source the skewness also leads to the descent of the plume centerline.

Surface type is very important factor in pollutants dispersion calculations. The modelling domain may contain water surface, urban and rural areas with different surface roughness, heat capacities and fluxes.

Therefore, surface characteristics in the form of albedo, surface roughness, Bowen ratio and meteorological observations (wind speed, wind direction, temperature, and cloud coverage) are Aermet's input data. Aermet then calculates the PBL parameters i.e. friction velocity, Monin-Obukhov length, convective velocity scale, temperature scale, mixing height, and surface heat flux. These parameters are then passed to the interface (which is within Aermod) for the model execution.

Aermap generates regular receptors (grid points) over a given terrain based on the modelling domain characteristics. Then, it uses gridded terrain data to calculate a representative terrain-influence height. The terrain height scale  $h_c$ , which is defined for each receptor location, is used to calculate the dividing plume streamline height. Aermap passes the following information to Aermod: the receptor's location ( $x, y$ ), its height above mean sea level, and the receptor specific terrain height scale ( $h_c$ ) for each receptor.

Further research may be necessary to ensure the model applications for non-continuous releases source i.e. puffs and fugitive gases. Updated Aermod code and supporting documents are available in the US EPA website (<http://www.epa.gov/>).

Commercially easy-to-use interfaces that integrate all model tools are commonly used, so that the modeller does not have to waste time sorting out all of the various input files and executable requirements. These interfaces are compatible with most workstations and laptops operating systems.

Lakes Environmental Company supplies graphical Windows-based interfaces of air dispersion modelling software. Its robust and user-friendly interfaces of air dispersion modelling software are used for research applications by consultancy companies, industries, governmental agencies and academia. Lakes Environmental offers a wide range of environmental software products, covering five major categories of air quality i.e. air dispersion modeling, compliance assurance, emergency release, emissions management and risk assessment. It developed interfaces for many air dispersion models including Aermod.

Breeze Company is also supplies uniform graphical interfaces of air dispersion modelling software. Its developed software products are compatible with Microsoft/Windows operating systems and applications. Breeze products include an integrated Geographic Information System (GIS), an intuitive data analysis and visualisation interface tool, that enables modeled objects and results to interact and be displayed with a variety of geophysical data.

In the present work, Aermod system package is obtained from Lakes Environmental Company.

#### **4.12 Features of Aermod**

There are some special features of Aermod, which improve its ability, to deal with the vertical in-homogeneity of the planetary boundary layer, extraordinary treatment of surface releases and irregular shaped area sources.

Dispersion options include the treatment of surge terrain with the help of stack-tip downwash and a routine for processing averages when calm winds or missing meteorological data occur. This includes on-default options for suppressing the use of stack-tip downwash and to disable the data checking for non-sequential meteorological data files.

Aermod can handle multiple emission sources, including point, volume and area sources. Line sources may also be modeled as a string of volume sources or as elongated area sources. Several source groups may be specified in a single run with the source contributions combined for each group. The model contains algorithms for modeling the effects of aerodynamic downwash due to nearby buildings on point source emissions. Source emission rates treated constant throughout the modeling period or may be varied by month, season, hour-of-day, or other periods of variation. These variable emission rate factors may be specified for a single source or for a multiple sources.

Aermod is designed to handle all types of terrain, flat or complex. Rather than to provide a separate file of terrain data for complex terrain applications, modeling of receptor in elevated or complex terrain requires solid information for surrounding terrain. Aermod includes a height scale and base elevation for each receptor in the run stream file. The terrain preprocessor, Aermap has considerable flexibility in the specification of receptor locations. It is developed to obtain the base elevation and height scale for a receptor. The receptors are specified in a manner identical to the Aermod dispersion model. Aermap allows the users to specify discrete receptors as well as Cartesian and Polar grid networks.

Aermet is the meteorological preprocessor that serves to organise and processes the meteorological data to estimates the necessary boundary layer parameters for dispersion calculations in Aermod. Aermet runs in a three-stage process and operates on three types of data National Weather Service (NWS) hourly surface observations, NWS twice - daily upper air soundings, and data collected from an on-site measurement program. In the present work meteorological data are obtained for spatially resolved for cast model (MM5 prognostic model).

The first stage extracts data and then assesses data quality. The second stage combines the available data for 24-hr periods and writes these data to an intermediate file. The third and final stage reads the merged data file and develops the necessary boundary layer parameters for

dispersion calculations by Aermid. These parameters are developed as two separate files - file of surface boundary layer parameters and a file of profile variables including wind speed, direction, and turbulence parameters.

Aermid shows computed outputs mainly in form of top values, which are recorded by receptor for each averaging period and source group combination, and overall maximum value for each averaging period and source group combination.

### **4.13 Advantages of Aermid Over ISCST3**

Aermid model has edges over ISCST3 as it is applicable to rural and urban areas, flat and complex terrain, surface and elevated releases with multiple sources (including, point, area and volume sources), where as ISCST3 is applicable for urban option either on or off with no other specification available. Moreover Aermid provides variable urban treatment as a function of city population and can selectively model sources as rural or urban. ISCST3 is one level data accepted model for Aermid any arbitrary large number of data level can be accumulated.

One of the major improvements that Aermid has over other dispersion models is the ability to differentiate the PBL (pressure boundary layer) with both surface and mixed layer scaling. It constructs vertical profiles of required meteorological variables based on measurements and extrapolations of those measurements using similarity (scaling) relationships. Vertical profiles of wind speed, wind direction, turbulence, temperature and temperature gradient are estimated using all available meteorological observations. Aermid captures the effect of flow above and below the dividing streamline by weighting the plume concentration associated with two possible extreme states of the boundary layer (horizontal plume and terrain-following).

ISCST3 can only work with Gaussian treatment in horizontal and in vertical for stable conditions; but Aermid can work with non-Gaussian probability density function in vertical for unstable conditions. Aermid's unstable treatment of vertical dispersion is a more accurate portrayal of actual conditions.



## 4.14 Applications of Aermom

Aermom is extensive performance evaluation designed software. On the contractor to ISCST3, Aermom contains new and improved algorithms. Aermom can estimate the concentrations in comparisons with a variety of independent databases and to assess the adequacy of the model for the use in regulatory decision-making, following points are discussed.

- i. Handle dispersion in both the convective and stable boundary layers.
- ii. Plume rise and buoyancy that can penetrate into elevated inversions.
- iii. Could deal with the treatment of elevated, near-surface, and surface level sources.
- iv. Computation of vertical profiles of wind, turbulence, and temperature easily achievable.
- v. Treatment of receptors on all types of terrain from the surface up to and above the plume height, (i.e., simple, intermediate, and complex terrain).

## 4.15 Selection of Dispersion Model

Selection of an appropriate model is the key element in assessing the scale of impact and complexity of particular emissions. The choice of models for different complexities is shown in Figure 4.4. The major factors affecting on the calculations and selection of dispersion models are:

- i. Emissions parameters e.g. as source location, source height, stack diameter, gas exit velocity, gas exit temperature and emission rate should be under reflection.
- ii. Terrain characteristics.
- iii. Dispersion models uses meteorological conditions, such as wind speed, wind direction, stability class, temperature and mixing height.
- iv. Building parameters, such as location, height and width need attention.

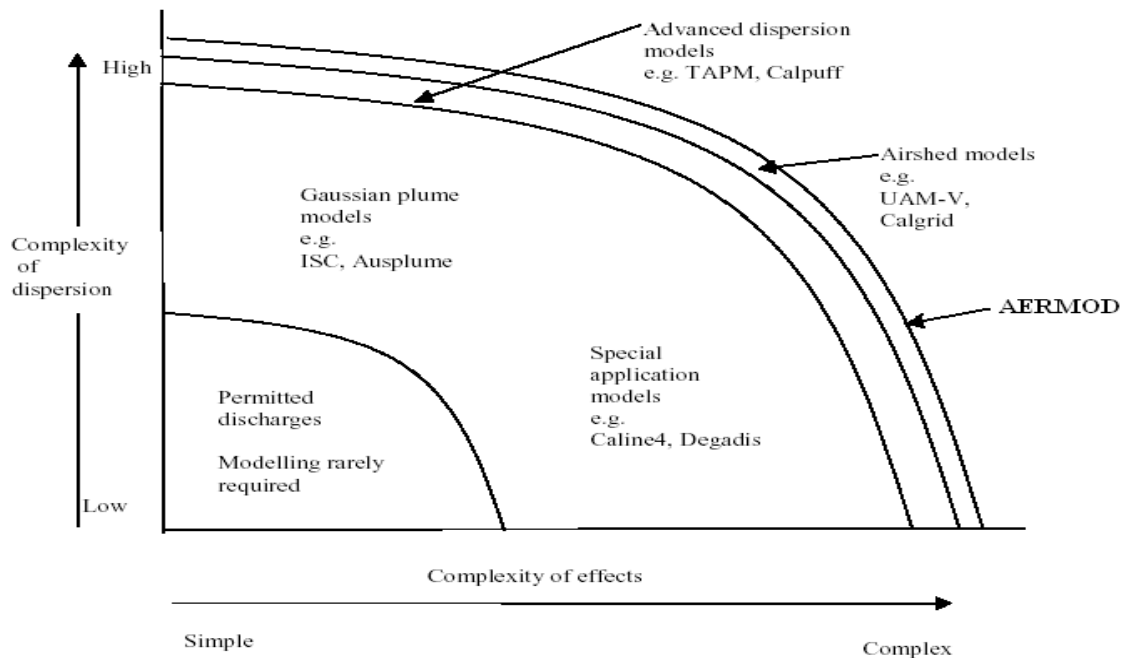


Fig. 4.4: Type of model applied according to the complexity of the problem (US EPA approved Good Practice Guide for Atmospheric Dispersion Modeling)

## 4.16 Meteorological Data Sensitivity

Ground-level concentrations of contaminants are primarily controlled by meteorological elements i.e. wind direction, speed (for transport), turbulence and mixing height of the lower boundary layer (for dispersion). Meteorological data are one of the most important inputs into air dispersion model. The meteorological data is processed in Aermet to generate.

- i. Boundary layer structure.
- ii. Atmospheric turbulence.
- iii. Modeling domain topography.
- iv. Meso-scale meteorology (air-pollution meteorology).

Table 4.1: Comparison of dispersion model features: Aermom vs. ISCST3  
(US EPA approved Good Practice Guide for Atmospheric Dispersion Modeling)

<b>Feature</b>	<b>ISCST3</b>	<b>Aermom</b>	<b>Comments</b>
Types of sources modeled	Point, area, and volume sources	Same as ISCST3	Models are comparable
Meteorological Data Input	One level of data accepted	An arbitrarily large number of data levels can be accommodated	Aermom can adapt multiple levels data to various stack and plume heights
Plume Dispersion: General Treatment	Gaussian treatment in horizontal and vertical	Gaussian treatment in horizontal and vertical for stable conditions; non-Gaussian probability density function in vertical for unstable conditions	Aermom's unstable treatment of vertical dispersion is a more accurate portrayal of actual conditions
Urban Treatment	Urban option either on or off; no other specification available; all sources must be modeled either rural or urban	Population is specified, so treatment can consider a variety of urban conditions; sources can individually be modeled rural or urban	Aermom provides variable urban treatment as a function of city population, and can selectively model sources as rural or urban
Characterization of Modeling Domain surface Characteristics	Choice of rural or urban	Selection by direction and month of roughness length, albedo, and Bowen ratio, providing user flexibility to vary surface characteristics	Aermom provides the user with considerably more options in the selection of the surface characteristics
Boundary Layer Parameters	Wind speed, mixing height, and stability class	Friction velocity, Monin-Obukhov length, convective velocity scale, mechanical and convective mixing height, sensible heat flux	Aermom provides parameters required for use with up-to-date planetary boundary layer (PBL) parameters; while ISCST3 does not
Mixed Layer Height	Holzworth scheme; uses interpolation based upon maximum afternoon mixing height	Has convective and mechanical mixed layer height; convective height based upon hourly accumulation of sensible heat flux	Aermom's formulation is significantly more advanced than that of ISCST3, includes a mechanical component, and using hourly input data, which provide a more realistic sequence of the diurnal mixing height changes

**CHAPTER FIVE**  
**EMISSION INVENTORIES**

## 5.1 Introduction

In this work emission inventories from FCC unit in an oil refinery are calculated. Mainly both SO<sub>2</sub> and particulate matters (PM) have been evaluated accurately for years 2008 and 2009 independently, considering seasonal variations in the operational conditions of the FCC unit in a refinery.

Hot feedstock is charged into the reactor through the riser where, it comes in contact with hot regenerated catalyst from the regenerator. The feedstock vapourises at a temperature of 730 °C and catalytically cracked in the reactor. The velocity of the vapor drops in the reactor, due to expansion from riser to the main reactor. The reaction takes place in fluidised bed reactor with uniform temperature. Products with the catalyst pass through a set of cyclones to separate the catalyst fines from the products. The spent catalyst from cyclones is returned to the reactor. The coke and sulphur impregnated catalyst is then sent to the regenerator to restore its activity. Excess air is fed to the regenerator for complete combustion of coke and sulphur in a fluidised process producing flue gas. The flue gas passes through cyclone to recover catalyst particles. Catalyst attrition takes place; producing fines. These fines are discharged with the exit gas. Flue gas consists of SO<sub>2</sub>, CO<sub>2</sub>, N<sub>2</sub>, O<sub>2</sub> and fines. The activated catalyst at 730 °C is recharged to the reactor and makeup stream is added to compensate the catalyst loss in the flue gas. The products are sent to the fractionator for further separation.

## 5.2 Material Balance

To evaluate each stream in FCC unit, overall material balance is established in mass flow rate (T/hr), Figure 5.1.

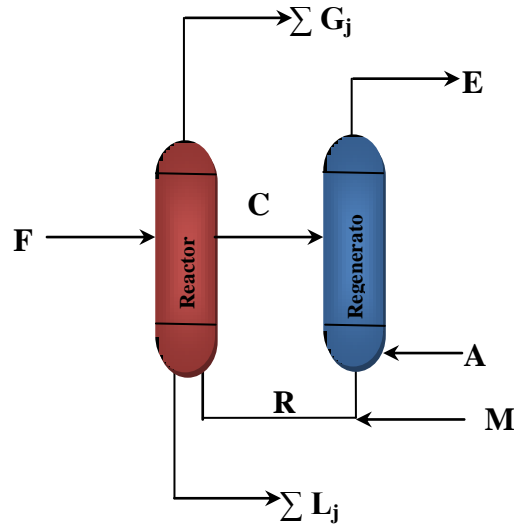


Fig. 5.1: Overall material balance around reactor and regenerator

$$F + M + A = L + G + E \quad (5.1)$$

Where:

F is the total feed consisting of heavy ends from various refining units M is makeup catalyst stream

A is the air supplied to the regenerator

G is a mixture of gaseous products (LPG and Off gas)

L is liquid products

E is the flue gas consisting of CO<sub>2</sub>, N<sub>2</sub>, SO<sub>2</sub>, O<sub>2</sub> and particulate matters (PM).

To calculate the emissions, material balance of the  $i^{\text{th}}$  component around the FCCU is considered:

For sulphur balance  $i = 1$ :

$$F \times x_{F1} = \sum (L_j \times x_{1j}) + \sum (G_j \times y_{1j}) + E \times y_{E1} \quad (5.2)$$

For PM balance  $i = 2$ :

$$M = L_j \times x_{2j} + E \times y_{E2} \quad (5.3)$$

The operational data for 24<sup>th</sup> of March 2008 are given as total feed equal to 255.1 t/hr, with sulphur composition ( $x_{F1}$ ) equal to 0.008. Total liquid and gaseous products are 173.6 and 62.3 t/hr respectively. Air fed to the regenerator is calculated based on complete combustion of all coke and sulphur to produce  $\text{SO}_2$  and  $\text{CO}_2$  with 10% excess and is equal to 233. T/hr. Total emission is calculated using equation (1) with known amount of catalyst makeup stream 0.1 t/hr.

$$E = 255.1 + 0.1 + 233.04 - 173.6 - 62.3 = 252.4 \text{ t/hr} \quad (5.4)$$

Sulphur in flue gas, E (252.4 t/hr) is calculated using equation (5.2)

$$E y_{E1} = (255.1 \times 0.008) - 0.614 - 0.204 = 1.2 \text{ t/hr.} \quad (5.5)$$

$$\text{SO}_2 \text{ emission is equal to } = 1.2 \frac{64}{32} = 2.4 \text{ t/hr}$$

Particulate Matter (PM) in flue gas, E (252.4 t/hr) is calculated using equation (5.3)

$$E y_{E2} = 0.1042 - 0.0007 = 0.1035 \text{ t/hr} \quad (5.6)$$

### 5.3 Emission Inventories for Year 2008

SO<sub>2</sub> and PM emissions inventories during the period from December 2007 to November 2008 are calculated for four different seasons. Kuwait is located in the north east of Arabian Peninsula and has four seasons, starting winter season from December till end of February, followed by spring season from March to May. Summer season starts from June till August, followed by autumn season from September to November. Figure 5.2 shows a regional map Kuwait and Figure 5.3 illustrates the seasonal temperature variation for the year 2008. In winter season, hourly minimum temperature is 6 °C recorded on 10<sup>th</sup> of January at 00:00 hour and the hourly maximum temperature is 26.5 °C on 20 February at 12:00 hour. The average seasonal temperature in winter is 16 °C. The hourly minimum temperature for spring season is 14.5 °C measured on 3<sup>rd</sup> of March at 6:00 hour and the hourly maximum temperature measured is 43 °C on 22<sup>nd</sup> of May at 10:00 hour. The average seasonal temperature in spring is 25 °C. In the summer season, hourly minimum temperature is 32 °C observed on 4<sup>th</sup> of August at 3:00 hour and the hourly maximum observed in the same season is 48 °C on 7<sup>th</sup> of August at 14:00 hour. The average seasonal temperature in summer is 40 °C. The hourly minimum temperature recorded in autumn season is 9 °C on 24<sup>th</sup> of November at 6:00 hour and the hourly maximum temperature recorded is 35.5 °C on 14<sup>th</sup> of October at 12:00 hour. The average seasonal temperature in the autumn is 28 °C.



Fig. 5.2: Regional map of Kuwait



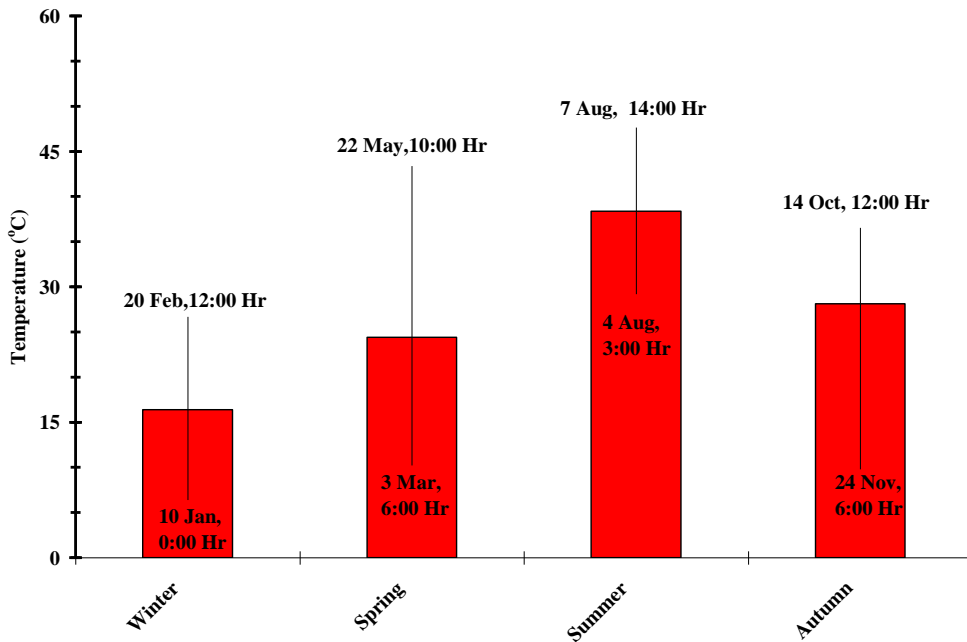


Fig. 5.3: Hourly maximum, minimum and seasonal average temperatures in Kuwait

Figures 5.4 to 5.7 show all the emission variation of SO<sub>2</sub> for different seasons respectively.

In winter season, the emission rates are evaluated from operational data for 11 weeks and the maximum value is 530 g/s on 2<sup>nd</sup> of December 2007 and the minimum value is 376 g/s on 9<sup>th</sup> of December 2007. The emission rate for the entire period is  $480 \pm 2\sigma$  g/s, where standard deviation is equal to 46 g/s. SO<sub>2</sub> emissions rates for spring season are observed providing maximum value of 680 g/s on 24<sup>th</sup> of March 2008, which is higher than the winter maximum emission rate. The minimum calculated value is 356 g/s on 26<sup>th</sup> of May 2008, which is lower than the winter minimum value. The emission rate for 13 weeks is  $600 \pm 2\sigma$  g/s, where standard deviation is equal to 90 g/s. The maximum value for SO<sub>2</sub> emissions rates is found to be 654 g/s on 2<sup>nd</sup> of June 2008, which is lower than the spring maximum value but higher than the winter maximum value. For the summer season, the minimum emission rate is 404 g/s same on 7<sup>th</sup> of July and 21<sup>st</sup> of August 2008, which is higher than both winter and spring minimum values. For summer season the emission rate calculated for 11 weeks is  $458 \pm 2\sigma$  g/s, where standard deviation is equal to 77 g/s. SO<sub>2</sub> emissions rates for autumn season are evaluated for 12 weeks. The maximum value is 653 g/s on 23<sup>rd</sup> of September 2008, which is almost similar to maximum value during spring

season. The minimum computed value is 357 g/s on 5<sup>th</sup> of October 2008 which is similar to the minimum value of spring season. The emission rate for whole autumn period is  $540 \pm 2\sigma$  g/s, where standard deviation is equal to 91 g/s.

In winter season emission rates are consistent with minimum fluctuation, while in spring season the emission rates are high in the beginning of the season then decreasing gradually. Whereas in summer season the emission rates are high at the start of the season and later become almost constant. Finally variation in emission rates is lower in beginning of the autumn season then increased. The highest and the lowest emission rates in all seasons reflect the operational conditions, mainly sulphur contents in the feedstock and the total amount of heavy ends charged to the FCCU.

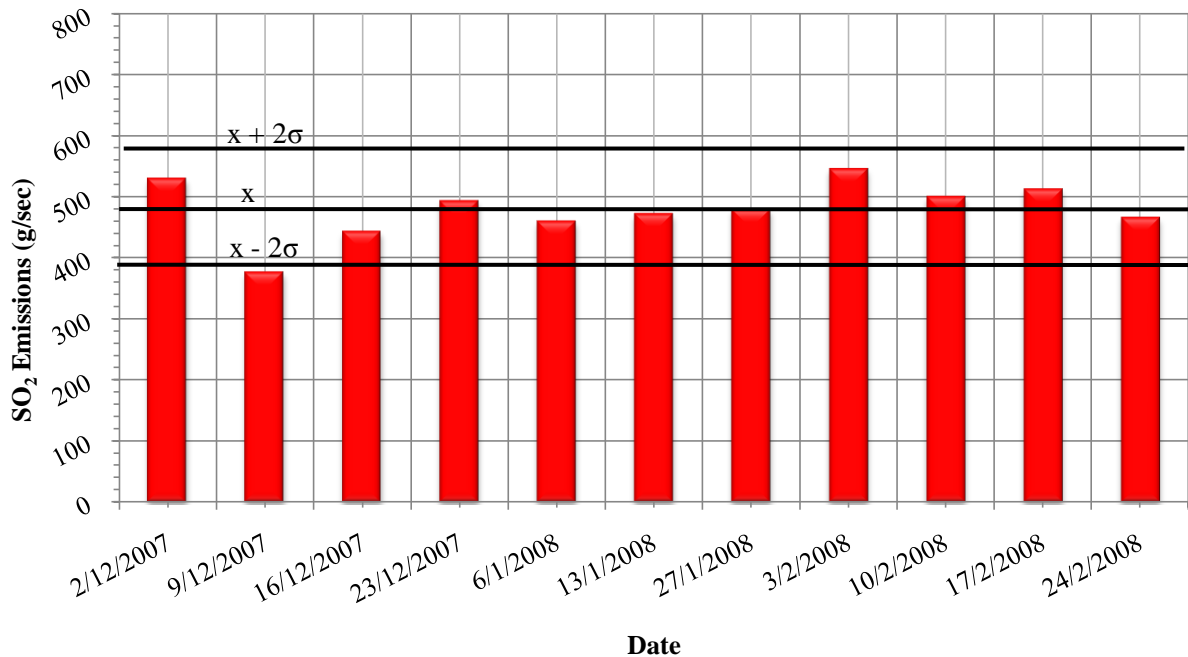


Fig. 5.4: SO<sub>2</sub> emissions rates (g/s) for winter season for year 2008

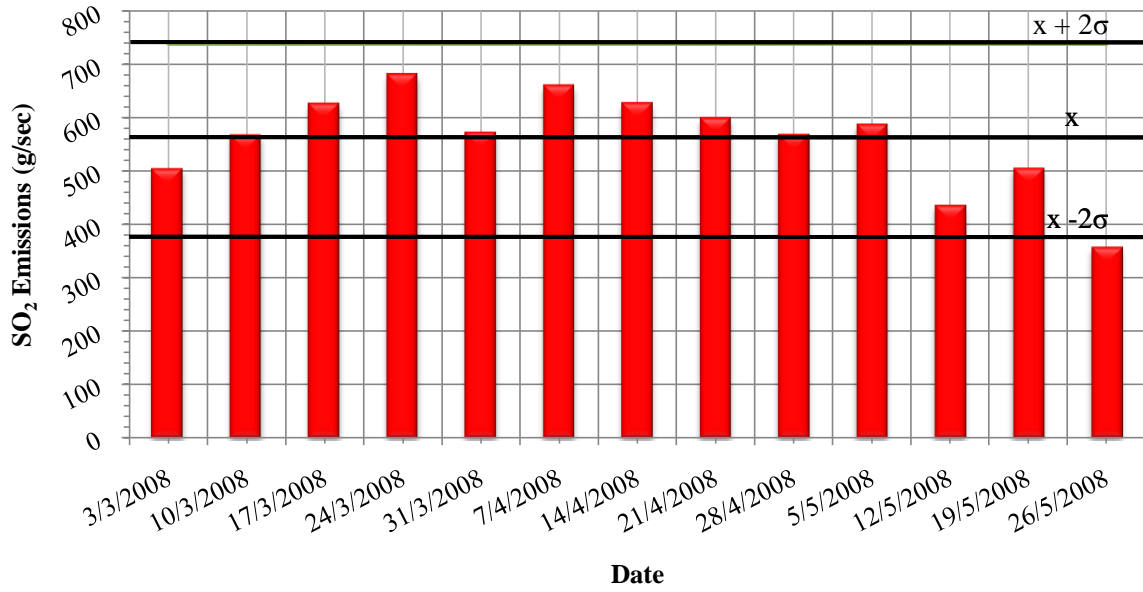


Fig. 5.5: SO<sub>2</sub> emissions rates (g/s) for spring season for year 2008

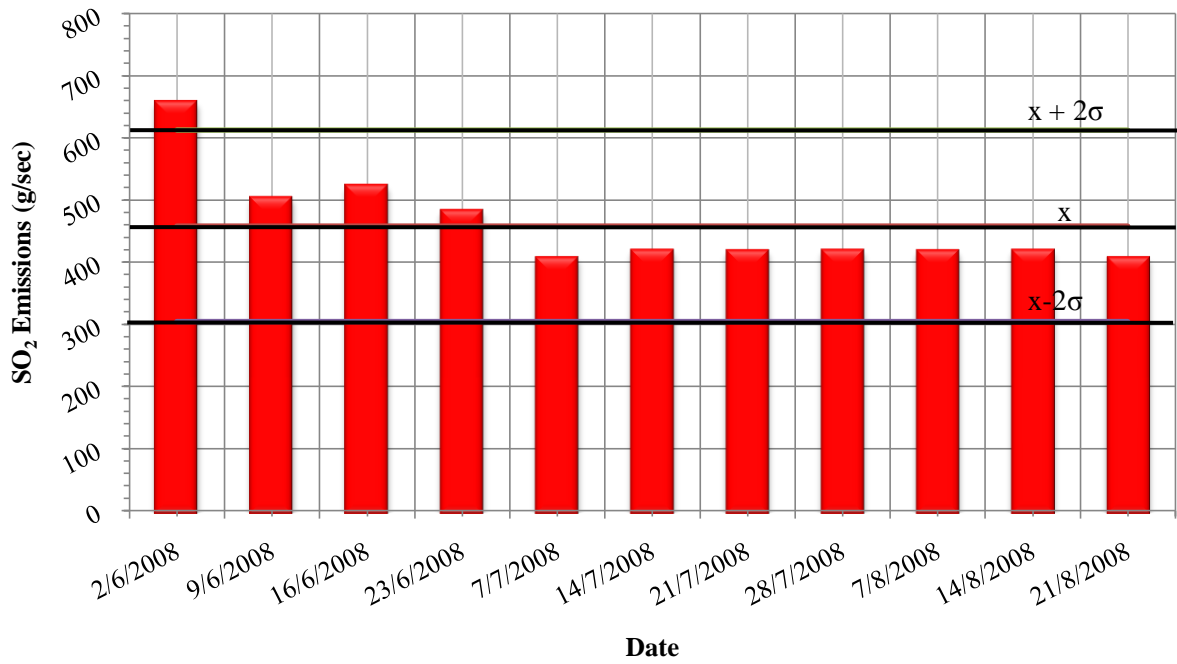


Fig. 5.6: SO<sub>2</sub> emissions rates (g/s) for summer season for year 2008

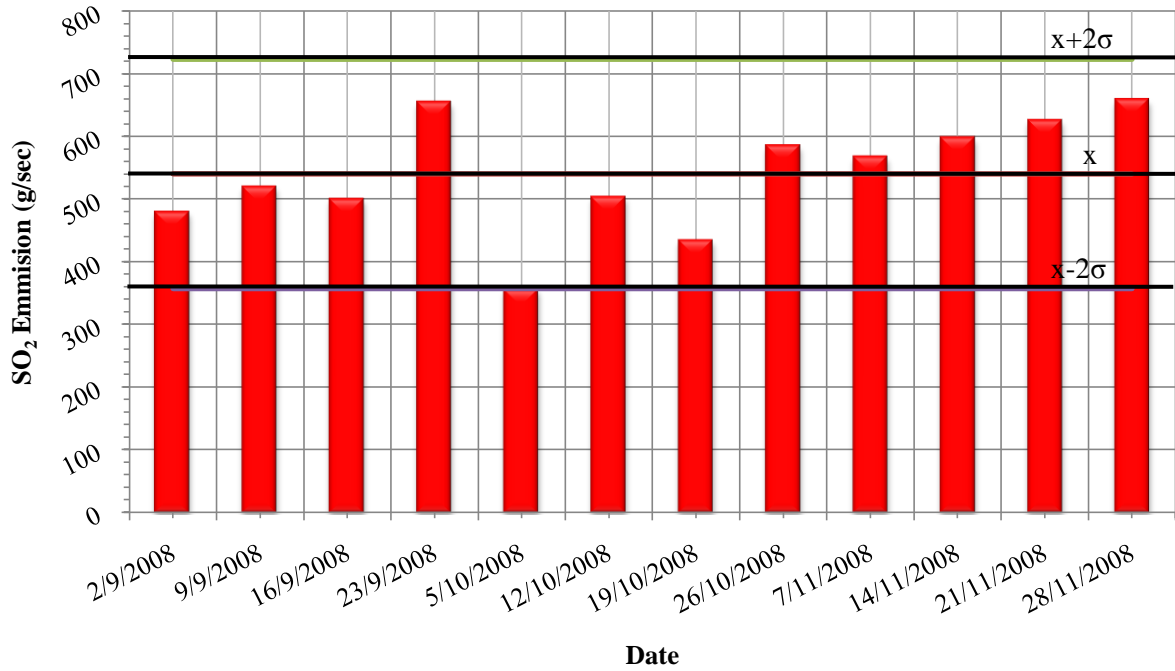


Fig. 5.7: SO<sub>2</sub> emissions rates (g/s) for autumn season for year 2008

Similarly the PM emissions related to the process operating conditions. Figures 5.8 to 5.11 show the behavior of PM emissions during different seasons. The maximum value is 40 g/s on 13<sup>th</sup> of January 2008 and the minimum value is 23 g/s on 23<sup>rd</sup> of December 2007 for winter season. The emission rate in this season is  $27 \pm 2\sigma$  g/s where standard deviation is 6 g/s. Similarly PM emission rates for spring season are calculated providing maximum value of 28 g/s on 17<sup>th</sup> of March 2008, which is lower than winter maximum value. The minimum value is 24 g/s on two occasions, 12<sup>th</sup> and 26<sup>th</sup> of May 2008. The emission rate for 13 weeks is  $25 \pm 2\sigma$  g/s, where standard deviation is equal to 2 g/s. The minimum calculated values for both winter and spring seasons are almost similar. For summer season the maximum value for PM emissions rates is 26 g/s on three consecutive occasions, 2<sup>nd</sup>, 9<sup>th</sup>, and 16<sup>th</sup> of June 2008. Whereas the minimum computed value is 18 g/s on 14<sup>th</sup> of July and 14<sup>th</sup> of August 2008. The emission rate calculated for 11 weeks is  $21 \pm 2\sigma$  g/s, where standard deviation is equal to 3 g/s. Finally PM emissions rates for autumn season are evaluated for 12 weeks. The maximum value found to be 27 g/s on three consecutive occasions, 09<sup>th</sup>, 16<sup>th</sup> and 23<sup>rd</sup> September 2008. While the minimum computed value is 24 g/s on 5<sup>th</sup> and 19<sup>th</sup> of October 2008. The emission rate for whole autumn period is  $25 \pm 2\sigma$  g/s, where standard deviation is equal to 1 g/s. The highest PM maximum value is in the winter

season and the lowest value is in the summer season, while minimum emission rate is similar to the maximum emission values, high in winter and low summer seasons.

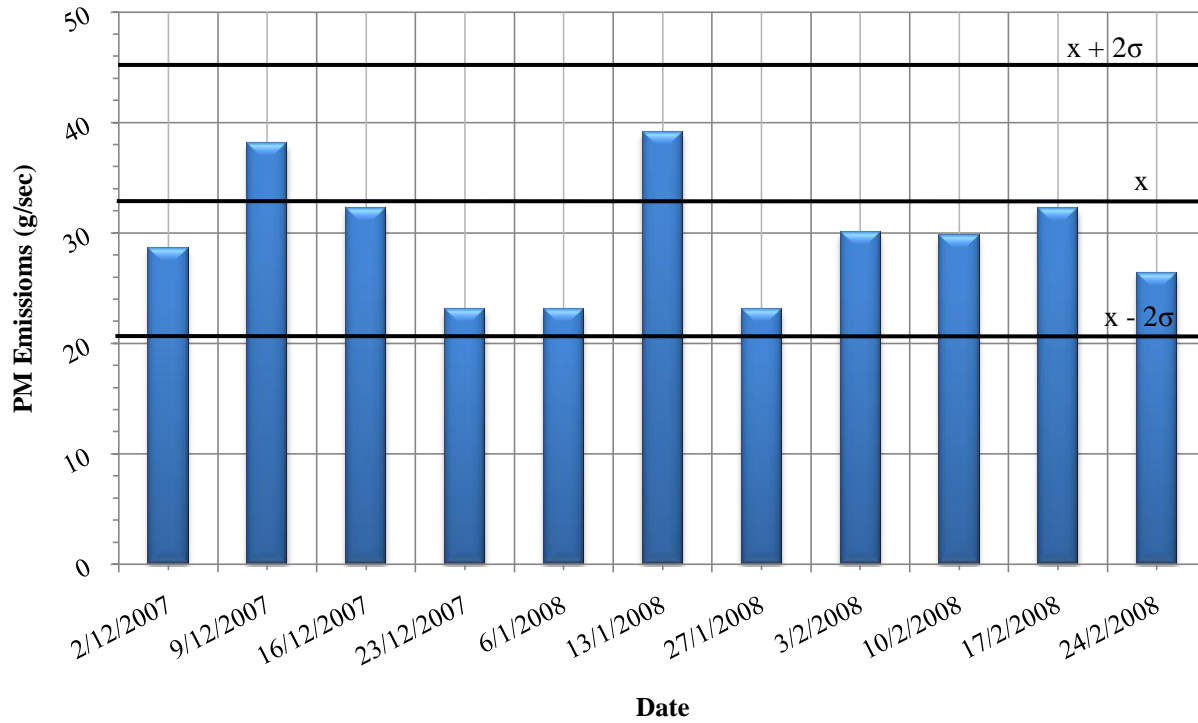


Fig. 5.8: Particulate Matter (PM) emissions rates (g/s) for winter season for year 2008

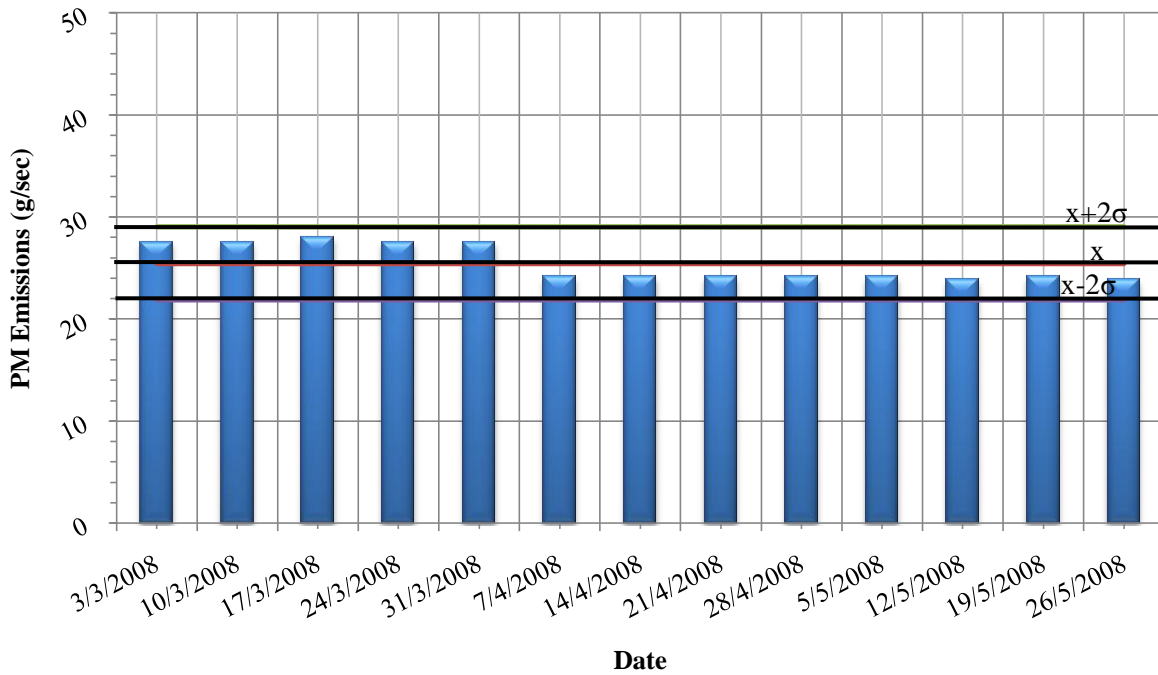


Fig. 5.9: Particulate Matter (PM) emissions rates (g/s) for spring season for year 2008

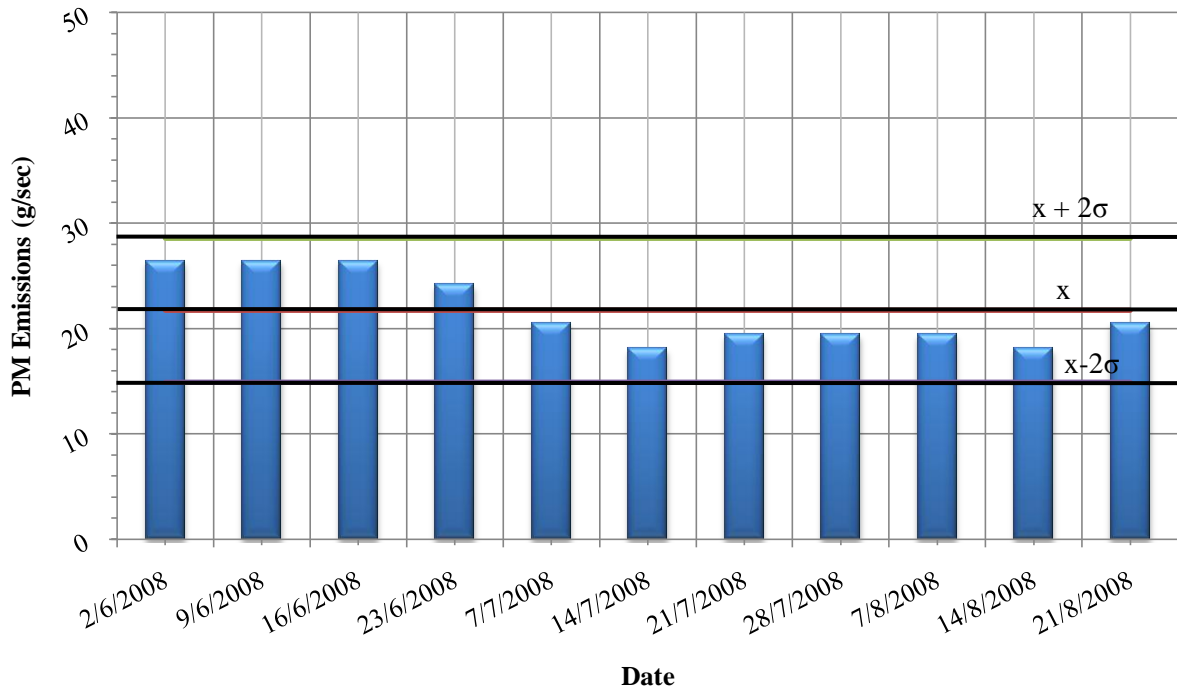


Fig. 5.10: Particulate Matter (PM) emissions rates (g/s) for summer season for year 2008

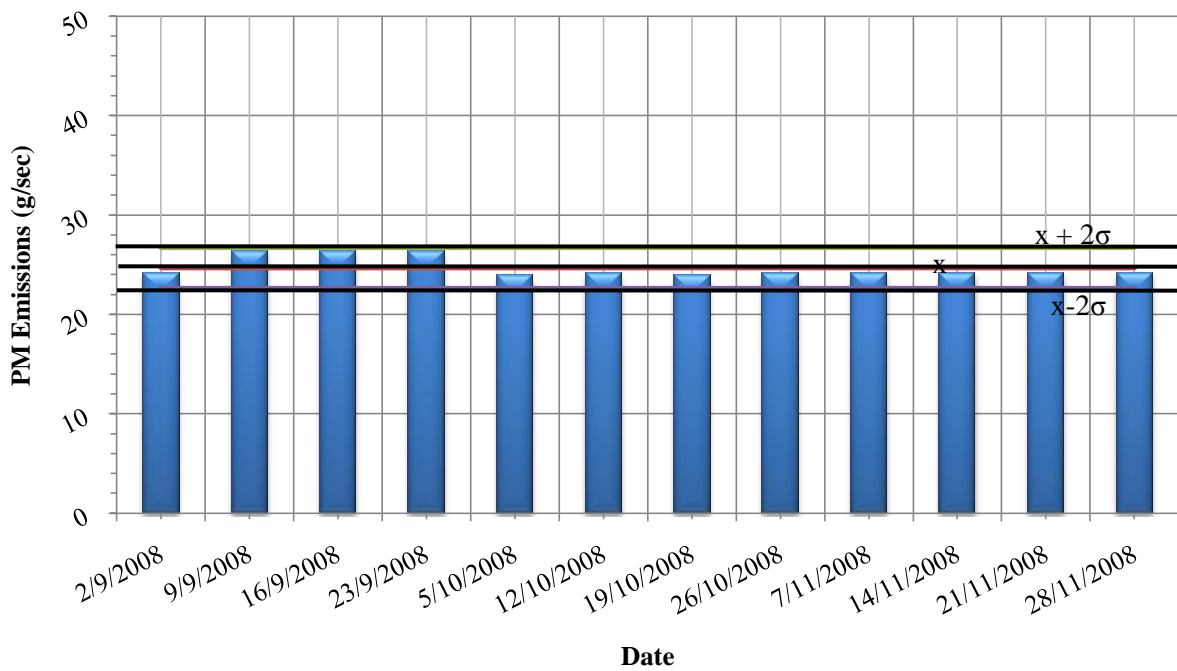


Fig. 5.11: Particulate Matter (PM) emissions rates (g/s) for autumn season for year 2008

## 5.4 Emission Inventories for Year 2009

Emission inventories for year 2009 for SO<sub>2</sub> and PM are prepared as the refinery increased the production rate of FCC unit due to the high local and international demands, mainly for energy production.

Figures 5.12 to 5.15 show all the emission variation of SO<sub>2</sub> for different seasons respectively.

In winter season, the emission rates are calculated from operational data for 11 weeks and the highest value of SO<sub>2</sub> is equal to 611 g/s on 3<sup>rd</sup> of February 2009 and the lowest value is 422 g/s on 9<sup>th</sup> of December 2008. The emission rate for the entire period is  $534 \pm 2\sigma$  g/s, where standard deviation is equal to 52 g/s. SO<sub>2</sub> emissions rates for spring season are computed providing highest value of 747 g/s of SO<sub>2</sub> on 24<sup>th</sup> of March 2009, which is higher than the winter maximum emission rate. The lowest calculated value is 392 g/s on 26<sup>th</sup> of May 2009, which is lower than the winter minimum value. The emission rate for 13 weeks is  $619 \pm 2\sigma$  g/s, where standard deviation is equal to 102. g/s. The maximum value for SO<sub>2</sub> emissions rates for the summer season is found to be 733 g/s on 2<sup>nd</sup> of June 2009, which is lower than the spring maximum value but higher than the winter maximum value. The minimum emission rate for the same season is equal to 444 g/s, observed on 7<sup>th</sup> of July, which is higher than both winter and spring minimum values. For summer season, the emission rate calculated for 11 weeks is  $510 \pm 2\sigma$  g/s, where standard deviation is equal to 88 g/s. SO<sub>2</sub> emissions rates for autumn season are evaluated for 12 weeks. The highest value of SO<sub>2</sub> is 724 g/s on 28<sup>th</sup> of November 2009. The minimum computed value is 400 g/s on 5<sup>th</sup> of October 2009, which is almost similar to the minimum value of spring season. The emission rate for the entire autumn period is  $597 \pm 2\sigma$  g/s, where standard deviation is equal to 98 g/s.

In winter season emission rates are consistent with minimum fluctuation, while in spring season the emission rates are high in the beginning of the season then decreasing gradually. Whereas in summer season the emission rates are high at the start of the season and later become almost constant. Finally variation in emission rates is lower in beginning of the autumn season then increased.

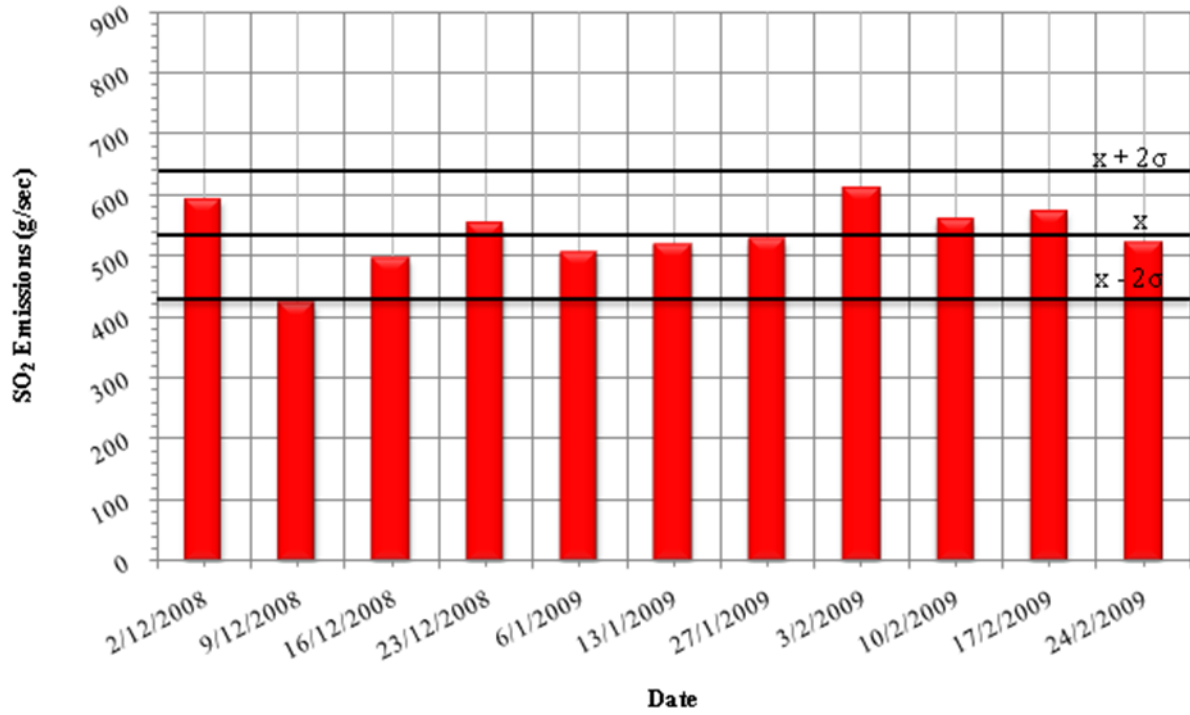


Fig. 5.12: SO<sub>2</sub> emissions rates (g/s) for winter season for year 2009

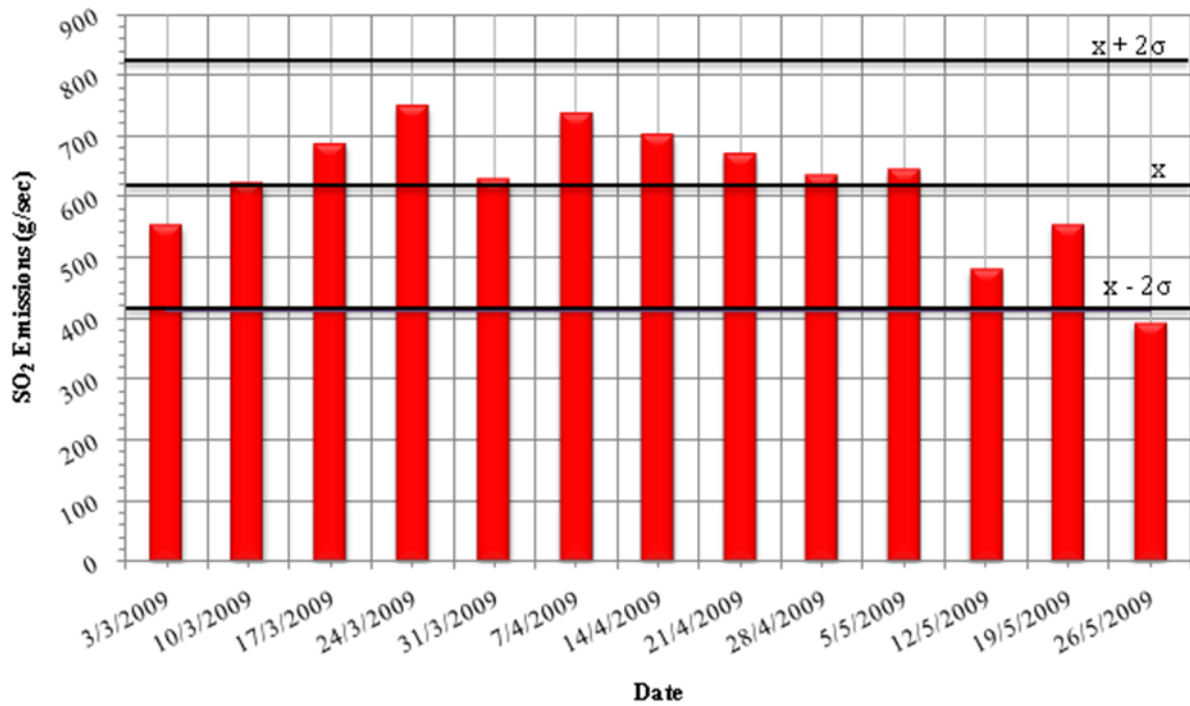


Fig. 5.13: SO<sub>2</sub> emissions rates (g/s) for spring season for year 2009



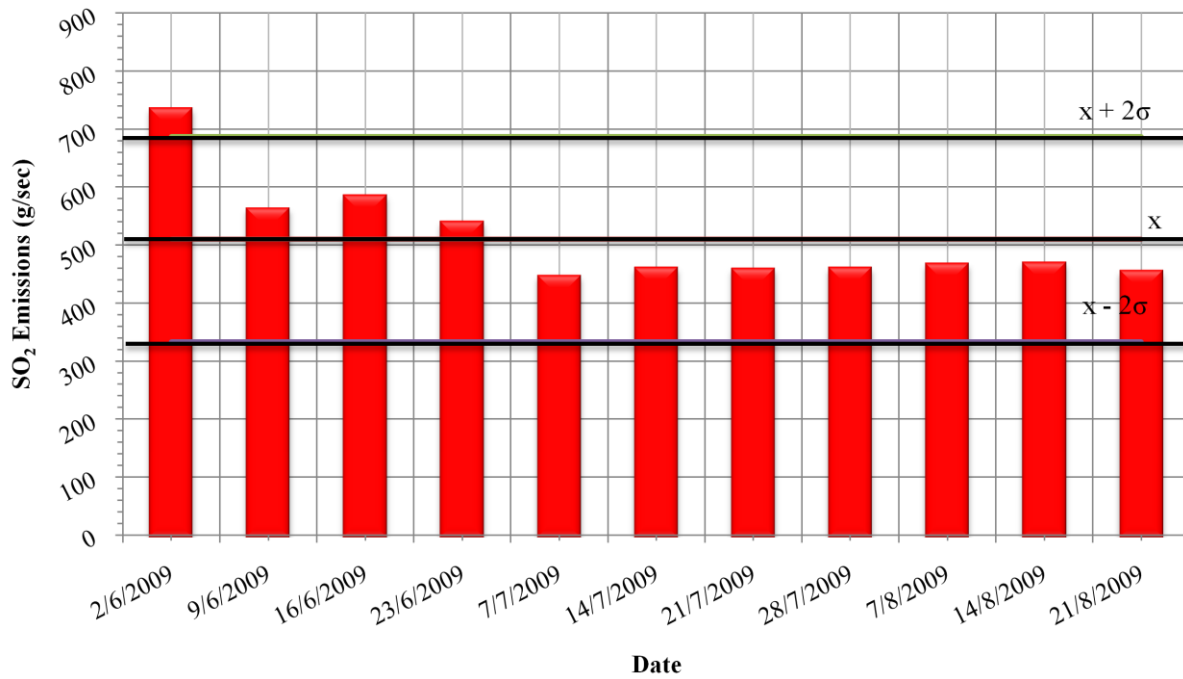


Fig. 5.14: SO<sub>2</sub> emissions rates (g/s) for summer season for year 2009

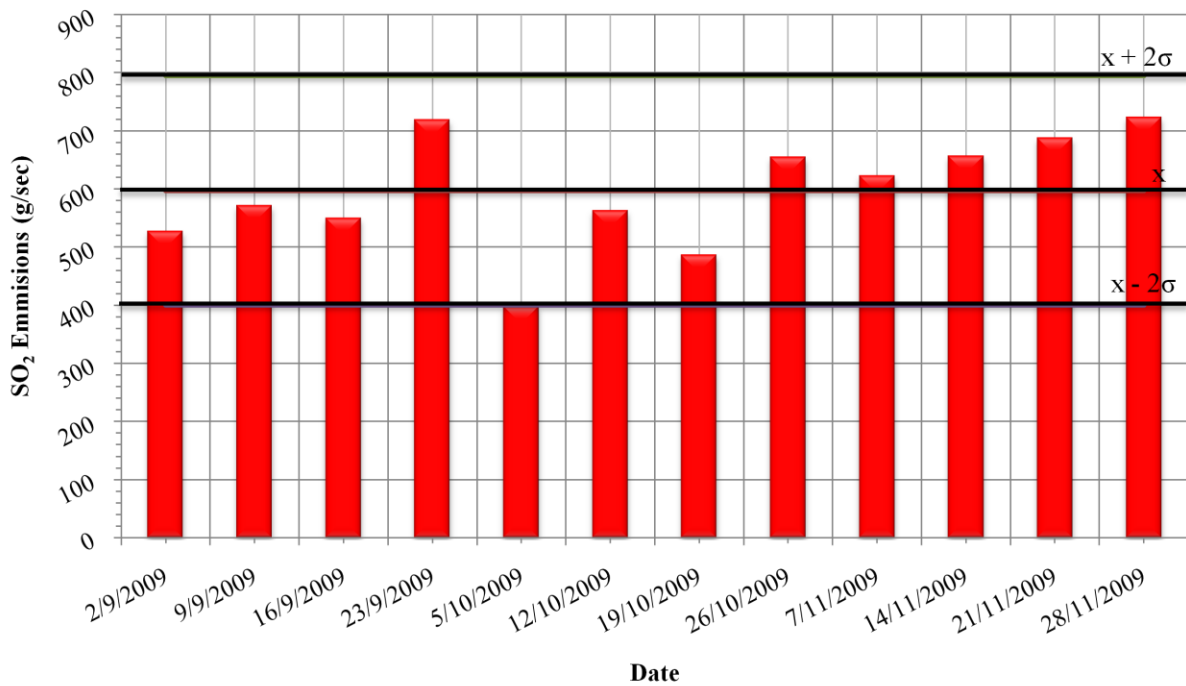


Fig. 5.15: SO<sub>2</sub> emissions rates (g/s) for autumn season for year 2009

Figures 5.16 to 5.19 show PM emission rates for all the seasons of year 2009. The highest value of PM emission rates for the winter season is equal to 43 g/s, observed on 13<sup>th</sup> of January 2009 and the lowest value is 25 g/s, observed on 6<sup>th</sup> and 27<sup>th</sup> of January 2009. The emission rate in this season is  $33 \pm 2\sigma$  g/s where standard deviation is 6 g/s. PM emission rates for spring season are calculated providing maximum value of 31 g/s on 17<sup>th</sup> of March 2009, which is lower than winter maximum value. The minimum value is 26 g/s on two occasions, 12<sup>th</sup> and 26<sup>th</sup> of May 2009. The emission rate for 13 weeks is  $28 \pm 2\sigma$  g/s, where standard deviation is equal to 2 g/s. For summer season the maximum value for PM emissions rates is 30 g/s on three consecutive occasions, 2<sup>nd</sup>, 9<sup>th</sup>, and 16<sup>th</sup> of June 2009. Whereas the minimum computed value is 20 g/s on 14<sup>th</sup> of August 2009. The emission rate calculated for 11 weeks is  $24 \pm 2\sigma$  g/s, where standard deviation is equal to 4 g/sec. PM emissions rates for autumn season are evaluated for 12 weeks. The maximum value found to be 34 g/s on 7<sup>th</sup> of November 2009, while the minimum computed value is 27 g/s on 2<sup>nd</sup> of September 2009. The emission rate for the entire autumn season is  $30 \pm 2\sigma$  g/s, where standard deviation is equal to 3 g/s. The highest PM maximum value is in the winter season and the lowest value is in the summer season, while minimum emission rate is similar to the maximum emission values, high in winter and low summer seasons.

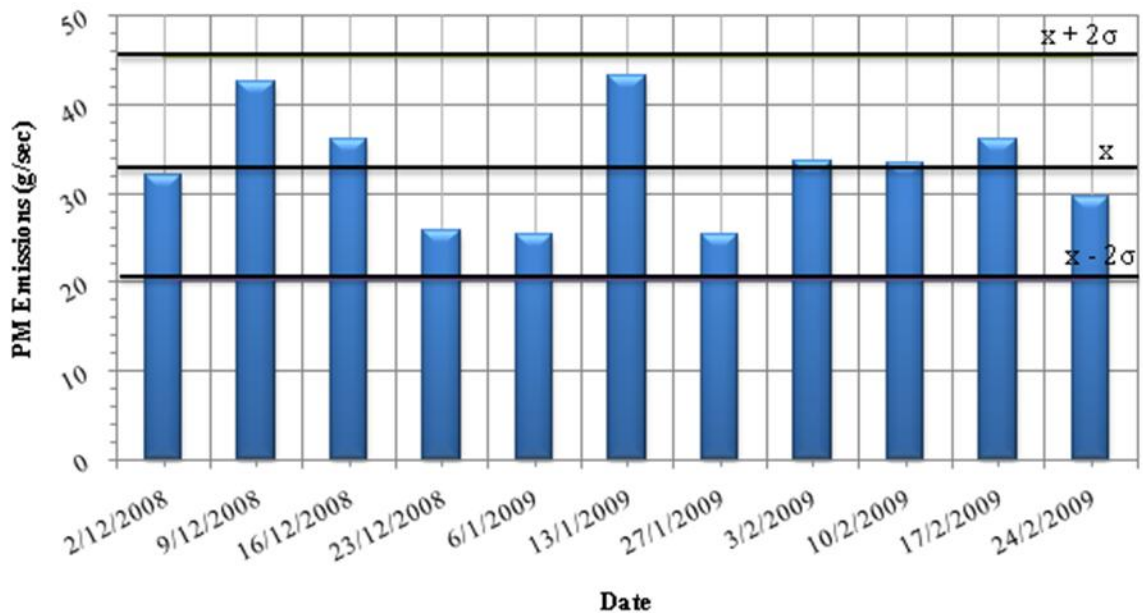


Fig. 5.16: Particulate Matter (PM) emissions rates (g/s) for winter season for year 2009

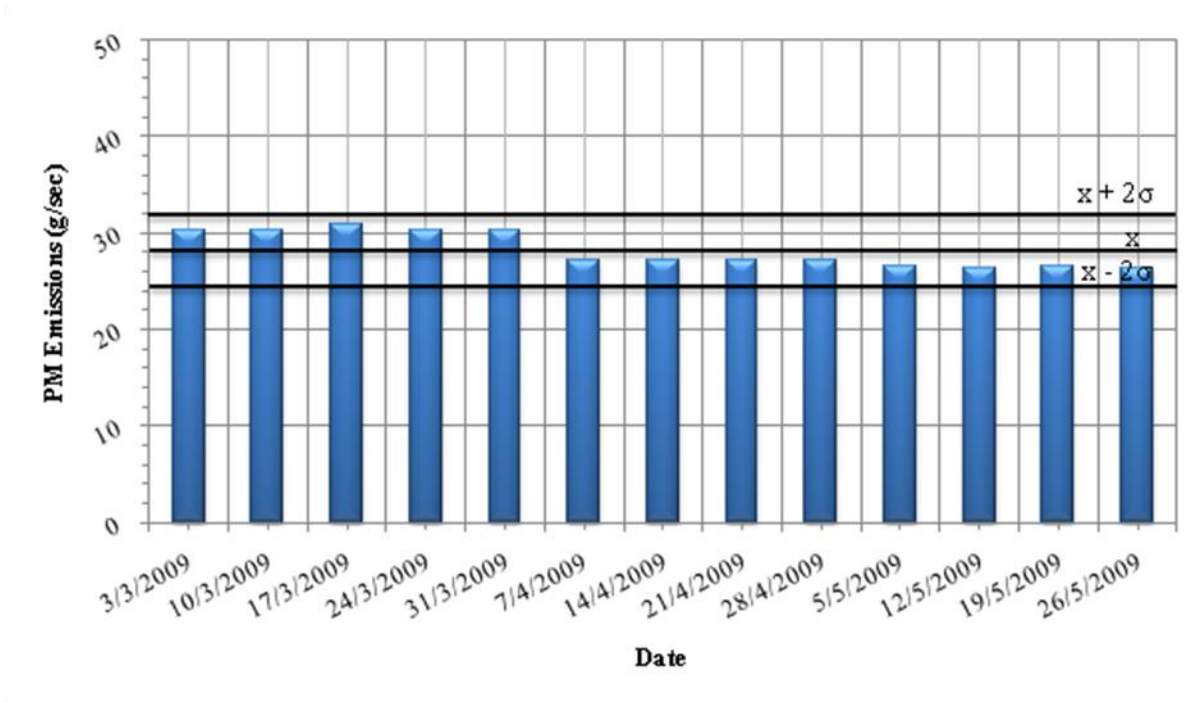


Fig. 5.17: Particulate Matter (PM) emissions rates (g/s) for spring season for year 2009

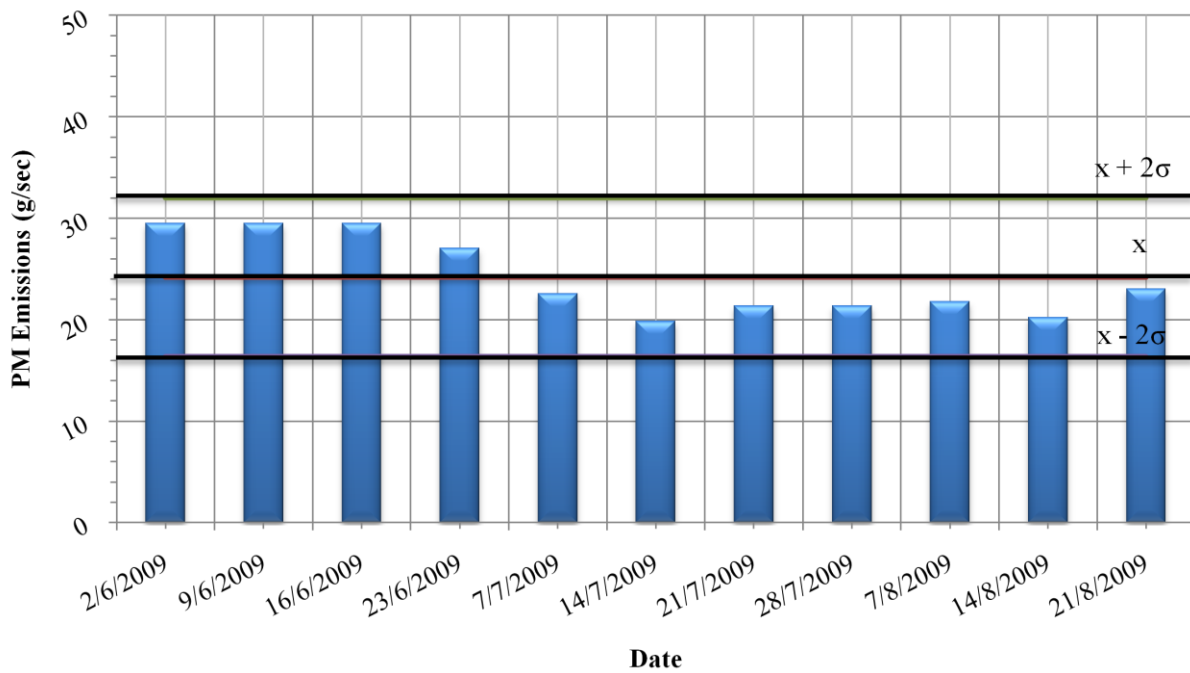


Fig. 5.18: Particulate Matter (PM) emissions rates (g/s) for summer season for year 2009

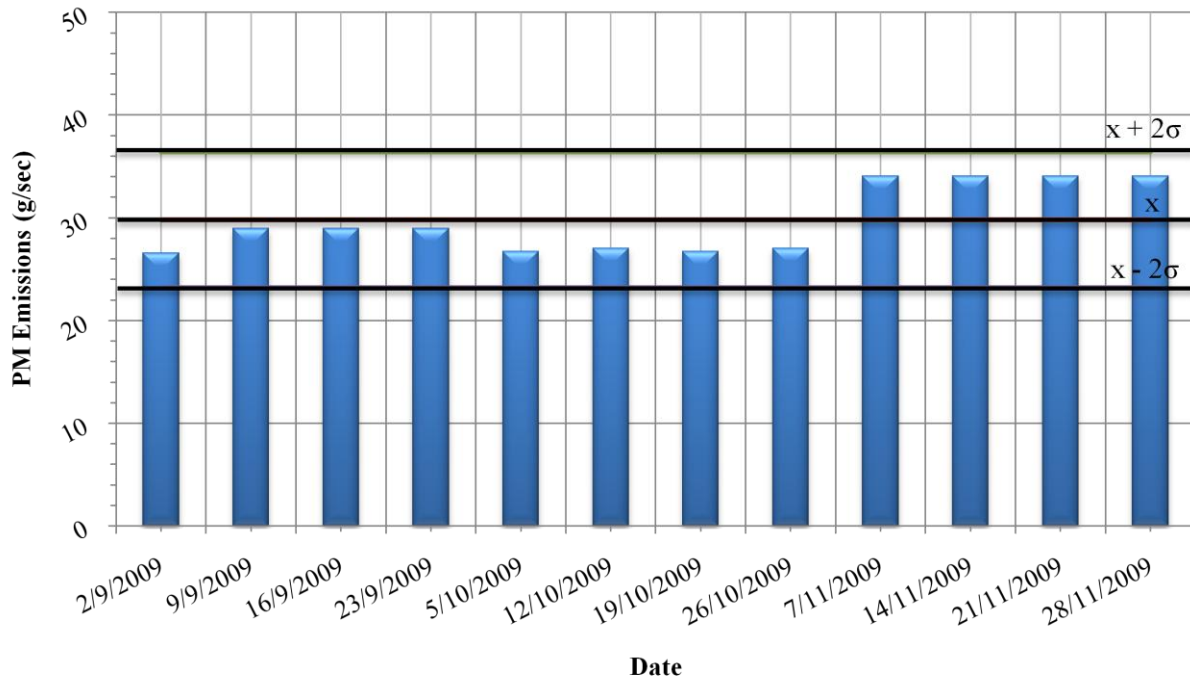


Fig. 5.19: Particulate Matter (PM) emissions rates (g/s) for autumn season for year 2009

Tables 5.1 to 5.4 show the emission factors for both pollutants for years 2008 and 2009.

Table 5.1: SO<sub>2</sub> monthly emission factors for year 2008

January	February	March	April	May	June
0.077	0.083	0.096	0.1	0.077	0.088
July	August	September	October	November	December
0.067	0.067	0.088	0.077	0.1	0.075

Table 5.2: PM monthly emission factors for year 2008

January	February	March	April	May	June
0.093	0.097	0.091	0.079	0.079	0.085
July	August	September	October	November	December
0.064	0.063	0.085	0.079	0.079	0.1

Table 5.3: SO<sub>2</sub> monthly emission factors for year 2009

<b>January</b>	<b>February</b>	<b>March</b>	<b>April</b>	<b>May</b>	<b>June</b>
0.076	0.083	0.096	0.1	0.077	0.089
<b>July</b>	<b>August</b>	<b>September</b>	<b>October</b>	<b>November</b>	<b>December</b>
0.067	0.068	0.087	0.077	0.1	0.075

Table 5.4 PM monthly emission factors for year 2009

<b>January</b>	<b>February</b>	<b>March</b>	<b>April</b>	<b>May</b>	<b>June</b>
0.093	0.098	0.09	0.08	0.078	0.086
<b>July</b>	<b>August</b>	<b>September</b>	<b>October</b>	<b>November</b>	<b>December</b>
0.063	0.064	0.084	0.08	0.079	0.1

FCC unit in a refinery is major contributor of SO<sub>2</sub> and PM emissions those are responsible for adverse impact on the immediate neighborhood of the refinery. A complete comprehensive emission inventories for years 2008 and 2009 have been prepared for both SO<sub>2</sub> and Particulate Matters. The refinery operations are not dependent on seasons but controlled by market driven conditions to maximize the profit. The seasonal impact on refinery emissions is minimal due to its operation at optimum capacity fulfilling the international and local market demand.

SO<sub>2</sub> emissions are high in spring while PM emissions are high in winter, mainly due to operational conditions that are dependent on feed rate, sulphur contents in the feed. PM emissions are mainly due to high attrition of cold makeup catalyst charge and operating conditions, vapor velocity, particle velocity, particle collision and particle degradation.

These inventories are prepared based on real operational data of FCC unit obtained from the refinery. In the year 2009, the unit is operated at its maximum capacity to fulfil the market demand, leading to higher emission rates of both pollutants.

These inventories are used in Aermol dispersion model to thoroughly investigate the impact of FCC unit emissions in the vicinity of the petroleum refinery, using five years comprehensive meteorological data of Kuwait to cover all expected meteorological events as FCC unit is operating at its maximum capacity for the coming years. In general, Kuwait meteorology does

not show significant variation and the obtained meteorological inputs will provide adequate information about the expected levels of pollution in the coming years.

**CHAPTER SIX**  
**MODEL APPLICATIONS**

## 6.1 Introduction

The application of Aermid dispersion model is more frequent than any other model for the evaluation of the ground level concentrations of the selected pollutants. The advantages associated with the use of Aermid include the calculation of the planetary boundary layer parameters through both surface and mixed layer scaling, the applicability to rural and urban areas, flat and complex terrain, surface and elevated releases with multiple sources (including, point, area and volume sources). Aermid can also construct vertical profiles of required meteorological variables based on measurements and extrapolations of those measurements using similarity (scaling) relationships. It applies Gaussian plume treatment horizontally and vertically for stable conditions and non-Gaussian probability density function for unstable conditions. Aermid provides reliable predicted concentrations if turbulent wind velocity measurements are used to estimate plume dispersion, Venkatram et al., (2004).

## 6.2 Model Input Data

Aermid dispersion model implementation requires three main input data. These are:

1. Source information input: including pollutant emission rate (g/s), location coordinates in Universal Transverse Mercator (UTM) (m), base elevation from the sea level (m), stack height (m), exit stack inner diameter (m), exit stack gas velocity (m/s), and exit stack gas temperature (K).
2. Meteorological information input: includes anemometer height (m), wind speed (m/s), wind direction (flow vector from which the wind is blowing) (in degrees clockwise from the north), ambient air temperature ( $^{\circ}\text{C}$ ), stability class at the hour of measurement (dimensionless) and hourly mixing height (m) for the region of interest (Ahmadi).
3. Receptors information input: These are uniform Cartesian grid and discrete receptors which are specified by defining an optimum mesh size and selecting critical locations respectively to compute pollutants ground level concentrations.



The entire required source input data are obtained from FCC unit in the refinery. A stack of 80 m height, an inner diameter of 2.3 m, with an average exit gas velocity of 20 m/s and exit gas temperature of 550 K are fed into the model. Monthly emission variation is considered with total SO<sub>2</sub> emission rate of 6089 g/s for year 2008, 6758 g/s for year 2009 and total PM emission rate of 302 g/s for year 2008, 336 g/s for year 2009 as presented in detail, Yateem et al., (2010).

### 6.3 Area of Study

The area of study in this work covers portion of Ahmadi governorate in the state of Kuwait. Fahaheel area is adjacent to the petroleum refinery has one of the Kuwait EPA air quality monitoring station located at a polyclinic. Both areas Fahaheel and Ahmadi are surrounded by arid desert from the west side and bordered by the Gulf from the east. Figure 6.1 shows the area of study including the refinery and its vicinity map.



Fig. 6.1: Map of the refinery and its vicinity

Two different types of receptor coordinates are used as input to the Aermol model to predict the ground level concentration of pollutants, these are:

1. Discrete Cartesian receptors specified at the sensitive areas viz., a school, a shopping area and EPA monitoring stations in Fahaheel. A hospital and petroleum services companies' offices are selected in Ahmadi.
2. Uniform Cartesian Grid receptors covering the entire area of study, where the FCC stack (emissions source) is located almost in the centre of the mesh grid.

The grid sensitivity is examined by selecting 21 x 21 up to 72 x 72 grids for prediction of ground level concentrations of pollutants for specified emission rate. Figure 6.2 shows the percentage value with respect to 72 x 72 grid, reflecting the accuracy of predicted concentrations with grids variation. The predicted concentrations are gradually decreased with selection of coarser grid. It is observed that the accuracy of the predicted values is above 99 % for 42 x 42 grid and higher. Therefore, 42 x 42 grid is selected for the rest of the computational process.

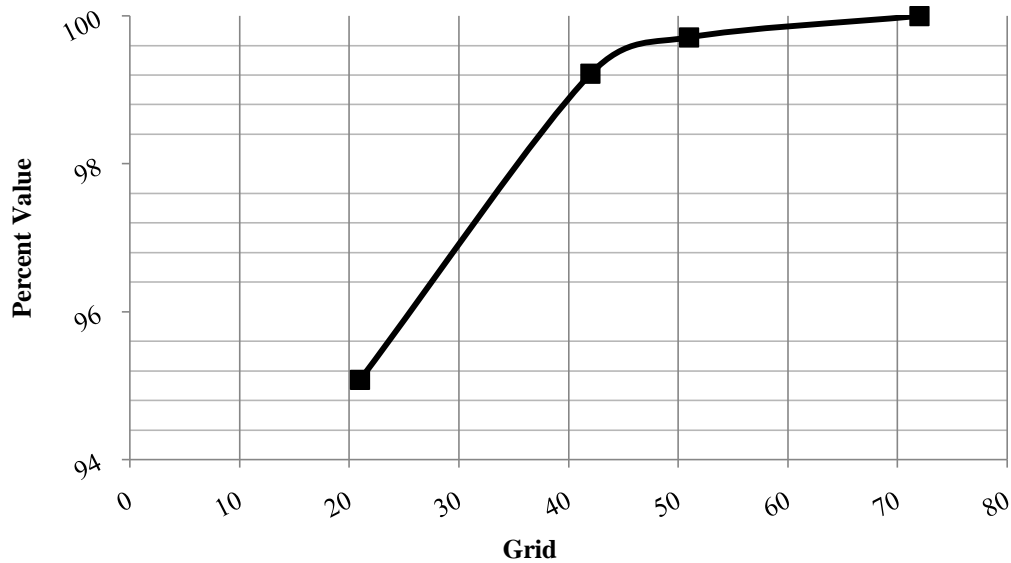


Fig. 6.2: Percent value Vs. mesh grid

The receptors selected are based on the actual sites in a UTM location coordinate of the area of interest map. Table 6.1 shows the selected discrete receptors information.

The uniform grid of total 1764 receptors (42 x 42) is considered with ( $\Delta x = 350$  m and  $\Delta y = 350$  m) to cover about 12 x 10 km area of study. The optimum selection of the mesh size is based on the computational accuracy and time.

Table 6.1: Selected discrete receptors information

<b>ID Number</b>	<b>Discrete receptor identity</b>	<b>X-coordinate</b>	<b>Y-coordinate</b>
1	Fahaheel Polyclinic	219854.25	3219765.79
2	Petroleum Services Offices in Ahmadi	216666.87	3220105.63
3	Primary school in Fahaheel	220300.00	3219820.85
4	Ahmadi Hospital	213458.86	3221523.64
5	Shopping area in Fahaheel	219274.32	3219554.21

## 6.4 Meteorological Data

Five years long comprehensive meteorological data are processed by Aermet to generate boundary layer parameters and to pass all meteorological observations to AERMOD. MM5 prognostic meteorological input data for these five years of 2005 – 2009 at anemometer height of 14 m and base elevation above Mean Sea Level (MSL) of 39 m are used in Aermet. These are consistent in describing sea breeze related to flow patterns, wind direction estimation for the coastal areas and provide adequate estimates of the maximum mixing layer heights, Isakov et al., (2007).

A yearlong comprehensive meteorological data is processed by Aermet to generate boundary layer parameters and to pass all meteorological observations to Aermod. Figure 6.3 shows wind direction and magnitude for a period of year 2008. It is observed that most of the time; the prevailing wind is from North West. There is strong influence of the neighboring Gulf as the refinery is located at the coast, resulting into strong sea breeze blowing from northeast and southeast direction.

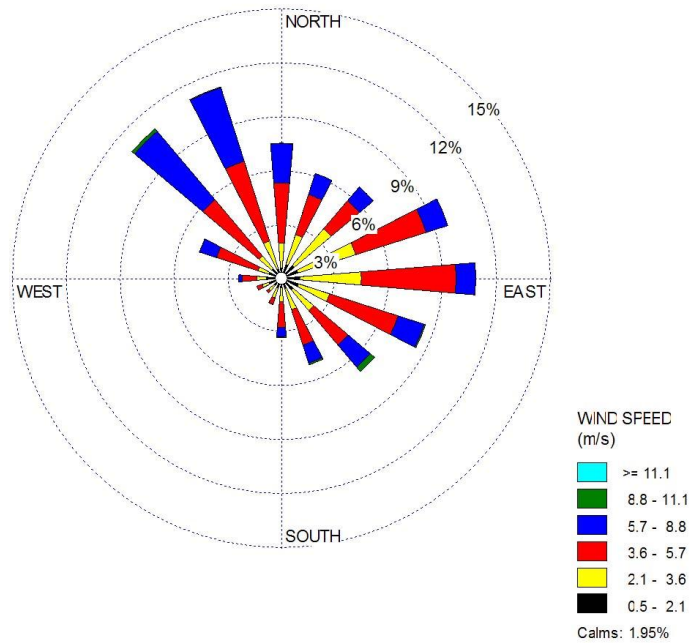


Fig. 6.3: Wind rose for year 2008

Figure 6.4 shows wind class frequency distribution for the entire year confirming 2 % calm conditions, while 39.8 % wind class is between 3.6 - 5.7 m/s. the highest wind class 8.8-11.1 m/s is less than 1%.

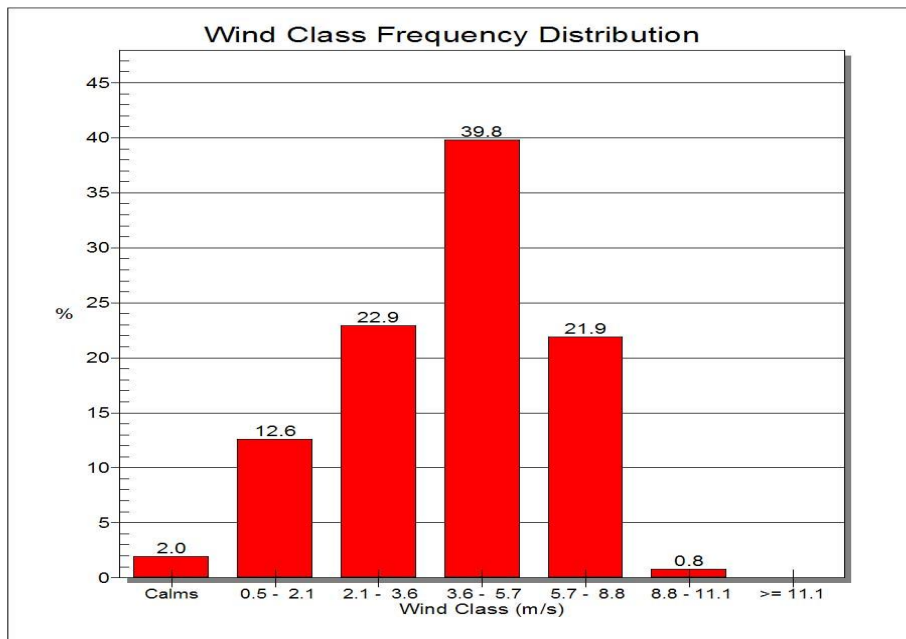


Fig. 6.4: Wind class distribution for year 2008

Figures 6.5 and 6.6 shows wind direction and magnitude for a period of five years (2005 – 2009). The prevalent wind is from northwest for the entire 5 years. Due to the location of the refinery at the coast, there is notable effect from the neighboring Gulf, resulting into strong sea breeze blowing from East direction. Wind class frequency distribution for the entire five years period confirming 1.3 % calm conditions, while 48.3 % is between 3.6 - 5.7 m/s. the highest wind class 8.8-11.1 m/s is less than 0.5%.

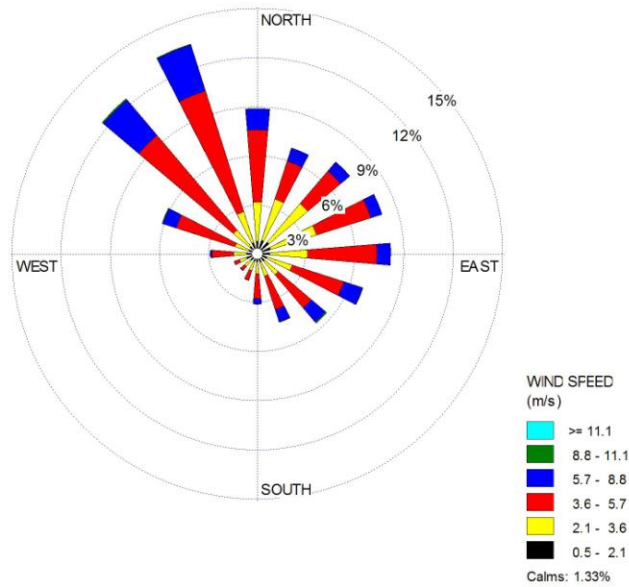


Fig. 6.5: Wind rose for years (2005- 2009)

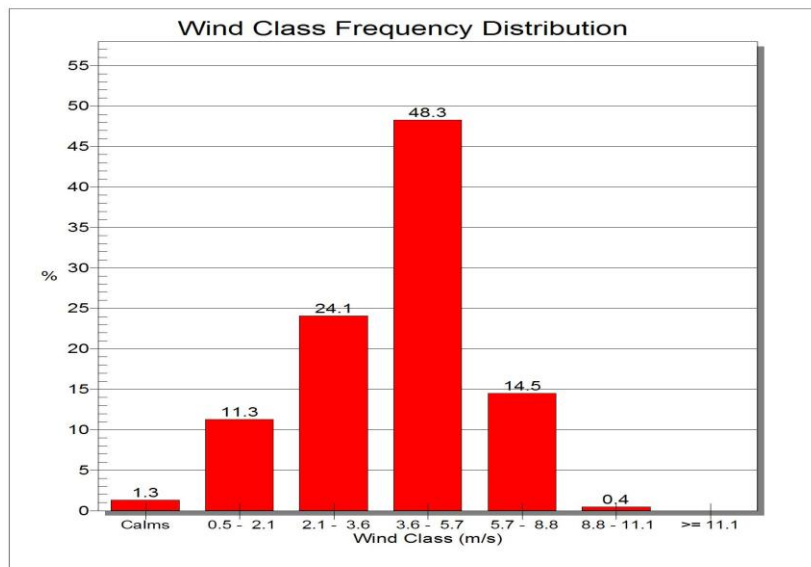


Fig. 6.6: Wind class distribution for years (2005 – 2009)

## 6.5 Meteorological Effects

In order to study the influence of yearly meteorological data on the prediction of the ground level concentrations of the pollutant, a model run is performed for fixed monthly SO<sub>2</sub> emission rate of 500 g/s using 2008 meteorological data for each month separately. Figure 6.7 shows the monthly maximum hourly predicted SO<sub>2</sub> ground level concentration for year 2008.

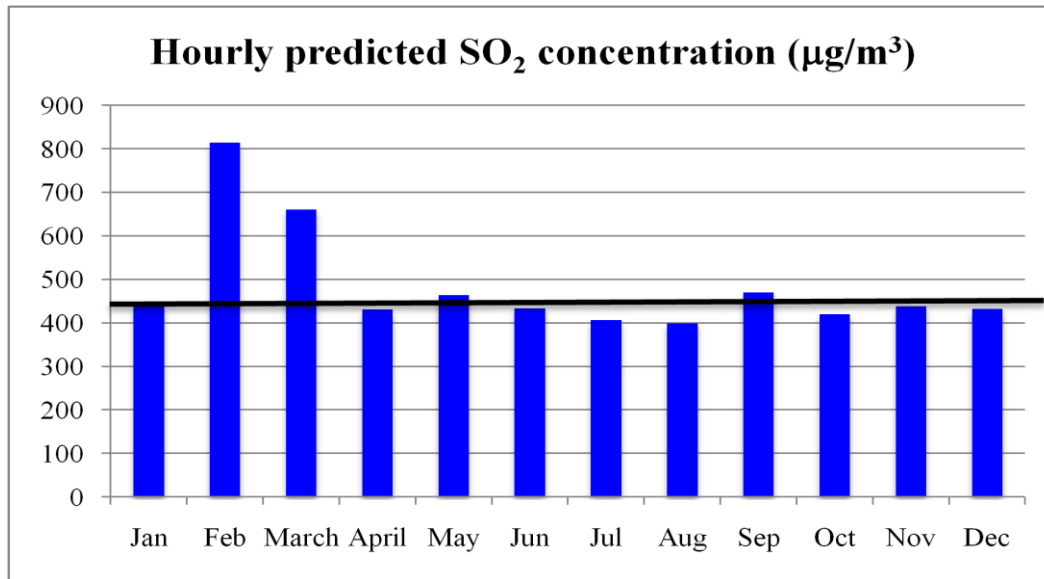


Fig. 6.7: Maximum hourly predicted SO<sub>2</sub> ground level concentration for each month for year 2008.

The highest hourly predicted SO<sub>2</sub> ground level concentration is equal to 814 µg/m<sup>3</sup> for the month of February on 27<sup>th</sup> day at 7:00 hours. The corresponding wind velocity is 0.8 m/s and the temperature is 15 °C. The second highest hourly predicted SO<sub>2</sub> ground level concentration is equal to 660 µg/m<sup>3</sup> for the month of March on 8<sup>th</sup> day at 8:00 hours. The respective wind velocity is 1 m/s and the temperature is 19 °C. These two high values are due to the prevailing meteorological conditions i.e. low temperatures, low inversion layers, low convective currents transfer and planetary boundary layer parameters and sea breeze effect in the early morning hours, resulting into inadequate dispersion.

Figure 6.7 depicts the highest predicted ground level concentrations for the month of July and August are  $406 \mu\text{g}/\text{m}^3$  and  $400 \mu\text{g}/\text{m}^3$  respectively, being the lowest among the rest of the months in year 2008. These are hot summer months where temperature soars to  $50^{\circ}\text{C}$  with strong winds, which stimulate dust storms. As a consequence, results into high inversion layer and leading to high dispersion.

A model run performed for actual monthly emission variation of year 2008 with total monthly  $\text{SO}_2$  emission rate of  $6089 \text{ g/s}$  using monthly emission factors for  $\text{SO}_2$  tabulated in Table 5.1 with the corresponding meteorological data.

A discrete receptor is selected at Kuwait Environmental Public Authority monitoring station located at polyclinic in Fahaheel area as mentioned in Table 6.1. Concentrations of  $\text{SO}_2$ ,  $\text{NO}_x$ ,  $\text{H}_2\text{S}$ ,  $\text{O}_3$ ,  $\text{CO}$ ,  $\text{CO}_2$ , methane, non-methane hydrocarbon, benzene, toluene, o-m-p xylenes, ethylbenzene, total suspended particulates and meteorological parameters are continuously recorded on hourly basis.

Hourly predicted ground level concentrations at specified discrete receptor showed large scatter due to variation in meteorological conditions and the recorded values influenced by the contribution of various emission sources has made the comparison erroneous. Therefore, daily measured concentrations of  $\text{SO}_2$  are compared with the daily-predicted concentrations to validate the model output. Figure 6.8 shows the plot between the predicted top 20 values to the corresponding measured values at the specified discrete receptor.

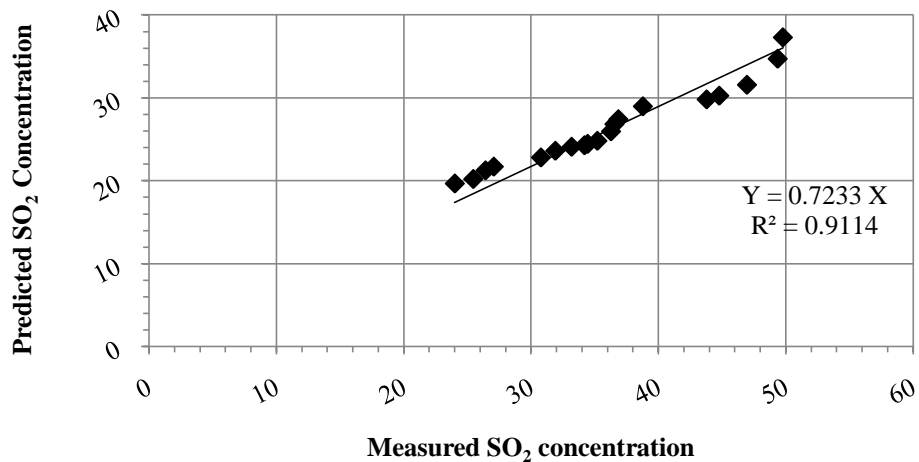


Fig. 6.8: Predicted  $\text{SO}_2$  concentrations Vs. Measured  $\text{SO}_2$  concentrations

The slope of the trend line is equal to 0.7, reflecting high measured values compared to predicted values, depicting the contribution of other emission sources. The correlation coefficient is equal to 0.91.

Venkatram (2004) studied the role of the metrological data on the dispersion. Air dispersion Aermid is used in this study. The performance of the model is evaluated by comparing the observed values with the model-estimated values. The comparison indicated that the model is under predicted the ground level concentrations. The observed values are greater than the computed values. The model estimated values are within a factor of two of the observations.

Isakov et al (2007) evaluated different meteorological inputs in air quality modelling applications. Most of the estimated concentrations are within a factor of two of the measured values when MM5 meteorological input is used.

In the present work, the predicted values are almost within the factor of two of the measured values, reflecting an acceptable validation of the model's output. The observed values are higher due to the contribution of the line source emissions. EPA monitoring station is located in Fahaheel area. The additional SO<sub>2</sub> levels are mainly due to heavy vehicles, busses and trucks, using sulphur-containing fuel viz., diesel.

Sulphur hexafluoride SF<sub>6</sub> is commonly used as tracer gas to assess the performance of air dispersion models. A known amount of SF<sub>6</sub> can be released at fixed flow rate. Air dispersion model can be used to predict ground level concentration of the tracer gas using different meteorological inputs. And ambient air sample either at regular grid point or at discrete receptor can be sampled for estimation of SF<sub>6</sub> ground level concentration. The performance of the dispersion model can be accurately evaluated and its output can be validated.

Yuan et al. (2006) showed that a simple dispersion model that used onsite meteorological data i.e. mean wind and turbulence as an input predicted an adequate description of the ground level concentrations observed during the tracer (SF<sub>6</sub>) experiment. This model has the basic structure and input requirements similar to those of Aermid.

It is recommended to conduct a tracer gas study (SF<sub>6</sub>) to ascertain the performance of Aermid with greater confidence for future work.



**CHAPTER SEVEN**  
**RESULTS & DISCUSSION**

## 7.1 Introduction

The execution of Aermid dispersion model for total monthly emission rates of year 2008 the corresponding yearly meteorological data has shown top 300 hourly and daily ground level concentrations for both pollutants i.e. SO<sub>2</sub> and PM considering monthly emission variations. The stack parameters are already mentioned in the previous chapter.

Aermid is also applied to total monthly emission rates of year 2009 for both pollutants, SO<sub>2</sub> and PM with wider range of meteorological data (2005-2009), in order to thoroughly investigate the pattern of Kuwait weather variation for the said period and its impact on the prediction of the ground level concentrations.

## 7.2 Simulation of Concentrations for Year 2008

Sixteen sectors of spiral plot indicate the maximum and average hourly concentrations (top 300 values) profiles for year 2008 computational results of total emission rate of 6089 g/s. Figure 7.1 shows the maximum hourly concentration of SO<sub>2</sub> equal to 838 µg/m<sup>3</sup> in the northwest (NW) direction from the stack and the average hourly in the southwest south (SWS) direction from the stack is equal to 533 µg/m<sup>3</sup>, reflecting influence of eastern wind (sea breeze). This sea breeze is obviously drifting the pollutants towards the west direction affecting the areas located at downwind. The highest hourly concentration computed is on 8<sup>th</sup> of March 8:00 hours and at a distance of 1.6 km from the stack at 311° bearing north. The corresponding wind velocity is 1 m/s and temperature is 19 °C. Similarly the second highest is 826 µg/m<sup>3</sup> on 27<sup>th</sup> of February 7:00 hours at the distance of 1.8 km from the emission source at 303° bearing north.

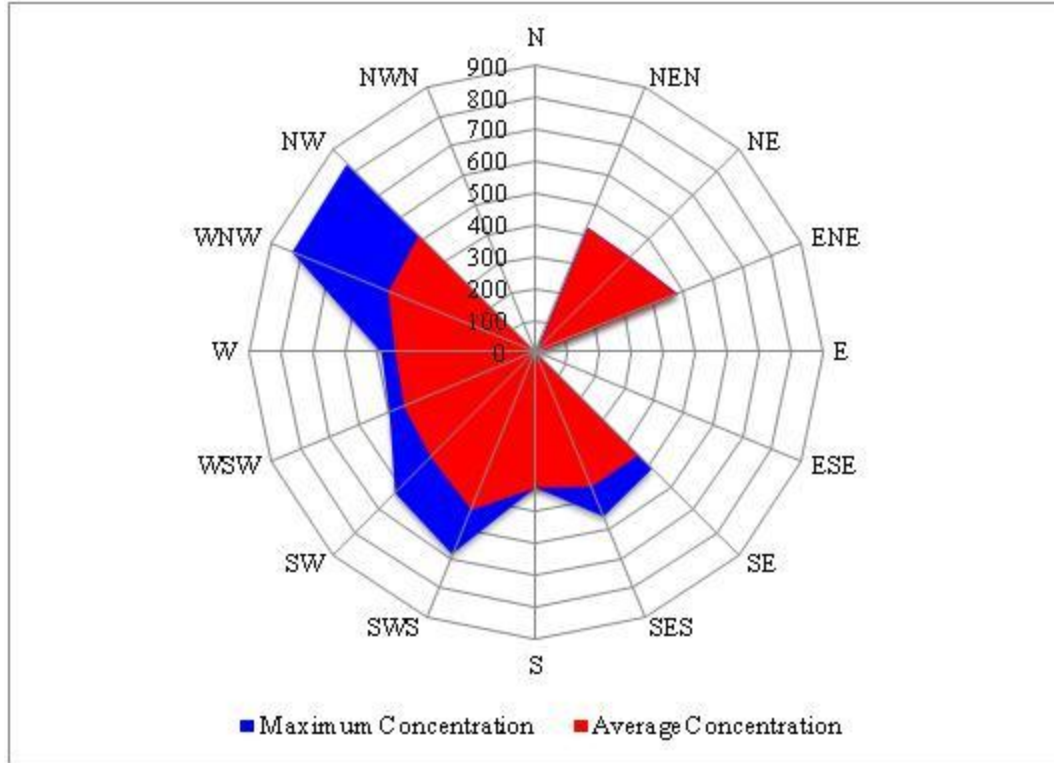


Fig. 7.1: Spiral plot shows top 300 hourly ground level concentration of SO<sub>2</sub> for year 2008 emission rate

Daily maximum and average concentrations of SO<sub>2</sub> (top 300 values) for year 2008 emission rate profiles are shown in sixteen sectors of spiral plot in Figure 7.2.

The maximum concentration of SO<sub>2</sub> is 341 µg/m<sup>3</sup> from east to southeast south (SES) direction, reflecting influence of prevailing northwest wind. The average concentration of SO<sub>2</sub> is equal to 157 µg/m<sup>3</sup>.

The influence of the dominant northwestern wind is clearly shown in Figure 7.2, dispersing the pollutants toward southeast direction and affecting downwind area.

The highest computed daily concentration of SO<sub>2</sub> is on 9<sup>th</sup> of November at the distance of 0.9 km from the stack at 128° bearing north. The second highest is equal to 267 µg/m<sup>3</sup> on 17<sup>th</sup> of November at the distance of 1.2 km from the emission source at 142° bearing north.

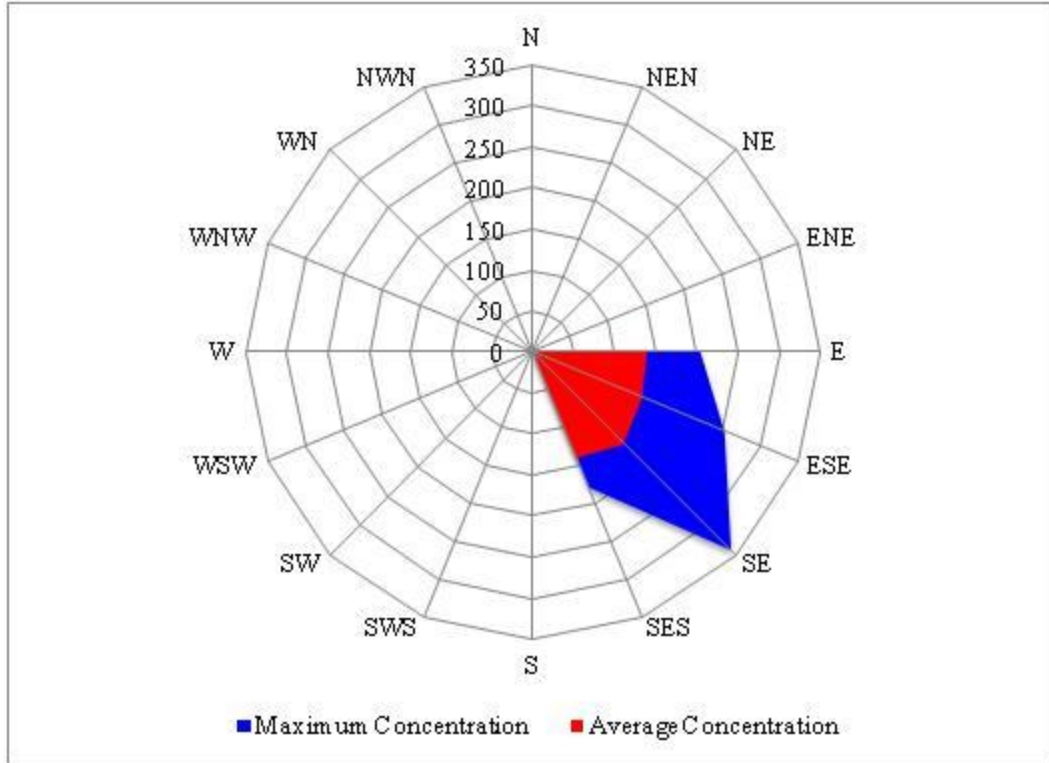


Fig. 7.2: Spiral plot shows top 300 daily maximum and average ground level concentration of SO<sub>2</sub> for year 2008 emission rate

The maximum and average hourly ground level concentrations of SO<sub>2</sub> (top 300 values) profiles for total emission rate of 6758 g/s for year 2009, using 5 years meteorological data of Kuwait (2005 – 2009) are shown in Figure 7.3.

The maximum predicted ground level concentration of SO<sub>2</sub> is equal to 930 µg/m<sup>3</sup> in the northwest (NW) direction. The application of the model for prediction of SO<sub>2</sub> hourly ground level concentration, using 5 years meteorological data of Kuwait showed the strong eastern wind (sea breeze) influence on the dispersion process. The highest predicted concentration is at a distance of 1.5 km from the stack at 311° bearing north, corresponding to the meteorological conditions of 8<sup>th</sup> of March 2008, at 8:00 hours. The corresponding wind velocity is 1 m/s and temperature is 19 °C. The average concentration is equal to 676 µg/m<sup>3</sup> in the southeast direction from the emission source. The second highest is 917 µg/m<sup>3</sup>, corresponding to meteorological conditions of 27<sup>th</sup> of February 2008, 8:00 hours at the distance of 1.9 km from the emission source at 304° bearing north.

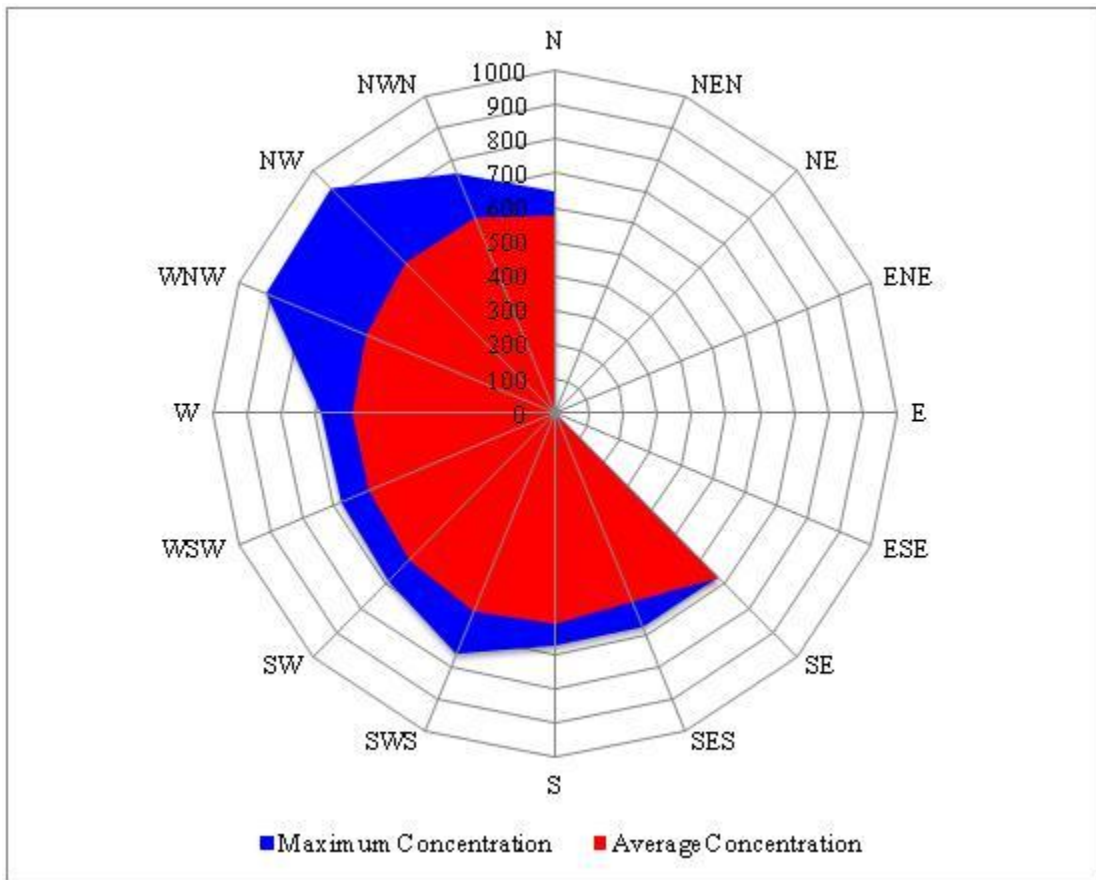


Fig. 7.3: Spiral plot shows top 300 hourly ground level concentration of SO<sub>2</sub> for year 2009 emission rate

Daily maximum and average concentrations of SO<sub>2</sub> (top 300 values) for year 2009 emission rate profiles are shown in sixteen sectors of spiral plot in Figure 7.4.

The daily maximum concentration of SO<sub>2</sub> is 379 µg/m<sup>3</sup> in the southeast south (SE) direction and the average concentration of SO<sub>2</sub> is equal to 200 µg/m<sup>3</sup>. The effect of the average daily northwestern wind of Kuwait meteorological data for 5 years is dominant, dispersing the pollutants toward southeast direction of the emission source.

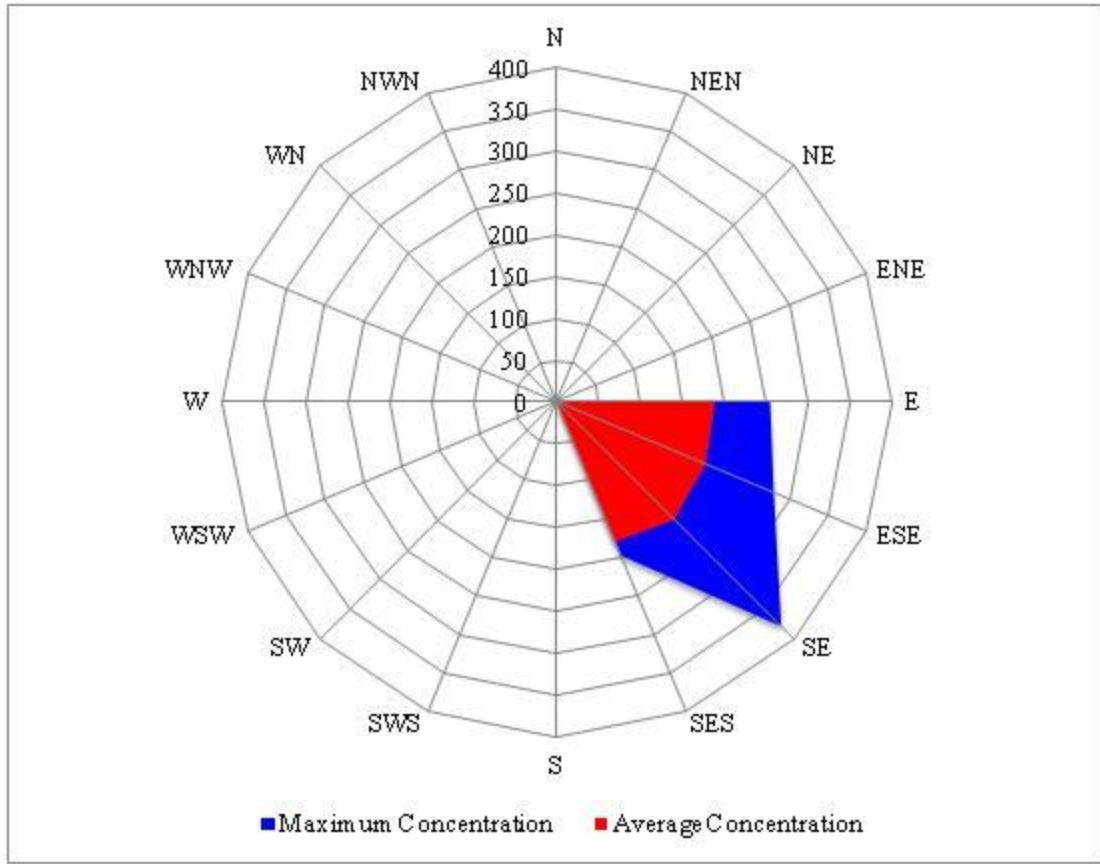


Fig. 7.4: Spiral plot shows top 300 daily maximum and average ground level concentration of SO<sub>2</sub> for year 2009 emission rate

The highest computed daily concentration of SO<sub>2</sub> is at the distance of 0.9 km from the stack at 128° bearing north, corresponding to meteorological conditions of 9<sup>th</sup> of November 2008. The second highest is equal to 297 µg/m<sup>3</sup> corresponding to meteorological conditions 17<sup>th</sup> of November 2008, at the distance of 1.2 km from the emission source at 141° bearing north.

### 7.3 Model Results for Year 2008 Emission Data

The predicted hourly average ground level concentrations of SO<sub>2</sub> for years 2008 emission rate, are compared with Kuwait-EPA Ambient Air Quality Standards (AAQS) at all of the selected receptors. The maximum allowable limit for the hourly average concentration of SO<sub>2</sub>, specified by Kuwait-EPA, is 444 µg/m<sup>3</sup>. Figure 7.5 shows the isopleths of the predicted hourly average ground level concentration of SO<sub>2</sub> calculated at the selected uniform grid receptors.

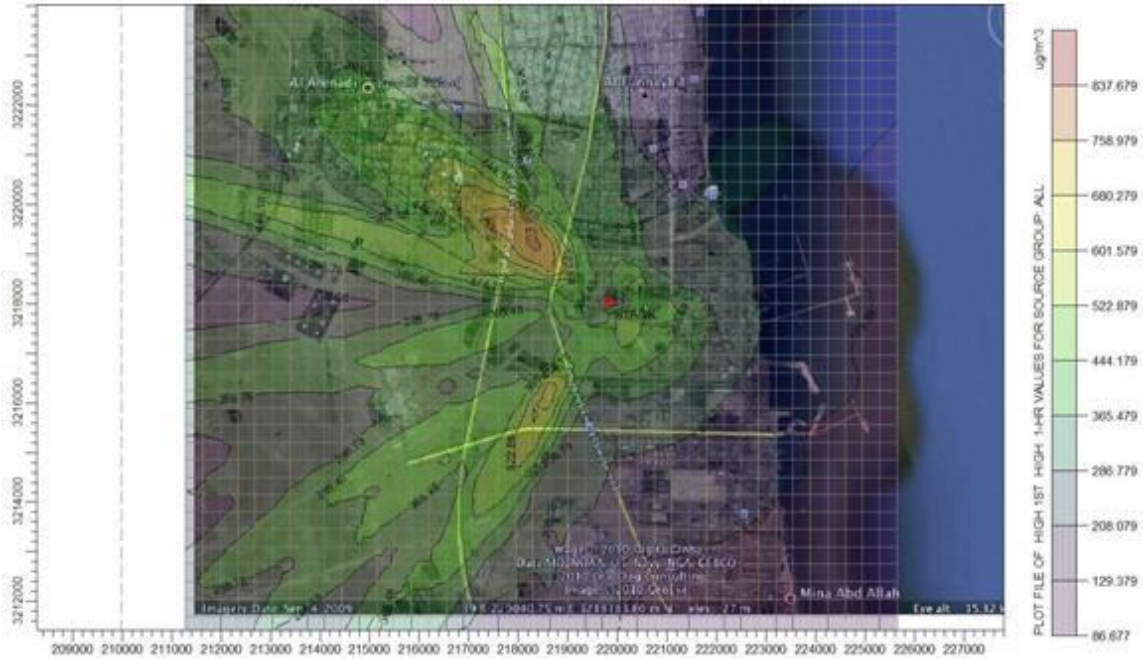


Fig. 7.5: Isopleths plot of the predicted hourly average ground level concentration of  $\text{SO}_2$  for year 2008

The isopleths indicate the predicted spatial variations of the ground level concentrations of  $\text{SO}_2$ . The maximum predicted hourly average ground level concentration of  $\text{SO}_2$  in the vicinity of the refinery exceeded by as much as  $400 \mu\text{g}/\text{m}^3$ . The highest predicted concentration is equal to  $838 \mu\text{g}/\text{m}^3$ , observed on the 8<sup>th</sup> of March 2008 at 8:00 hour and about 1.6 km in the northwest direction from the FCC stack, and not far from Fahaheel and Ahmadi areas at the receptor coordinates of  $X = 218648$ ,  $Y = 3219048$ . This high value of the predicted  $\text{SO}_2$  concentration is expected due to the elevated  $\text{SO}_2$  emission rate, which resulted from the high sulphur content in the FCC feedstock in this particular month and other operational conditions i.e. (reaction temperature, pressure, catalyst characteristics) and the prevailing meteorological conditions (ambient temperature, humidity, wind speed, wind direction, stability class, planetary boundary layer).

A thorough inspection on Figure 7.5 indicates that predicted concentrations of  $\text{SO}_2$  exceed the allowable hourly limit at 6 % of the study area from northwest and southwest directions from the stack.



Similarly, the predicted daily average ground level concentration of SO<sub>2</sub> is compared with Kuwait EPA ambient air quality standards at all receptors. The allowable limit for the daily average concentration of SO<sub>2</sub> is 157 µg/m<sup>3</sup>. Figure 7.6 shows the isopleths of the predicted daily average ground level concentration of SO<sub>2</sub> computed at the selected uniform grid receptors.

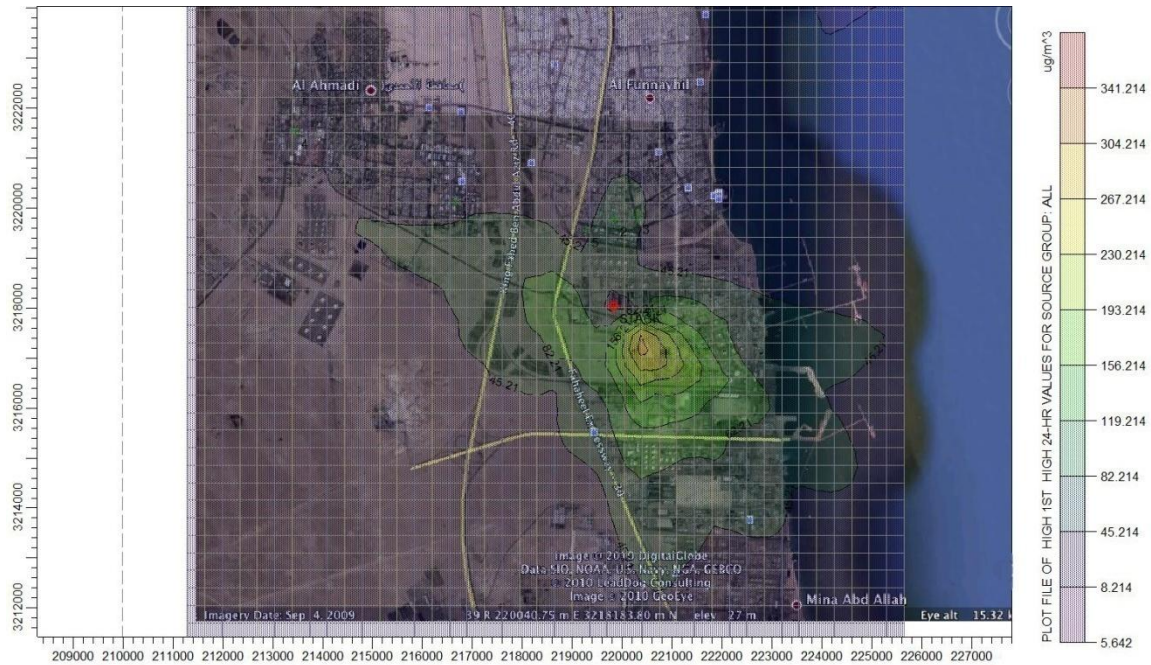


Fig. 7.6: Isopleths plot of the predicted daily average ground level concentration of SO<sub>2</sub> for year 2008

The isopleths indicate the daily predicted spatial variations of the ground level concentrations of SO<sub>2</sub> in the area of study. The highest daily predicted concentration is equal to 341µg/m<sup>3</sup>, observed on the 9<sup>th</sup> of November 2008 and about 0.9 km in the southeast direction from the stack, at a receptor coordinates of X = 220398, Y = 3217298 affecting the neighboring Shuaiba industrial area, Kuwait main industrial complex. This high value of the daily predicted SO<sub>2</sub> concentration exceeded the allowable level by 157 µg/m<sup>3</sup> and obviously influenced by the prevailing meteorological conditions, especially the predominant northwest wind and other meteorological factors.

Discrete receptor 2, is located at Petroleum services offices, has shown the highest SO<sub>2</sub> hourly concentration equal to 609 µg/m<sup>3</sup> on 27th February at 8:00 hours. The hourly exceedance



occurred four times at this location throughout the study period. The highest daily concentration, which is below the Kuwait EPA allowable limit, at the same receptor is equal to  $41 \mu\text{g}/\text{m}^3$  on 8<sup>th</sup> March.

Discrete receptor 3, is located at primary school, has shown the highest  $\text{SO}_2$  hourly concentration equal to  $279 \mu\text{g}/\text{m}^3$  on 2<sup>nd</sup> March at 4:00 hours. The daily highest concentration is equal to  $57 \mu\text{g}/\text{m}^3$  on 2<sup>nd</sup> March. The hourly and daily concentrations are below the corresponding Kuwait EPA standards.

Discrete receptor 4, is located at Ahmadi hospital, has shown the highest  $\text{SO}_2$  hourly ground level concentration equal to  $314 \mu\text{g}/\text{m}^3$  on 27<sup>th</sup> February at 8:00 hours. This value is also below the specified hourly limit set by Kuwait EPA. The daily predicted concentration is equal to  $26 \mu\text{g}/\text{m}^3$  on 30<sup>th</sup> April.

Discrete receptor 5, is located at shopping area, has shown the highest  $\text{SO}_2$  hourly ground level concentration is equal to  $351 \mu\text{g}/\text{m}^3$  on 23<sup>rd</sup> October at 8:00 hours. The daily predicted concentration is equal to  $40 \mu\text{g}/\text{m}^3$  on 2<sup>nd</sup> April. Both hourly and daily predicted values are below Kuwait EPA hourly and daily ambient air quality standards.

Kulkarni et al., (2007) have reported that lanthanum and lanthanides are used as markers for particulate matters pollution as  $\text{PM}_{2.5}$  in petroleum refineries, mainly from FCC units.

US EPA daily  $\text{PM}_{2.5}$  standard is  $35 \mu\text{g}/\text{m}^3$ . In the present work, the application of Aermid to predict ground level concentration of PM is considered as  $\text{PM}_{2.5}$  for rare earth metals i.e. lanthanum and cerium.  $\text{PM}_{2.5}$  is inhalable and has adverse impact on public health causing cardiovascular diseases. Kuwait EPA has no standard for  $\text{PM}_{2.5}$  and has only specified daily and yearly standard for  $\text{PM}_{10}$ . Figure 7.7 shows the isopleths of the predicted hourly average ground level concentration of PM calculated at the selected uniform grid receptors.

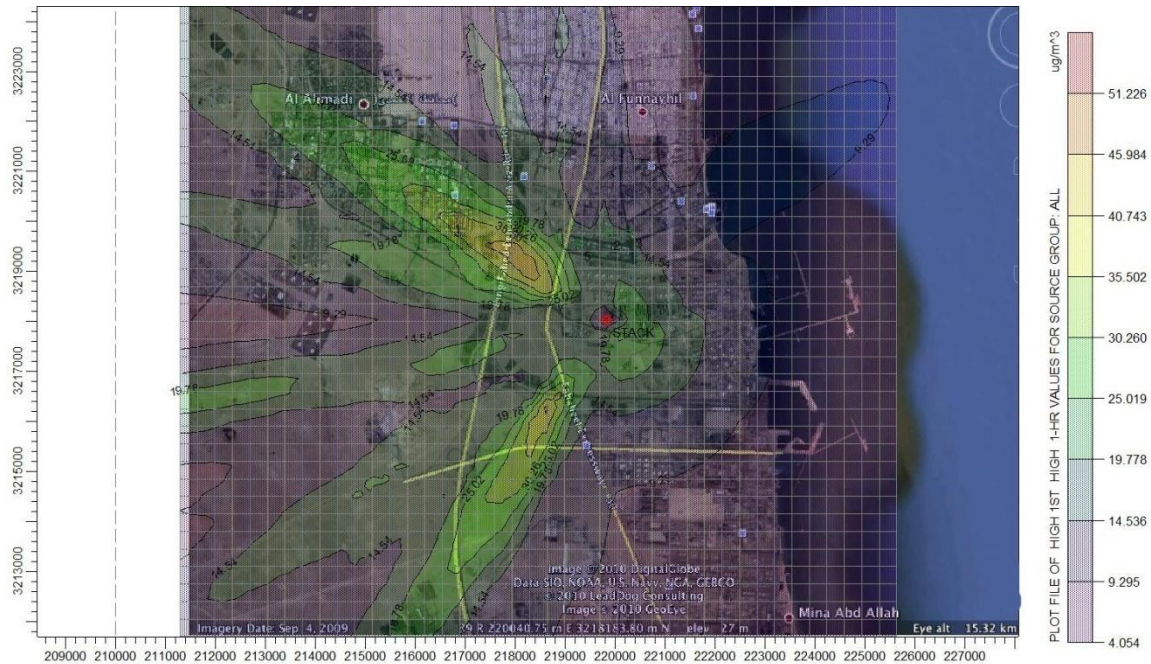


Fig. 7.7: Isopleths plot of the predicted hourly average ground level concentration of PM for year 2008

The isopleths indicate the hourly predicted spatial variations of the ground level concentrations of PM. The maximum hourly predicted average ground level concentration of PM is equal to  $51 \mu\text{g}/\text{m}^3$ , observed on the 27<sup>th</sup> of February 2008 at 8:00 hour and about 1.85 km in the northwest direction from the FCC stack. The top value is predicted in the early morning confirming the strong influence of the sea breeze. The receptor coordinates are  $X = 218298$ ,  $Y = 3219048$ .

Similarly, the predicted daily average ground level concentration of PM is compared with US EPA ambient air quality standards for  $\text{PM}_{2.5}$  at all receptors. Figure 7.8 shows the isopleths of the predicted daily average ground level concentration of PM computed at the selected uniform grid receptors.

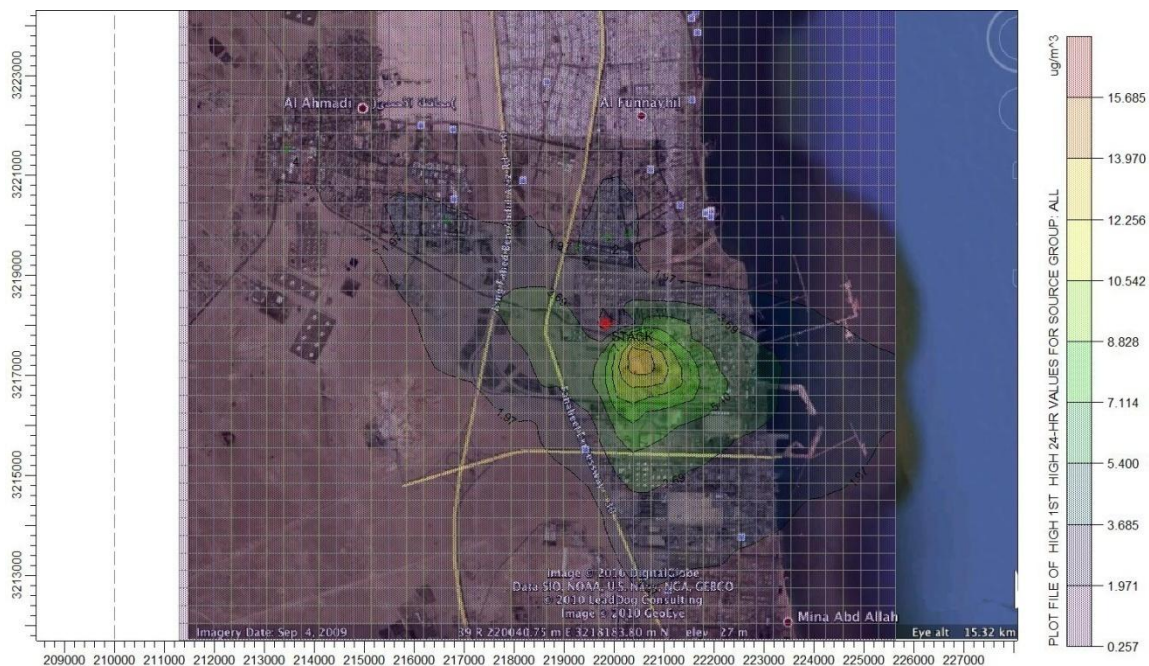


Fig. 7.8: Isopleths plot of the predicted daily average ground level concentration of PM for year 2008

The isopleths indicate the daily average predicted spatial variations of the ground level concentrations of PM in the area of study. The highest daily predicted concentration is equal to  $16 \mu\text{g}/\text{m}^3$ , observed on the 29<sup>th</sup> of December 2008 and about 0.9 km in the southeast direction from the stack, at a receptor coordinates of  $X = 220748$ ,  $Y = 3217298$  due to the influence of the prevailing meteorological conditions, especially the predominant northwest wind and other meteorological factors. The predicted value is below the US EPA allowable 24 hours limit. This value is computed based on the assumption of zero background concentration, which can exceed the limit with a fair contribution of other local or far distant sources.

#### 7.4 Model Results for Year 2009 Emission Data

The hourly predicted spatial variation of  $\text{SO}_2$  ground level concentration is shown in Figure 7.9 using emission rate for year 2009 with 5 years meteorological data of Kuwait (2005 – 2009). The highest predicted concentration is equal to  $930 \mu\text{g}/\text{m}^3$ , observed corresponding to 8<sup>th</sup> of March 2008 at 8:00 hour meteorological conditions and about 1.6 km in the northwest direction from the emission source, at the receptor coordinates of  $X = 218648$ ,  $Y = 3219048$ .



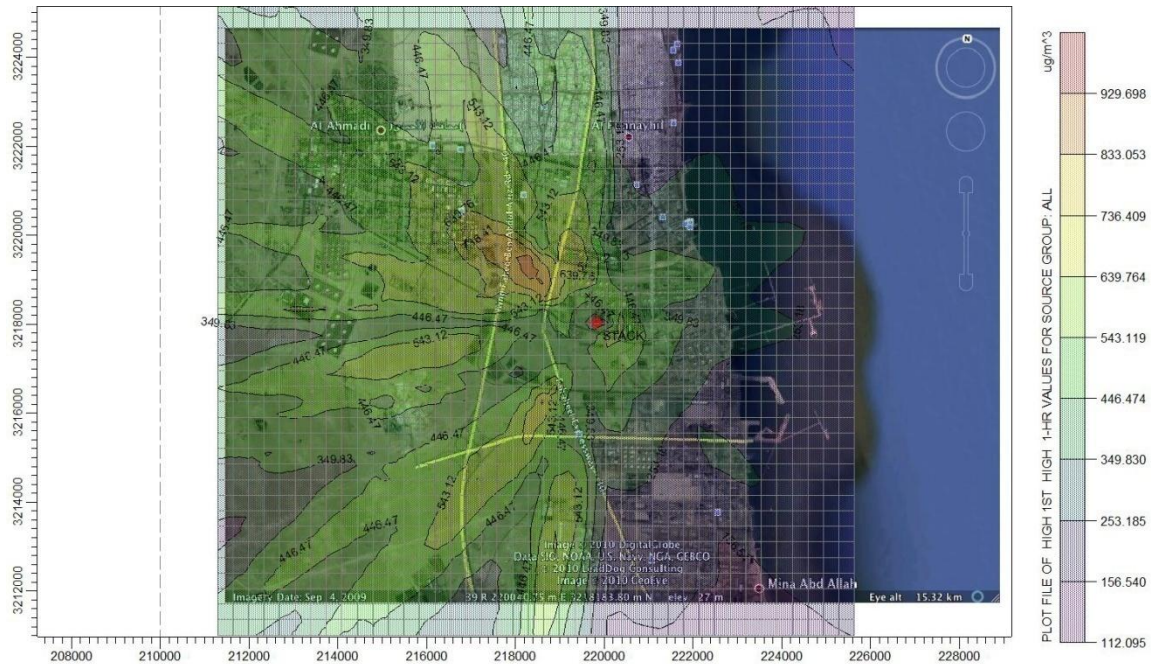


Fig. 7.9: Isopleths plot of the predicted hourly average ground level concentration of  $\text{SO}_2$  for year 2009

The high sulphur content in the feedstock, high FCC unit production rate and low sulphur products resulted from local and international market demands boosted  $\text{SO}_2$  emission rate, resulting into elevated  $\text{SO}_2$  ground level concentration. High emission rates of  $\text{SO}_2$  is also affected by the FCC unit operational conditions i.e. (reaction temperature, pressure, catalyst characteristics) and the prevailing meteorological conditions (ambient temperature, humidity, wind speed, wind direction, stability class, planetary boundary layer). The highest predicted  $\text{SO}_2$  ground level concentration is exceeded the Kuwait EPA allowable limit by almost  $500 \mu\text{g}/\text{m}^3$ . The hourly  $\text{SO}_2$  ground level concentration isopleths indicate the influence of high  $\text{SO}_2$  emission rate on the ambient air quality of the neighboring areas of the refinery i.e. Fahaheel and Ahmadi. Figure 7.9 also indicates that the predicted concentrations of  $\text{SO}_2$  exceed the allowable hourly limit at 31 % of the study area from western directions, influenced by strong sea breeze in the early morning hours.

Figure 7.10 shows the isopleths of the predicted daily average ground level concentration of  $\text{SO}_2$  computed at the selected uniform grid receptors.

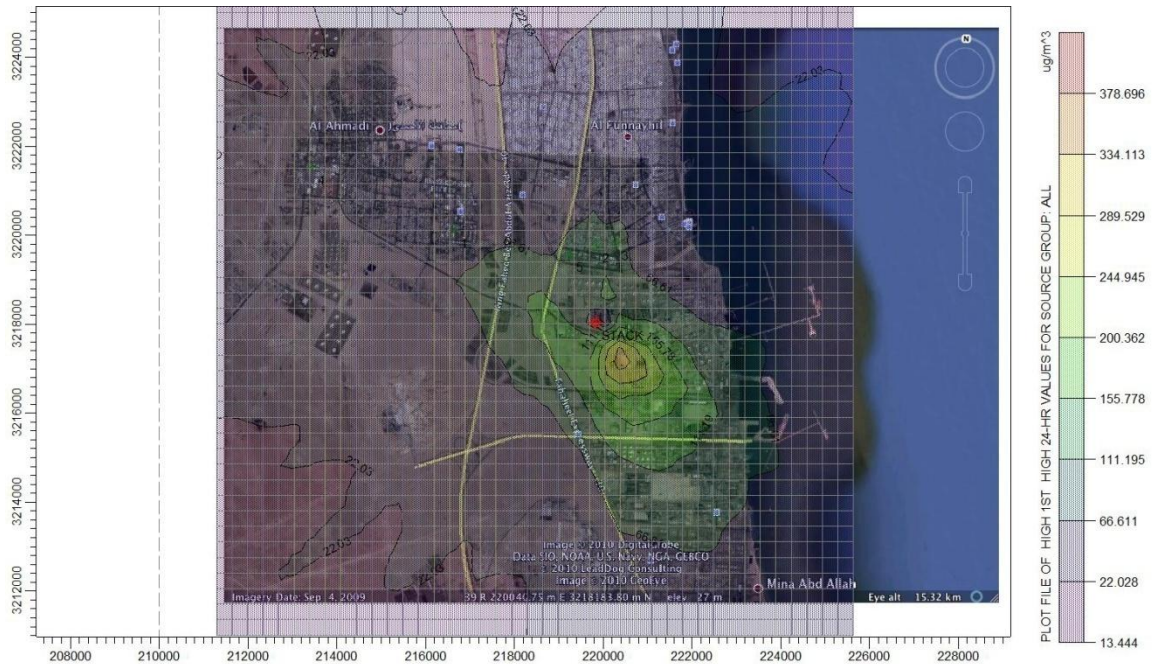


Fig. 7.10: Isopleths plot of the predicted daily average ground level concentration of SO<sub>2</sub> for year 2009

The highest daily predicted concentration is equal to 379  $\mu\text{g}/\text{m}^3$ , observed corresponding to 9<sup>th</sup> of November 2008 and about 0.9 km in the southeast direction from the stack, at a receptor coordinates of X = 220398, Y = 3217298. This high value of the daily predicted SO<sub>2</sub> concentration is exceeded the allowable level by 157  $\mu\text{g}/\text{m}^3$  and obviously influenced by the prevailing meteorological conditions, especially the predominant northwest wind and other meteorological factors. This high predicted ground concentration is also affecting the ambient air quality of Shuaiba, Kuwait main industrial area.

Discrete receptor 2 showed the highest SO<sub>2</sub> hourly concentration is equal to 676  $\mu\text{g}/\text{m}^3$  corresponding to meteorological condition of 27<sup>th</sup> of February 2008, at 8:00 hours. The highest daily concentration, which is below the Kuwait EPA allowable limit, at the same receptor is equal to 47  $\mu\text{g}/\text{m}^3$  corresponding to meteorological condition of 27<sup>th</sup> of April 2006.

Discrete receptor 3 showed the highest SO<sub>2</sub> hourly concentration is equal to 347  $\mu\text{g}/\text{m}^3$  corresponding to meteorological condition of 9<sup>th</sup> of April 2006, at 3:00 hours. The daily highest

concentration is equal to  $90 \mu\text{g}/\text{m}^3$  corresponding to meteorological condition of 29<sup>th</sup> October 2006. Both hourly and daily concentrations are below the corresponding Kuwait EPA standards.

Discrete receptor 4, is located at Ahmadi hospital, has shown the highest  $\text{SO}_2$  hourly ground level concentration equal to  $500 \mu\text{g}/\text{m}^3$  corresponding to meteorological condition of 30<sup>th</sup> March 2005, at 7:00 hours. This value is above the specified hourly limit set by Kuwait EPA. The daily predicted concentration is equal to  $33 \mu\text{g}/\text{m}^3$  corresponding to meteorological condition of 25<sup>th</sup> March 2005.

Discrete receptor 5, is located at shopping area, has shown the highest  $\text{SO}_2$  hourly ground level concentration is equal to  $744 \mu\text{g}/\text{m}^3$  corresponding to meteorological condition of 16<sup>th</sup> April 2007, at 7:00 hours. The daily predicted concentration is equal to  $80 \mu\text{g}/\text{m}^3$  on 10<sup>th</sup> April 2007. The hourly predicted ground level concentration is exceeded Kuwait EPA hourly ambient air quality standard by almost  $300 \mu\text{g}/\text{m}^3$ .

Figure 7.11 indicates the hourly predicted ground level concentrations of PM for year 2009 emission rate. The highest hourly predicted average ground level concentration of PM is equal to  $57 \mu\text{g}/\text{m}^3$ , observed corresponding to meteorological conditions 27<sup>th</sup> of February 2008, at 8:00 hour and about 1.85 km in the northwest direction from the FCC stack. The receptor coordinates are  $X = 218298$ ,  $Y = 3219048$ .

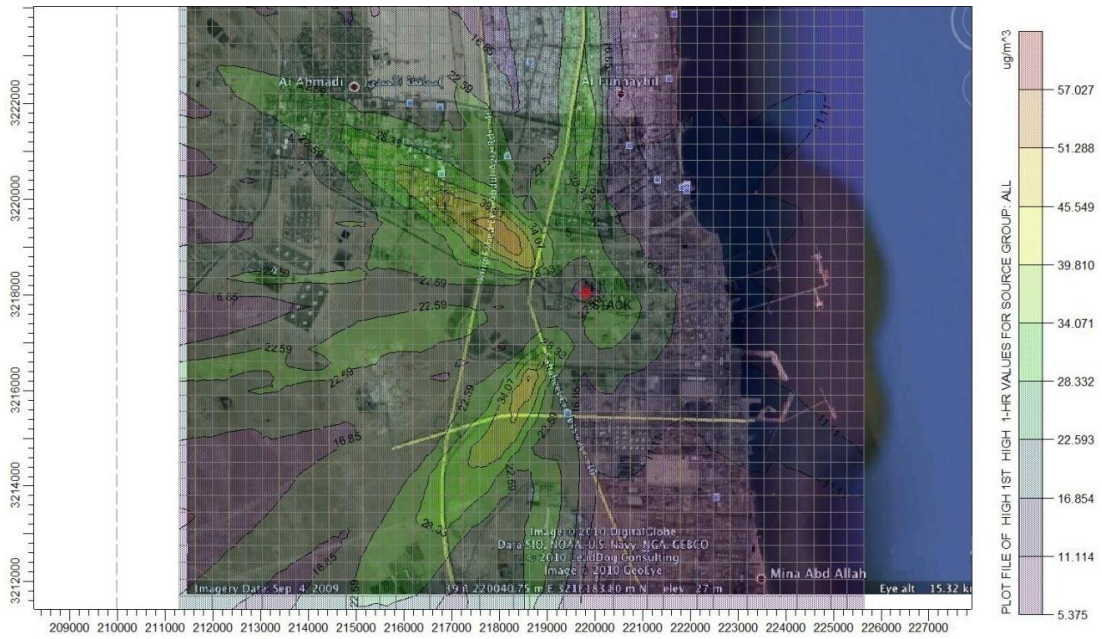


Fig. 7.11: Isopleths plot of the predicted hourly average ground level concentration of PM for year 2009

Similarly, the predicted daily average ground level concentration of PM is compared with US EPA ambient air quality standards for  $\text{PM}_{2.5}$  at all receptors. Figure 7.12 shows the isopleths of the predicted daily average ground level concentration of PM computed at the selected uniform grid receptors.

The isopleths indicate the daily average predicted spatial variations of the ground level concentrations of PM in the area of study. The highest daily predicted concentration is equal to  $17 \mu\text{g}/\text{m}^3$ , observed corresponding to meteorological conditions of 29<sup>th</sup> of December 2008 and about 0.9 km in the southeast direction from the stack, at a receptor coordinates of  $X = 220748$ ,  $Y = 3217298$  due to the influence of the prevailing meteorological conditions, especially the average northwest wind and other meteorological factors. The predicted concentration is also calculated based on the assumption of zero background concentration, which can exceed the limit with a fair contribution of other local or far distant sources.



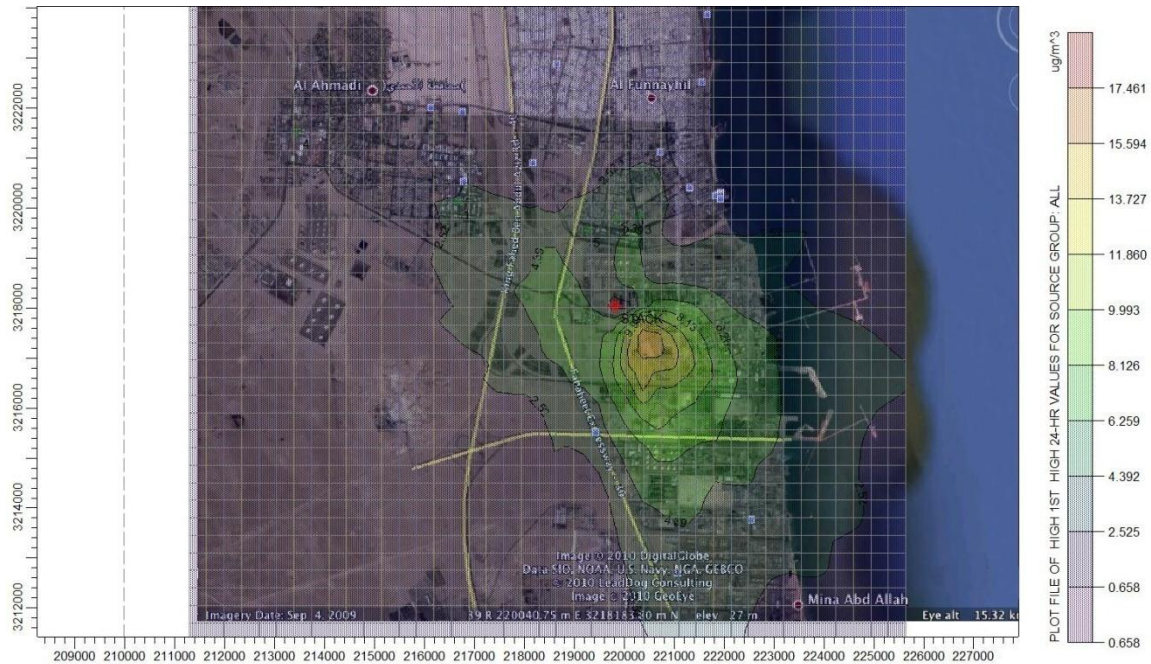


Fig. 7.12: Isopleths plot of the predicted daily average ground level concentration of PM for year 2009

## 7.5 Parametric Sensitivity Study

In order to observe the computational model sensitivity, another scenario run is performed adding two finer meshes consisting of 21 x 21 uniform receptor points, the first one covering hourly highest ground level concentration area, the other one covering daily highest predicted ground level concentration area. The output accuracy has improved for both pollutants due to application of interpolation using small values of  $\Delta x = 150$  m,  $\Delta y = 110$  m for the first mesh and  $\Delta x = 100$  m,  $\Delta y = 100$  m for the second mesh. There is 0.7% increase in the hourly highest ground level concentration and 3% increase in the daily highest ground level concentration, which are insignificant. Therefore, the only parent mesh is used in the computational process for all the other scenarios considered in the parametric studies.

FCC stack sensitivity analysis is performed on 3 scenarios (stack height, SO<sub>2</sub> emission rate and stack diameter).



In scenario 1, analysis for stack heights 50 m, 80 m, 120 m, 160 m and 200 m is conducted while keeping all other parameters constant i.e. (emission rate, exit flue gas velocity, exit temperature, stack diameter).

The computed concentrations for different stack heights are shown in figure 7.13. It is obvious from the figure that the highest predicted hourly and daily ground level concentrations of SO<sub>2</sub> are reduced substantially as stack height is increased. The reduction in the highest computed hourly ground level concentration of SO<sub>2</sub> is almost 50 % when stack height is doubled. The reduction in the evaluated hourly SO<sub>2</sub> concentration as a function of stack height is given as an exponential expression  $C (\mu\text{g}/\text{m}^3) = 1600e^{0.01h}$  and  $r^2$  is 0.99, where h is the stack height (m). The hourly predicted concentration gradient  $dC/dh = 14.5e^{0.01h}$  becomes insignificant at higher stack elevations (>200 m). The highest daily predicted ground level concentration as a function of stack height is given as  $C (\mu\text{g}/\text{m}^3) = 1410e^{0.017h}$  and  $r^2$  is 0.98. The daily highest predicted concentration gradient is  $dC/dh = 24e^{0.017h}$ . The locations of hourly highest predicted concentrations of SO<sub>2</sub> from the stack, as a function of stack height is shown in Figure 7.13 and related as  $D (\text{km}) = 0.6e^{0.0116h}$  and  $r^2$  is 0.98.

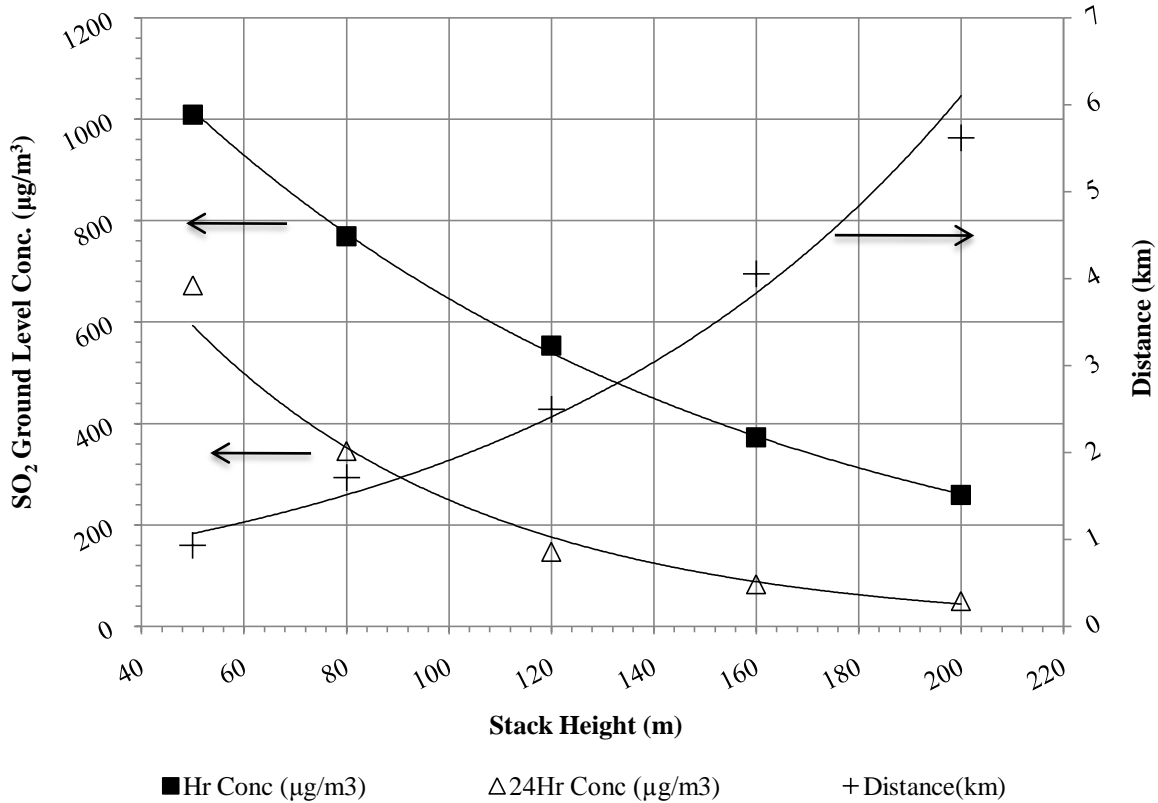


Fig. 7.13: Hourly and daily predicted ground level concentrations of SO<sub>2</sub> versus stack height

In scenario 2, SO<sub>2</sub> emission rate effect from FCC stack is tested at stack height of 80 m for different yearly emission rates of 3000 g/s, 4000 g/s, 5000 g/s, 6000 g/s, 7000 g/s and 8000 g/s, taking into consideration the monthly emission variations (by using emission factors, Table 5.1 and fixing other stack parameters i.e. exit temperature, exit flue gas velocity and stack diameter.

It is noticed from Fig. 7.14 that the highest predicted hourly and daily ground level concentration of SO<sub>2</sub> is substantially decreased as SO<sub>2</sub> emission rate is reduced. At 50% reduction in the emission rate, the highest hourly and daily ground level concentrations decreased by about 48%.

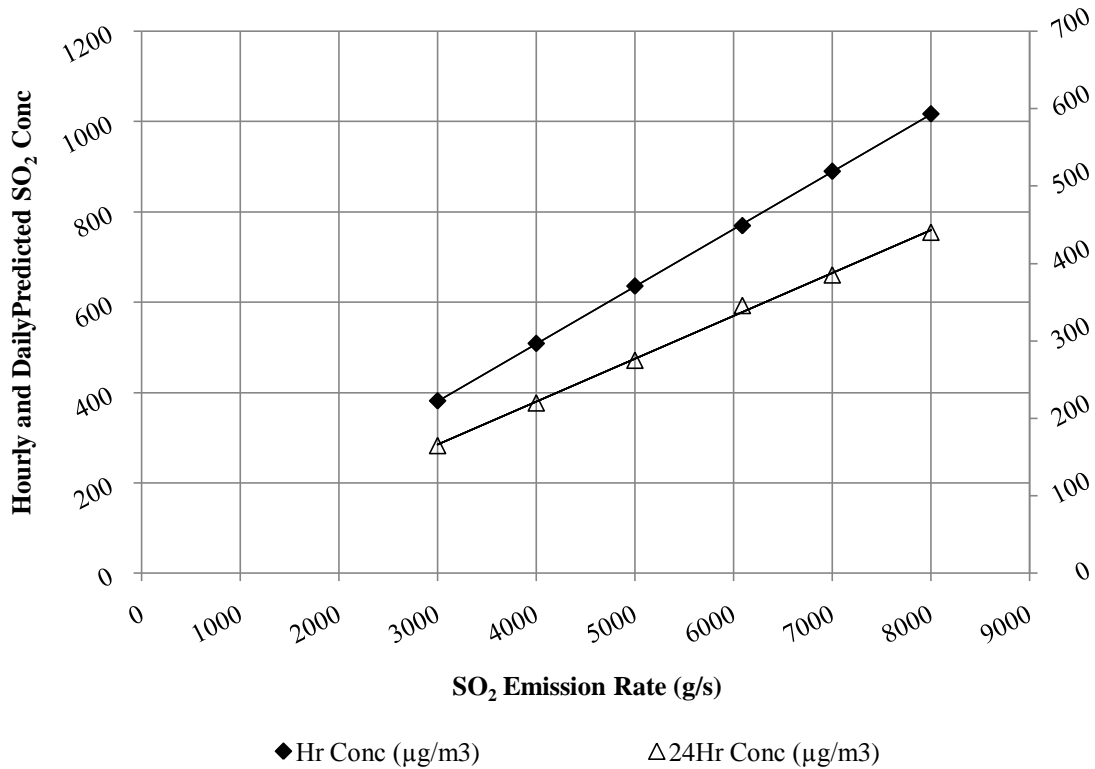


Fig. 7.14: Hourly and daily predicted SO<sub>2</sub> ground level concentrations versus SO<sub>2</sub> emission rate

In scenario 3, FCC stack diameter effect is examined at stack height of 80 m for different diameters of 1.5 m, 2.3 m, 3 m and 4 m. The exit flue gas velocity is directly related to the square of the diameter for a fixed exit flue gas flow rate. It is observed that the dispersion and rise of the plume are not affected by diameter variation and the predicted ground level concentration of SO<sub>2</sub> remained almost unaltered. The hourly and daily predicted concentrations of SO<sub>2</sub> are almost identical for all stack diameters calculations.

In the convective boundary layer, Aermid estimates the plume rise using wind speed at the stack tip as the stack momentum and stack buoyant fluxes are influenced by turbulence in this layer. In the stable boundary layer, Aermid calculates the plume rise and the effective height using stack momentum, stack buoyant fluxes and Brunt–Vaisala frequency at effective wind speed. These parameters are depending mainly on stack exit velocity, radius, temperature and potential temperature gradient. Both stack momentum and buoyant fluxes are directly proportional to stack exit velocity and radius. For fixed flue gas flow rate, the exit velocity is

changed with the change in stack diameter, compensating the effect of the stack diameter in the estimation of the plume rise and the effective height.

The plume rise,  $\Delta h_s$  is calculated in Aermoc using the following equation:

$$\Delta h_s = 2.66 \left( \frac{F_b}{u N^2} \right)^{\frac{1}{3}} * \left( \frac{F_m N'}{F_b} \sin \frac{x N'}{u} \right) + 1 - \cos \frac{x N'}{u} \Big)^{\frac{1}{3}} \quad (7.1)$$

Where the stack momentum flux,  $F_m$  and stack buoyant flux,  $F_b$  are calculated using:

$$F_m = (T/T_s) w_s^2 r_s^2 \quad (7.2)$$

$$F_b = (\Delta T/T_s) g w_s r_s^2 \quad (7.3)$$

And Brunt–Vaisala frequency is calculated using:

$$N = \left( \frac{g}{T_p} \frac{\partial T}{\partial z} \right)^{\frac{1}{2}} \quad (7.4)$$

Where:

$$N' = 0.7 N$$

$$x = 49 F_b^{\frac{5}{8}} \quad (7.5)$$

$$\text{The effective stack height} = \text{plume rise} + \text{actual stack height} \quad (7.6)$$

$u$  is the wind speed at the maximum plume rise, m/s

$x$  is the distance to the final plume rise, metre.

$T$  is the ambient temperature, °C.

$T_s$  is the exit flue gas temperature, °C

$g$  is the gravitational acceleration, m/s

Table 7.1 shows the values of effective stack height for different values of stack radius and plume rise. These values are based on the following assumed values:

Flue gas flow rate = 50 m<sup>3</sup>/s

$$T = 20 \text{ }^{\circ}\text{C}$$

$$T_s = 227 \text{ }^{\circ}\text{C}$$

$$u = 10 \text{ m/s}$$

$$N = 0.018 \text{ s}^{-1}$$

Table 7.1: Effective stack heights for different of stack radius and plume rise

Stack radius (m)	Plume rise, $\Delta h_s$ (m)	Effective height, $H_{\text{eff}}$ (m)
0.75	61.56	141.56
1	61.53	141.53
1.5	61.50	141.50
2	61.50	141.50

As shown in Table 7.1 the stack momentum flux,  $F_m$  changes significantly with the change of the stack radius. However, it is noticed that there is no significant change in the plume rise and the effective stack height with respect to the change in the stack radius.

## 7.6 Mitigation Methods of Sulphur Oxides

$\text{SO}_2$  emissions are controlled by the introduction of  $\text{SO}_x$  reduction additives in a typical FCC unit. These additives are mainly hydrotalcites based or mix oxides (Mg/Al/Fe/Cu). In the literature, Vierheilig et al., (2003) have reported that  $\text{SO}_2$  reduction of 20 – 60 % can be achieved by the use of additives, which is almost about 1-10 % of the total catalyst inventory. Mg, Fe and Cu oxides react with  $\text{SO}_3$  to produce respective sulphates, which are re-circulated with the catalyst into the riser. The sulphates are reduced to respective oxides and  $\text{H}_2\text{S}$  is produced that is further reacted to generate elemental sulphur through Claus process.

In the preceding section, the effect of  $\text{SO}_2$  emission rates on predicted ground level concentrations is thoroughly examined in scenario 2 of the parametric study. The hourly maximum predicted  $\text{SO}_2$  concentration for year 2008 can be reduced to  $444 \mu\text{g}/\text{m}^3$ , Kuwait EPA

specified limit for an equivalent total annual emission rate of 3500 g/s by reduction of 43% of total 6089 g/s. Similarly, total annual emission rate for year 2009 may also be reduced by 57% of total 6758 g/s to achieve SO<sub>2</sub> concentration below the Kuwait EPA hourly standard. The reduction of SO<sub>2</sub> emissions is proportional to the amount of SO<sub>x</sub> additive charged. There are different types of additives commercially available that have to be tested and economically evaluated for the selection of the appropriate type and quantity of additives.

## **7.7 Particulates Emission Control**

Particulate fines are produced, mainly due to high attrition resulted from catalyst particle erosion and fracture during the process and of the thermal shock of the cold fresh catalyst charge (makeup) coming in contact with hot regenerated catalyst under operating conditions i.e. vapour velocity, particle velocity, particle collision and particle degradation.

Among the various available mitigation techniques for of PM emissions, cyclones and electrostatic precipitator, (ESP) are integral parts of FCC process. ESP has recently been installed to reduce substantially PM emissions. In the trail runs, 90 % reduction is observed, which has resulted into high reduction in ground level concentration in the vicinity of this unit. Total average annual emission of PM for year 2009 is 336 g/s before the installation of ESP and is reduced to almost 34 g/s after the commissioning of ESP. in lieu of this reduction; the highest daily predicted ground level concentration has decreased from 17µg/m<sup>3</sup> to almost 2 µg/m<sup>3</sup>.

**CHAPTER EIGHT**  
**CONCLUSION, RECOMENDATIONS AND FUTURE WORK**

FCC unit in a refinery is major contributor of SO<sub>2</sub> and PM emissions those are responsible for adverse impact on the immediate neighborhood of the refinery. A complete comprehensive emission inventories for years 2008 and 2009 have been prepared for both SO<sub>2</sub> and Particulate Matters based on real operational data obtained from the refinery.

SO<sub>2</sub> emissions are high in spring while PM emissions are high in winter in both years 2008 and 2009, mainly due to operational conditions that are dependent on feed rate and sulphur contents in the feed. PM emissions are mainly due to high attrition of cold makeup catalyst charge and operating conditions i.e. vapour velocity, particle velocity, particles collision and particles degradation.

The comprehensive meteorological data for year 2008 has been tested for fixed monthly SO<sub>2</sub> emission rate of 500 g/s using Aermid. The highest hourly predicted ground level concentration of SO<sub>2</sub> is equal to 814 µg/m<sup>3</sup> on 27<sup>th</sup> of February at 7:00 hours. The corresponding wind velocity is 0.8 m/s and the temperature is 15 °C. The second highest hourly predicted SO<sub>2</sub> ground level concentration is equal to 660 µg/m<sup>3</sup> for the month of March on 8<sup>th</sup> day at 8:00 hours. These values are mainly due to the prevailing calm meteorological conditions, low temperature, low inversion layer, lower convective currents transfer and other planetary boundary layer parameters resulting into inadequate dispersion. The hourly highest predicted SO<sub>2</sub> concentration for the month of August is equal to 400 µg/m<sup>3</sup>, which is the minimum value among the months of year 2008. August is a hot and dry summer month where temperature crosses 45 °C with strong dusty winds, resulting into high inversion layer and leading to high dispersion.

The mesh sensitivity is tested by selecting 21 x 21 up to 72 x 72 mesh size for the prediction of ground level concentrations of SO<sub>2</sub> for fixed emission rate. The predicted concentrations are gradually increased with selection of finer mesh. It is observed that the accuracy of the predicted values is above 99 % for 42 x 42 mesh and higher. Therefore, 42 x 42 mesh size is selected for the rest of the computational process.

A model runs performed for actual monthly emission variation with total SO<sub>2</sub> emission rate of 6089 g/s for years 2008, taking into consideration monthly emission factors for SO<sub>2</sub>. The daily predicted ground level concentrations of SO<sub>2</sub> are compared with the respective Kuwait EPA



monitoring station daily measured SO<sub>2</sub> concentrations at the same discrete receptor and showed acceptable validation of the model output.

Another run is performed for PM emission variation with total emission rate of 302 g/s for year 2008 using monthly PM emission factors. The highest hourly predicted concentration of SO<sub>2</sub> for year 2008 is equal to 838 µg/m<sup>3</sup>. It is observed on the 8<sup>th</sup> of March 2008 at 8:00 hour, due to elevated SO<sub>2</sub> emission rate in this month and the prevailing meteorological conditions, especially sea breeze effect in the early morning hours. The highest daily predicted concentration is equal to 341 µg/m<sup>3</sup>. It is observed on the 9<sup>th</sup> of November 2008, and obviously influenced by the predominant northwest wind. The maximum daily predicted concentration of PM is equal to 16 µg/m<sup>3</sup>. It is observed on the 29<sup>th</sup> of December 2008. The predicted concentrations of SO<sub>2</sub> exceeded the allowable hourly limit at 6 % of the study area.

Aermod is applied for year 2009 emission rates of both pollutants, using five years meteorological data (2005 – 2009). The highest hourly SO<sub>2</sub> predicted concentration is equal to 930 µg/m<sup>3</sup>, observed corresponding to 8<sup>th</sup> of March 2008 at 8:00 hour, mainly due to elevated SO<sub>2</sub> emission rate resulted from high products demand and the influence of the prevailing meteorological conditions. The highest daily SO<sub>2</sub> predicted concentration is equal to 379 µg/m<sup>3</sup>, observed corresponding to 9<sup>th</sup> of November 2008, influenced by the prevailing meteorological conditions, especially the predominant northwest wind. The maximum daily PM predicted concentration is equal to 17 µg/m<sup>3</sup>, observed corresponding to 29<sup>th</sup> of December 2008. The predicted concentrations of SO<sub>2</sub> exceeded the allowable hourly limit at 32 % of the study area.

High hourly values of SO<sub>2</sub> for both years are affecting the ambient air quality of Fahaheel and Ahmadi areas, while high daily values of SO<sub>2</sub> concentration affects the air quality of Shuaiba, Kuwait main industrial area.

The parametric sensitivity is explored by changing stack height, total emission rate and stack diameter independently. It is observed that the higher stack facilitated good dispersion, thus lowering the ground level average concentration of the pollutant up to 50% when the stack height is doubled.

It is notice that the highest predicted hourly and daily ground level concentrations of SO<sub>2</sub>

are substantially decreased as SO<sub>2</sub> emission rate is reduced. At 50% reduction in the emission rate, the highest hourly and daily ground level concentrations decreased by almost 48%.

The influence of stack diameter inherently changed the exit flue gas velocity due to invariable flue gas flow rate. The plume rise and dispersion are related to the exit flue gas velocity, which decreased with the increase of stack diameter because of proportionality to the square of diameter. For a fixed load there is no noticeable change in the average hourly and daily predicted ground level concentrations of SO<sub>2</sub>.

SO<sub>2</sub> emissions are controlled by the introduction of SO<sub>x</sub> reduction additives in a typical FCC unit. The additives charge is about 1-10 % of the total catalyst inventory, depending on sulphur deposition during coke formation. The hourly maximum predicted SO<sub>2</sub> concentration for year 2008 can be decreased to Kuwait EPA specified limit by reduction of 43% of total annual emission rate. Similarly, total annual emission rate for year 2009 may also be reduced by 57% of total emission to achieve SO<sub>2</sub> concentration below the Kuwait EPA hourly standard. The reduction of SO<sub>2</sub> emissions is proportional to the amount of SO<sub>x</sub> additive charged. There are different types of additives commercially available that have to be tested and economically evaluated for the selection of the appropriate type and quantity of additives.

Cyclones and electrostatic precipitator (ESP) are commonly used for PM emissions control. ESP has recently been installed and tested. The reduction in PM emissions is about 90 %, which has resulted into high reduction in ground level concentration in the vicinity of the refinery. As a result of this reduction; the daily highest predicted ground level concentration has decreased from 17 µg/m<sup>3</sup> to almost 2 µg/m<sup>3</sup>.

## **8.1 Recommendations and future work**

There are 101 stacks in the petroleum refinery emitting various pollutants with different rates. Comprehensive emission inventories shall be prepared and multi-pollutant dispersion model like Calpuff may be used to predicted various pollutant concentrations in a selected area,

considering interaction of different pollutants, photo-oxidation, dry and wet deposition. Model results shall be used for the evaluation of associated health risk to refinery employees as well as the residents of the neighboring area. Other potential emission sources like road vehicle, cottage industries, restaurants; fuel-dispensing stations etc shall be considered in ambient air quality assessments in neighboring urban and industrial localities.

It is recommended to conduct a tracer gas study ( $\text{SF}_6$ ) to ascertain the performance of AERMOD with greater confidence for future work.

Further research may be necessary for AERMOD to ensure the model applications for non-continuous releases source i.e. puffs and fugitive gases.

**CHAPTER NINE**  
**REFERENCES**

Abdul-Wahab A.S., 2006, "The role of meteorology on predicting SO<sub>2</sub> concentrations around a refinery: A case study from Oman" *Ecological modeling* **197**, 13-20

Ainslie B., Steyn D.G., Su J., Buzzelli M., Brauer M., Larson T., Rucker M., 2008, "A source area model incorporating simplified atmospheric dispersion and advection at fine scale for population air pollutant exposure assessment" *Atmospheric Environment* **42**, 2394–2404

Akeredolu F., 1989, "Atmospheric environment problems in nigeria-an overview", *Atmospheric environment* Vol. **23/4**, 783-792

Al-Rashidi M.S., Nassehi V., Wakeman R.J., 2005, "Investigation of the efficiency of existing air pollution monitoring sites in the state of Kuwait" *Environmental Pollution* **138**, 219 - 229

Babich I.V., Seshan K., Lefferts L., 2005, "Nature of nitrogen specie in coke and their role in NO<sub>x</sub> formation during FCC catalyst regeneration" *Applied Catalysis B: Environmental* **59**, 205–211

Barrett S.R.H., Britter R.E., 2008, "Development of algorithms and approximations for rapid operational air quality modeling" *Atmospheric Environment* **42**, 8105–8111

Barth J. O., Jentys A. Iliopoulou E. F., 2004, "Novel derivative of MCM-36 as catalysts for the reduction nitrogen oxides from FCC regenerator flue gas streams", *Journal of Catalysis* **227**, 117-129

Boerefijn R., Gudde N. J., and Ghadiri M., 2000, "A review of attrition of fluid cracking catalyst particles" *Advanced Powder Technology* **11**, 145–174

Bosco M.L., Varrica D., Dongarra G., 2005, "Case study: Inorganic pollutants associated with particulate matter from an area near a petrochemical plant" *Environmental Research* **99**, 18–30

Caputo M., Gimenez M., Schlamp M., 2003, “Intercomparison of atmospheric dispersion models” *Atmospheric Environment* **37**, 2435–2449

Centi G., Perathoner S., 2007, “Behaviour of SO<sub>x</sub>-traps derived from ternary Cu/Mg/Al hydrotalcite materials” *Catalysis Today* **127**, 219–229

Cerqueira H.S., Caeiro G., Costa L., Ribeiro F.R., 2008, “Deactivation of FCC catalysts” *Journal of Molecular Catalysis A: Chemical* **292**, 1-13

Chen Y.M., 2006, “Recent advances in FCC technology” *Powder Technology* **163**, 2–8

Cheng W.P., Yu X.Y., Wang W.J., Liu L., Yang J.G., He M.Y., 2008, “Synthesis, characterization and evaluation of Cu/Mg Al Fe as novel transfer catalyst for SO<sub>x</sub> removal” *Catalysis Communications* **9**, 1505–1509

Degrazia G.A., Anfossi D., Carvalho J.C., Mangia C., Tirabassi T., Velho H.F.C., 2000, “Turbulence parameterisation for PBL dispersion models in all stability conditions” *Atmospheric Environment* **34**, 3575-3583

Gary J.H., and Handwerk G. E., 2001, “Petroleum Refining: Technology and Economics” (4<sup>th</sup> edition) ISBN 0-8247-0482-7

Google Inc. 2010 “Google Earth” Version 5.1, [http:// www.earth.google.com](http://www.earth.google.com)

Holmes N.S., Morawsk L., 2006, “A review of dispersion modelling and its application to the dispersion of particles: An overview of different dispersion models available” *Atmospheric Environment* **40**, 5902–5928

Huang C., Wang Y., Wei F., 2008, “Solids mixing behavior in a nano-agglomerate fluidized bed” *Powder Technology* **182**, 334–341

Isakov V., Venkatram A., Touma J.S., Koracin D., Otte T.L., 2007, "Evaluating the use of outputs from comprehensive meteorological models in air quality modeling applications" *Atmospheric Environment* **41**, 1689–1705

Kesarkar A.P., Dalvi M., Kaginalkar A., Ojha A., 2007, "Coupling of the Weather Research and Forecasting Model with Aermოდ for pollutant dispersion modeling. A case study for PM<sub>10</sub> dispersion over Pune, India" *Atmospheric Environment* **41**, 1976–1988

Kikkinides E. S., Lappas A. A., Nalbadian A., Vasalos I. A., 2002, "Correlation of reactor performance with catalyst structural changes during coke formation in FCC processes", *Chemical Engineering Science* **57**, 1011 – 1025

Krishna R.T.V.B.P.S., Reddy M.K., Reddy R.C., Singh R.N., 2004, "Assimilative capacity and dispersion of pollutants due to industrial sources in Visakhapatnam bowl area" *Atmospheric Environment* **38**, 6775–6787

Krishna R.T.V.B.P.S., Reddy M.K., Reddy R.C., Singh R.N., 2005, "Impact of an industrial complex on the ambient air quality: Case study using a dispersion model" *Atmospheric Environment* **39**, 5395–5407

Kulkarni P., Shankaraman C., and Fraser M.P., 2007 "Tracking Petroleum Refinery Emission Events Using Lanthanum and Lanthanides as Elemental Markers for PM<sub>2.5</sub>" Preceding from annual meeting, 2007 American Institute of Chemical Engineering

Kumar A., Dixit S., Varadarajan C., Vijayan A., and Masuraha A., 2006, "Evaluation of the Aermოდ Dispersion Model as a Function of Atmospheric Stability for an Urban Area" *Environmental Progress* **25/2**

Long J., Zhu Y., Liu Y., Da Z., Zhou H., 2005, "Effects of vanadium oxidation number on desulfurization performance of FCC catalyst" *Applied Catalysis A: General* **282**, 295–301

Lopez J.L., Mandujano C., 2005, “Estimation of the impact in the air quality by the use of clean fuels (fuel oil versus natural gas)” *Catalysis Today* **106**, 176–179

Lushi E., Stockie J.M., 2010, “An inverse Gaussian plume approach for estimating atmospheric pollutant emissions from multiple point sources” *Atmospheric Environment* **44**, 1097 - 1107

McMillan J., Briens C., Berruti F., Chan E., 2007, “High velocity attrition nozzles in fluidized beds” *Powder Technology* **175**, 133–141

Mehdizadeh F., Rifai S.H., 2004, “Modeling point source plumes at high altitudes using a modified Gaussian model” *Atmospheric Environment* **38**, 821–831

Mizutani H., Korai Y., Mochida I., 2007, “Behavior of sulfur species present in atmospheric residue in fluid catalytic cracking” *Fuel* **86**, 2898–2905

Moreno T., Querol X., Alastuey A., Gibbons W., 2008, “Identification of FCC refinery atmospheric pollution events using lanthanoid and vanadium-bearing aerosols”, *Atmospheric Environment* **42**, 7851–7861

Olvera H.A., Choudhuri A.R., Li W.W., 2008, “Effects of plume buoyancy and momentum on the near-wake flow structure and dispersion behind an idealized building” *Journal of Wind Engineering and Industrial Aerodynamics* **96**, 209–228

Palomares A. E., Lopez-Nieto J. M., Lazaro F. J., Lopez A., Corma A., 1999, “Reactivity in the removal of SO<sub>2</sub> and NO<sub>x</sub> on Co/Mg/Al mixed oxides derived from hydrotalcites”, *Applied Catalysis B: Environmental* **20**, 257-266

Pang X., Zhang L., Sun S., Liu T., Gao X., 2007, “Effects of metal modifications of Y zeolites on sulfur reduction performance in fluid catalytic cracking process”, *Catalysis Today* **125**, 173–177



Perry S.G., Cimorelli A.J., Paine R.J., Brode R.W., Weil J.C., Venkatram A., Wilson R.B., Lee R.F., and Peters W.D., 2004, "Aermod: A Dispersion Model for Industrial Source Applications. Part II: Model Performance against 17 Field Study Databases" *Journal of Applied Meteorology* **44**, 694-708

Perry S.G., Cimorelli A.J., Paine R.J., Brode R.W., Weil J.C., Venkatram A., Wilson R.B., Lee R.F., and Peters W.D., 2004, "Aermod: A Dispersion Model for Industrial Source Applications. Part I: General Model Formulation and Boundary Layer Characterization" **44**, 682-693

Polato C.M.S., Henriques A.C., Rodrigues A.C.C., Monteiro J.L.F., 2008, "De-SO<sub>x</sub> additives based on mixed oxides derived from Mg,Al-hydroxalcalite-like compounds containing Fe, Cu, Co or Cr", *Catalysis Today* 133–135 and 534–540

Princevac M., Venkatram A., 2007, "Estimating micrometeorological inputs for modeling dispersion in urban areas during stable conditions" *Atmospheric Environment* **41**, 5345–5356

Ravichander N., Chiranjeevi T., Gokak D.T., Voolapalli R.K., Choudary N.V., 2009, "FCC catalyst and additive evaluation - A case study" *Catalysis Today* **141**, 115–119

Sabatino D.S., Buccolieri R., Pulvirenti B., Britter R., 2007, "Simulations of pollutant dispersion within idealized urban-type geometries with CFD and integral models" *Atmospheric Environment* **41**, 8316–8329

Sax T., Isakov V., 2003, "A case study for assessing uncertainty in local-scale regulatory air quality modeling applications" *Atmospheric Environment* **37**, 3481–3489

Siddiqui M.A.B., Ahmed S., Aitani A.M., Dean C. F., 2006, "Sulfur reduction in FCC gasoline using catalyst additives", *Applied Catalysis A: General* **303**, 116-120

Simpson M., Raman S., Lundquist J.K., Leach M., 2007, “A study of the variation of urban mixed layer heights” *Atmospheric Environment* **41**, 6923–6930

Speight J.G., 2006, “The Chemistry and Technology of Petroleum” (4<sup>th</sup> edition) ISBN 0-8493-9067-2.

Stein A.F., Isakov V., Godowitch J., Draxler R.R., 2007, “A hybrid modeling approach to resolve pollutant concentrations in an urban area” *Atmospheric Environment* **41**, 9410–9426

Touma S.J., Isakov V., Cimorelli J.A., Brode W.R., Anderson B., 2007, “Using Prognostic Model-Generated Meteorological Output in the Aermid Dispersion Model: An Illustrative Application in Philadelphia, PA” *Air & Waste Manage. Assoc.* **57**, 586 – 595

US Environmental Protection Agency 2003, “Aermid: Latest Features and Evaluation Results” EPA-454/R-03-003

US Environmental Protection Agency 2003,” Comparison of Regulatory Design concentrations Aermid V<sub>s</sub> ISCST3, CTDMPLUS, ISC-PRIME” EPA-454/R-03-002

US Environmental Protection Agency 2004, “Aermid: Description of Model Formulation” EPA-454/R-03-004

Valla J.A., Lappas A.A., Vasalos I.A., Kuehler C.W., Gudde N.J. 2004, “Feed and process effects on the in situ reduction of sulfur in FCC gasoline” *Applied catalyst A: General* **276**, 75–87

Venkatram A., 2004, “The role of meteorological inputs in estimating dispersion from surface releases” *Atmospheric Environment* **38**, 2439–2446

Venkatram A., Brodeur R., Cimarello A., Lee R., Paine R., Perry S., Peters W., Weil J., Wilson R., 2001, "A complex terrain dispersion model for regulatory applications" *Atmospheric Environment* **35**, 4211–4221

Venkatram A., Isakov V, Yuana J., Pankratz D., 2004, "Modeling dispersion at distances of meters from urban sources" *Atmospheric Environment* **38**, 4633–4641

Vierheilig A., Evans M., 2003, "The role of additives in reducing fluid catalytic cracking SO<sub>x</sub> and NO<sub>x</sub> Emissions" *Petroleum and Coal* **45**, 3-4 and 147- 153

Whitcombe J.M., Agranovski I.E., Braddock R.D., 2003, "Attrition due to mixing of hot and cold FCC catalyst particles" *Powder Technology* **137**, 120 – 130

Yassaa N., Cecinato A., 2005, "Composition of torched crude oil organic particulate emitted by refinery and its similarity to atmospheric aerosol in the surrounding area" *Chemosphere* **60**, 1660–1666

Yescas R. M., Villafuerte-Macias E.F., Aguilar R., Sotelo D.S., 2005, "Sulphur oxides emission during fluidized-bed catalytic cracking" *Chemical Engineering Journal* **106**, 145–152

Zannetti, P., 1990. "Air Pollution Modeling: Theories, Computational Methods, and Available Software". Computational Mechanics Publications

Zhang Q., Wei Y., Tian W., Yang K., 2008, "GIS-based emission inventories of urban scale: A case study of Hangzhou, China" *Atmospheric Environment* **42**, 5150 – 5165

Zhu H., Zhu J., 2008, "Characterization of fluidization behavior in the bottom region of CFB risers" *Chemical Engineering Journal* **141**, 169–179

Zou B., Wilson J. G., Zhan F.B., Zeng Y., 2009, "Spatially differentiated and source-specific population exposure to ambient urban air pollution" *Atmospheric Environment* **43**, 3981-3988

Zou B., Zhan F.B., Wilson J. G., Zeng Y., 2010, "Performance of Aermod at Different Time Scales" *Simulation Modeling Practices and Theory*. **18**, 612-623

## **APPENDIX - A**

# Inventories of SO<sub>2</sub> and Particulate Matter Emissions from Fluid Catalytic Cracking Units in Petroleum Refineries

Wael Yateem · Vahid Nassehi · Abdul R. Khan

Received: 14 October 2009 / Accepted: 30 March 2010 / Published online: 20 April 2010  
© Springer Science+Business Media B.V. 2010

**Abstract** Fluid catalytic cracking of heavy ends to high-value liquid fuels is a common unit operation in oil refineries. In this process, the heavy feedstock that contains sulfur is cracked to light products. Sulphur content is hence redistributed in the liquid and gaseous products and coke of the catalyst used in this process. The coke is later burnt in the regenerator releasing sulfur into the discharged flue gas as SO<sub>2</sub>. In the present work, comprehensive emission inventories for a fluid catalytic cracking unit in a typical oil refinery are prepared. These inventories are based on calculations that assume complete combustion of catalyst coke in the regenerator. Yearly, material balances for both SO<sub>2</sub> and particulate matters emissions are carried out taking into account seasonal variations in the operation of the process unit. The results presented in this article reflect the variation of sulfur in feedstock originating from various units in the refinery. The refinery operations are not dependant on seasons but controlled by market-driven conditions to maximize the profit. The seasonal

impact on refinery emissions is minimal due to its operation at optimum capacity fulfilling the international market demand. The data presented and analyzed here can be used to assess the hazardous impact of SO<sub>2</sub> and particulate matter emissions on surrounding areas of the refinery.

**Keywords** Emissions inventory · Particulates · SO<sub>2</sub> · FCC · Material balance

## Nomenclature

$F$	feed (T/h)
$L$	total liquid products (T/h)
$G$	total gas products (T/h)
$E$	total emission (T/h)
$A$	total air feed (T/h)
$M$	fresh catalyst (T/h)
$L_2$	is heavy cycle oil
$x_{F1}$	sulfur weight fraction in liquid feed
$x_{j1}$	sulfur weight fraction in liquid products
$x_{j2}$	PM weight fraction in HCO
$y_{j1}$	sulfur weight fraction in gaseous products
$y_{E1}$	sulfur weight fraction in flue gases
$y_{E2}$	PM weight fraction in flue gases

---

W. Yateem (✉) · V. Nassehi  
Department of Chemical Engineering,  
Loughborough University,  
Leicestershire, UK  
e-mail: w.yateem@lboro.ac.uk

A. R. Khan  
Department of Environment Technology and Management,  
College for Women, Kuwait University,  
Safat, Kuwait

## 1 Introduction

Ever-increasing demand for fossil fuels resulting from industrial and economic growth in the modern world

has forced the utilization of the state-of-the-art technologies by petroleum refining industry to obtain maximum yield. However, the environmental impact of the unit operations used in this industry is an issue that requires constant monitoring. In this respect, the main operation to be considered is processing of crude oil, which yields many valuable products such as gasoline, diesel, aviation turbine kerosene, liquefied petroleum gas, and others. Fluid catalytic cracking unit (FCC) has been one of the most important conversion processes since 1942. This process, which has developed considerably over the years, allows refineries to utilize their crude oil resources more efficiently.

Maya-Yescasa et al. (2004) described the FCC of heavy ends as a common practice in the oil refining industry, which produces highly valuable fuels. After 60 years of evolution, FCC has become one of the most important oil refining processes (Fig. 1). Currently, FCC operates in constrained regions of medium to high conversion, using synthetic catalysts.

The main objective of FCC unit is to upgrade the low-value feedstock to more valuable products. Its heavy feedstock (vacuum gas oil, coker gas oil, unconverted oil, and waxy distillate), coming from vacuum unit, delayed coker unit, and crude distillation units, respectively, is catalytically cracked into lighter products (liquefied petroleum gas, gasoline, diesel, and fuel oil). Environmental concerns about this process have increased during the last 10 years, because of its great contribution of sulfur oxides and particulate matters (PMs) emissions.

Chen (2006) demonstrated the FCC process technology as a primary conversion unit in the most refineries. It converts low-value heavy ends of the crude

oil into a variety of higher-value, light products. The primary function of FCC units is to produce gasoline. About 45% of worldwide gasoline production comes either directly from FCC units or indirectly from combination with downstream units, such as alkylation.

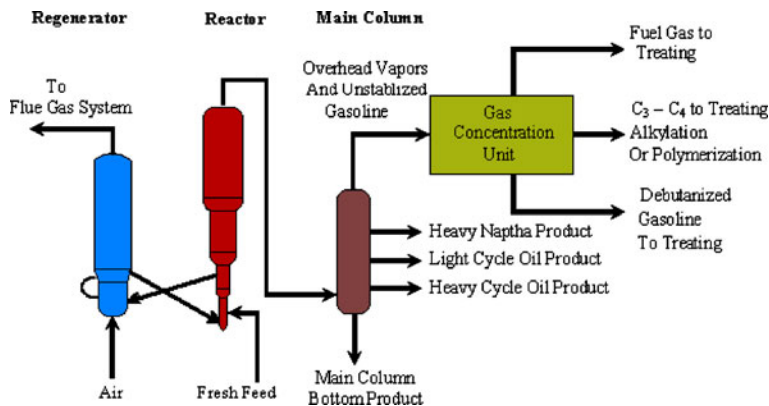
Venuto and Habib (1978) showed the most common FCC feedstock as a blend of gas oils, from vacuum and atmospheric distillation and delayed coking. Due to the inherent desulfurization during cracking reactions, that results of breaking of the C–S bonds in the feedstock. Sulphur in the feedstock distributes mainly to cyclic oils, gasoline, hydrogen sulphide, and coke.

The major units in the FCC process are discussed as a feed preheat section, reactor-regenerator section, main fractionator, and gas concentration section.

In the reactor, the catalytic cracking endothermic reaction takes place, and a catalyst is recovered from all products by passing through a set of multistage cyclones. The collected catalyst is sent to the regenerator. The coke impregnated catalyst is reactivated by combustion process producing SO<sub>2</sub>. This process is exothermic and energy generated and carried with the catalyst to the reactor to facilitate the endothermic catalytic cracking reaction.

Mitchell et al. (1993) studied the deposition of coke onto the catalyst particle during the oil cracking process and the impurities such as metal compounds, which are also deposited on the surface of the catalyst. Nickel, iron, vanadium, and sodium are just a few of the main contaminants that are deposited onto the catalyst particle. These contaminant metals lead to premature catalyst deactivation and the propagation of undesirable reactions, which reduce the quality of the product.

Fig. 1 FCC process



Whitcombe et al. (2003) studied the formation of fines in a fluidized catalytic cracker unit (FCCU) due to catalyst attrition, and fracture is a major source of catalyst loss. In addition to the generation of fine particles, a significant amount of aerosols have been identified in the stack emission of FCCUs. It was found that major quantities of metal-rich aerosols were generated by the thermal shock. This production of fine particles and aerosols is a new phenomenon that can help explain excessive catalyst emissions from operating FCCUs. The addition of cold makeup catalyst stream to the regenerated hot catalyst enhances attrition resulting into large quantity of fines that result into the increase of PM emissions.

The high heat transfer coefficients for fluidized systems are responsible for the temperatures uniformity within the reactor and help to provide a proper control of the system. The regenerator objective restores the catalyst activity and supplies heat to the reactor by burning off the coke deposited on the spent catalyst, whereas the main purpose of the fractionators is to desuperheat and recover liquid products from the products vapor. It accomplishes the fractionation by condensing and revaporizing the hydrocarbon vapors as they flow upward. Apart from the bottom product, which is called heavy cycle oil (HCO), the other products from the main column are light cycle oil (LCO), distillate, heavy gasoline, and the overhead vapors, which are unstabilized gasoline and lighters. The deposited sulfur in the coke leaves the FCC process as flue gas from the regenerator in the form of SO<sub>2</sub>, whereas SO<sub>2</sub> typically accounts for 80% to 90% of total SO<sub>2</sub>.

Akeredolu (1989) discussed the air pollution sources in Nigeria. PM constitutes the major atmospheric pollution problem. Both anthropogenic and nonanthropogenic sources of PM were found to be important. The Harmattan dust haze constitutes the largest anthropogenic source of PM. Severe visibility reduction and increased incidence of respiratory and chest congestion complaints are recorded during the Harmattan season. Dust remobilization resulting from vehicular traffic on unpaved as well as on unswept paved roads and from fugitive emissions from open surfaces and biomass burning are the major non-anthropogenic sources of PM. Industries generate and emit particulate as well as gaseous pollutants, which have manifested significant negative impact at local levels. Atmospheric environment problems such as air pollution and thermal stress are growing in many

tropical countries partly on account of their rapid rate of industrialization/urbanization which outpaces the urban planning process.

## 2 Fluid Catalytic Cracking Process

In the present work, emission inventories from FCC unit in an oil refinery are calculated. Mainly both SO<sub>2</sub> and PMs have been evaluated accurately for a period of 1 year considering seasonal variations in the operational condition of the FCC unit in a refinery.

Hot feedstock is charged into the reactor through riser where it comes in contact with hot regenerated catalyst from regenerator. The feedstock vaporizes at a temperature of 730°C and catalytically cracked in the reactor. The velocity of the vapor drops in the reactor, due to expansion from riser to the main reactor. The reaction takes place in fluidized bed reactor with uniform temperature. Products with catalyst pass through a set of cyclones to separate the catalyst fines from the products. The spent catalyst from cyclones is returned to the reactor. The coke- and sulfur-impregnated catalyst is then sent to a regenerator to restore its activity. Excess air is fed to the regenerator for complete combustion of coke and sulfur in a fluidized process producing flue gas. The flue gas passes through cyclone to recover catalyst particles. Attired catalyst fines are discharged with the exit gas. Flue gas consists of SO<sub>2</sub>, CO<sub>2</sub>, N<sub>2</sub>, O<sub>2</sub>, and fines. The activated catalyst at 730°C is recharged to the reactor, and makeup stream is added to compensate the catalyst loss in the flue gas. The products are sent to the fractionator for further separation.

## 3 Material Balance

To evaluate each stream in FCC unit, overall material balance is established in mass flow rate (T/h; Fig. 2).

$$F + M + A = L + G + E \quad (1)$$

where  $F$  is the total feed consisting of heavy ends from various refining units;  $M$  is makeup catalyst stream;  $A$  is the air supplied to the regenerator;  $G$  is a mixture of gaseous products (LPG and Off gas);  $L$  is a liquid product;  $E$  is the flue gas consisting of CO<sub>2</sub>, N<sub>2</sub>, SO<sub>2</sub>, O<sub>2</sub>, and PMs.



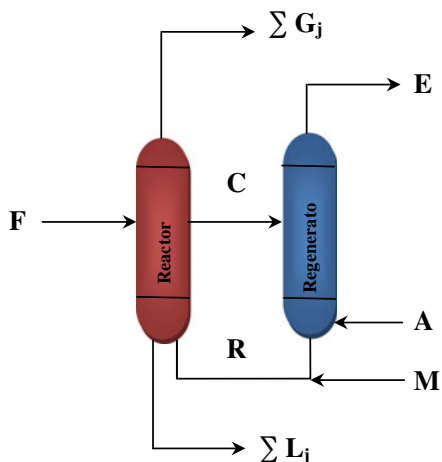


**Fig. 2** Overall material balance around reactor and regenerator

To calculate the emissions, material balance of *i*th component around the FCCU is considered:

For sulfur balance, *i*=1:

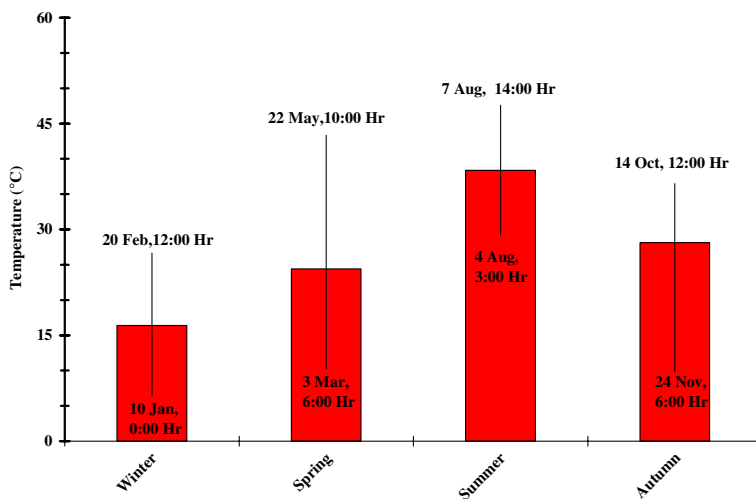
$$F \times x_{F1} = \sum (L_j \times x_{1j}) + \sum (G_j \times y_{1j}) + E \times y_{E1} \tag{2}$$

For PM balance, *i*=2:

$$M = L_j \times x_{2j} + E \times y_{E2} \tag{3}$$

The operational data for 24th of March 2007 are given as total feed equal to 255.1 T/h, with sulfur composition ( $x_{F1}$ ) equal to 0.008. Total liquid and gaseous products are 173.6 and 62.3 T/h, respectively.

**Fig. 3** Hourly maximum, minimum, and seasonal average temperatures in Kuwait



Air fed to the regenerator is calculated based on complete combustion of all coke and sulfur to produced SO<sub>2</sub> and CO<sub>2</sub> with 10% excess and is equal to 233.04 T/h. Total emission is calculated using Eq. 1, with known amount of catalyst makeup stream of 0.1 T/h.

$$E = 255.1 + 0.1 + 233.04 - 173.6 - 62.3 = 252.4 \text{ T/h} \tag{4}$$

Sulfur in flue gas, *E* (252.4 T/h) is calculated using Eq. 2:

$$E y_{E1} = (255.1 \times 0.008) - 0.614 - 0.204 = 1.222 \text{ T/h.} \tag{5}$$

SO<sub>2</sub> emission is equal to  $= 1.222 \frac{64}{32} = 2.444 \text{ T/h}$

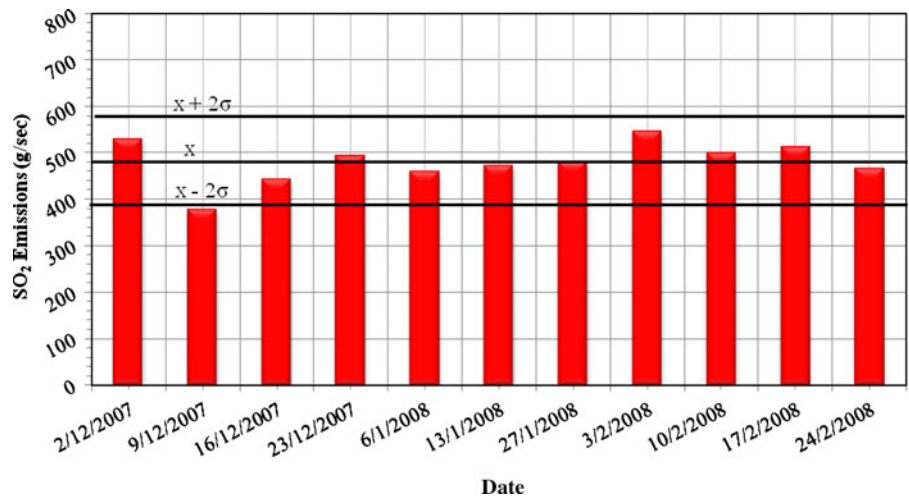
PMs in flue gas, *E* (252.4 T/h) is calculated using Eq. 3:

$$E y_{E2} = 0.1042 - 0.0007 = 0.1035 \text{ T/h} \tag{6}$$

### 4 Results and Discussion

SO<sub>2</sub> and PM emissions inventories during the period from December 2007 to November 2008 are calculated for four different seasons. Kuwait is located in the north east of Arabian Peninsula and has four seasons, starting winter season from December till end of February, followed by spring season from March to May. Summer season starts from June till

**Fig. 4** SO<sub>2</sub> emission rates (in grams per second) for winter season



August, followed by autumn season from September to November. Figure 3 illustrates the seasonal temperature variation for the year 2008. In winter season, hourly minimum temperature is 6°C recorded on 10th of January at 0000 hour and the hourly maximum temperature is 26.5°C on 20 February at 1200 hour. The average seasonal temperature in winter is 16°C. The hourly minimum temperature for spring season is 14.5°C measured on 3rd of March at 0600 hour, and the hourly maximum temperature measured is 43°C on 22nd of May at 1000 hour. The average seasonal temperature in spring is 25°C. In the summer season, hourly minimum temperature is 32°C observed on 4th of August at 0300 hour, and the hourly maximum observed in the same season is 48°C on 7th of August at 1400 hour. The average seasonal temperature in summer is 40°C. The hourly minimum temperature recorded in autumn season is 9°C on 24th

of November at 0600 hour, and the hourly maximum temperature recorded is 35.5°C on 14th of October at 1200 hour. The average seasonal temperature in the autumn is 28°C.

Figures 4, 5, 6, 7, 8, 9, 10, 11 show all the emission variation of SO<sub>2</sub> and PM for different seasons respectively.

In winter season, the emission rates are evaluated from operational data for 11 weeks; the maximum value is 529.2 g/s on 2nd of December 2007, and the minimum value is 376.4 g/s on 9th of December 2007. The emission rate for the entire period is  $479.3 \pm 2\sigma$  g/s, where standard deviation is equal to 45.9 g/s. SO<sub>2</sub> emissions rates for spring season are observed providing maximum value of 679.17 g/s on 24th of March 2008, which is higher than the winter maximum emission rate. The minimum calculated value is 356.39 g/s on 26th of May 2008, which is lower than

**Fig. 5** SO<sub>2</sub> emission rates (in grams per second) for spring season

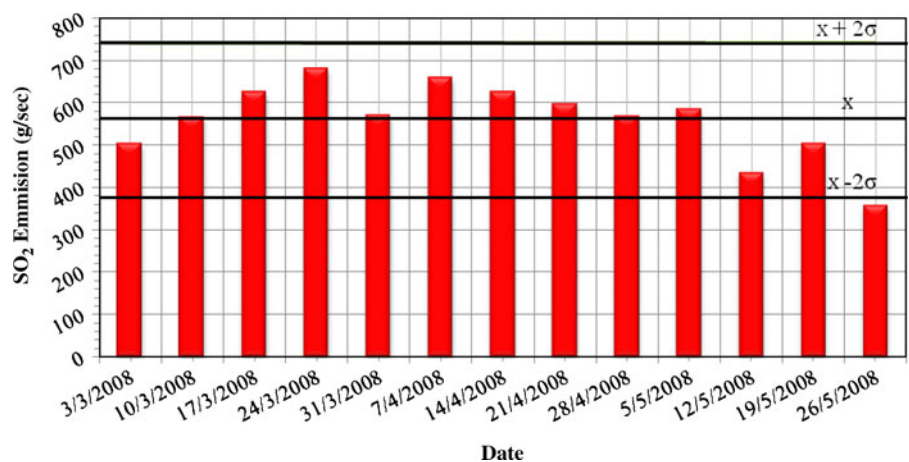
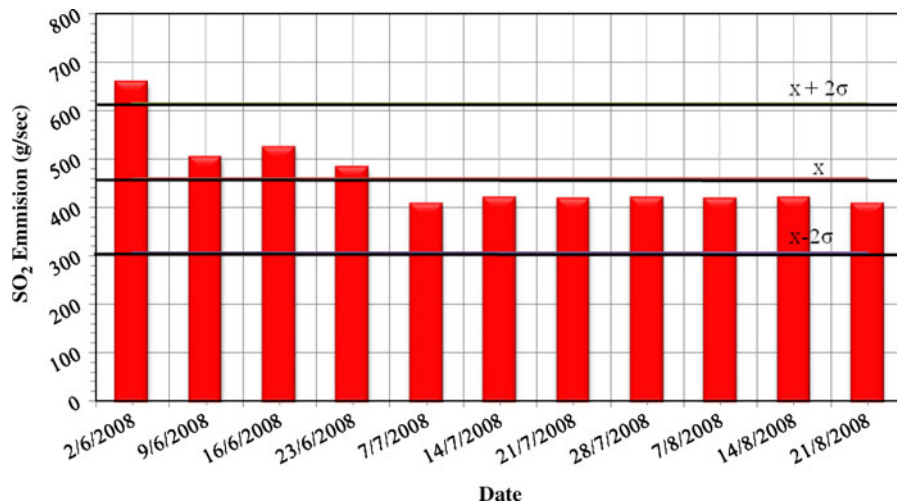


**Fig. 6** SO<sub>2</sub> emission rates (in grams per second) for summer season



the winter minimum value. The emission rate for 13 weeks is  $559.1 \pm 2 \sigma$  g/s, where standard deviation is equal to 90.42 g/s. The maximum value for SO<sub>2</sub> emissions rates is found to be 654.17 g/s on 2nd of June 2008, which is lower than the spring maximum value but higher than the winter maximum value. For the summer season, the minimum emission rate is 403.89 g/s same on 7th of July and 21st of August 2008, which is higher than both winter and spring minimum values. For summer season, the emission rate calculated for 11 weeks is  $458.30 \pm 2 \sigma$  g/s, where standard deviation is equal to 77.04 g/s. SO<sub>2</sub> emissions rates for autumn season are evaluated for 12 weeks. The maximum value is 653.4 g/s on 23rd of September

2008, which is almost similar to maximum value during spring season. The minimum computed value is 357.17 g/s on 5th of October 2008, which is similar to the minimum value of spring season. The emission rate for whole autumn period is  $540.1 \pm 2 \sigma$  g/s, where standard deviation is equal to 91.51 g/s.

In winter season, emission rates are consistent with minimum fluctuation, while in spring season, the emission rates are high in the beginning of the season then decreasing gradually, whereas in summer season, the emission rates are high at the start of the season and later become almost constant. Finally, variation in emission rates is lower in beginning of the autumn season then increased. The highest and the lowest

**Fig. 7** SO<sub>2</sub> emission rates (in grams per second) for autumn season

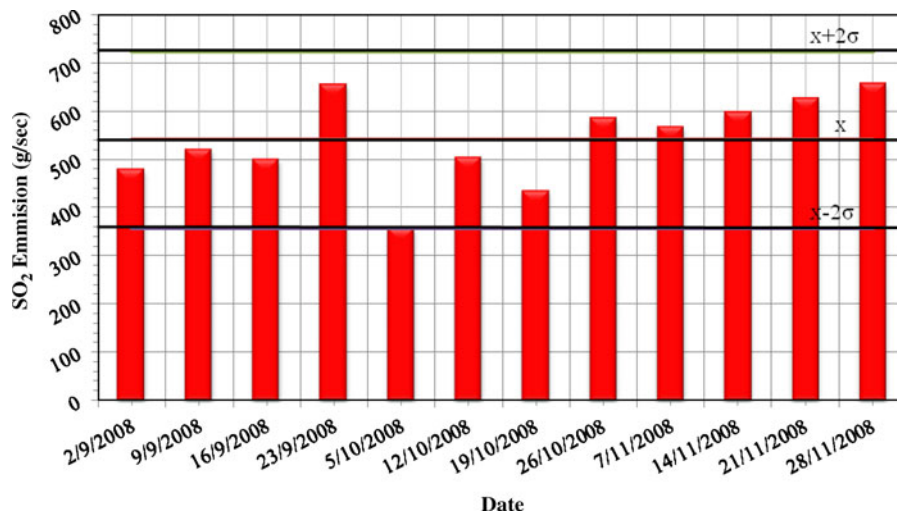
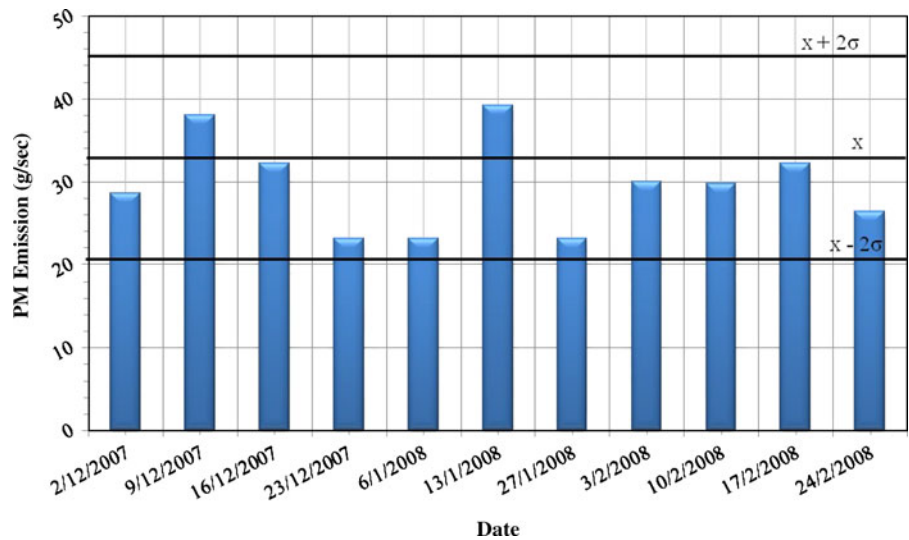


**Fig. 8** PM emissions rates (in grams per second) for winter season



emission rates in all seasons reflect the operational conditions, mainly sulfur contents in the feedstock and the total amount of heavy ends charged to the FCCU.

Similarly, the PM emissions related to the process operating conditions. Figures 8, 9, 10, 11 show the behavior of PM emissions during different seasons. The maximum value is 39.17 g/s on 13th of January 2008 and the minimum value is 23.06 g/s on 23rd of December 2007 for winter season. The emission rate in this season is  $26.6 \pm 2 \sigma$  g/s, where standard deviation is 5.63 g/s. Similarly, PM emission rates for spring season are calculated providing maximum value of 28.06 g/s on 17th of March 2008, which is lower than winter maximum value. The minimum value is 23.89 g/s on two occasions, 12th and 26th of May

2008. The emission rate for 13 weeks is  $25.45 \pm 2 \sigma$  g/s, where standard deviation is equal to 1.79 g/s. the minimum calculated values for both winter and spring seasons are almost similar. For summer season, the maximum value for PM emissions rates is 26.39 g/s on three consecutive occasions, 2nd, 9th, and 16th of June 2008, whereas the minimum computed value is 18.06 g/s on 14th of July and 14th of August 2008. The emission rate calculated for 11 weeks is  $21.72 \pm 2 \sigma$  g/s, where standard deviation is equal to 3.41 g/s. Finally, PM emissions rates for autumn season are evaluated for 12 weeks. The maximum value found to be 26.7 g/s on three consecutive occasions, 09th, 16th, and 23rd of September 2008, while the minimum computed value is 23.5 g/s on 5th and 19th of October

**Fig. 9** PM emissions rates (in grams per second) for spring season

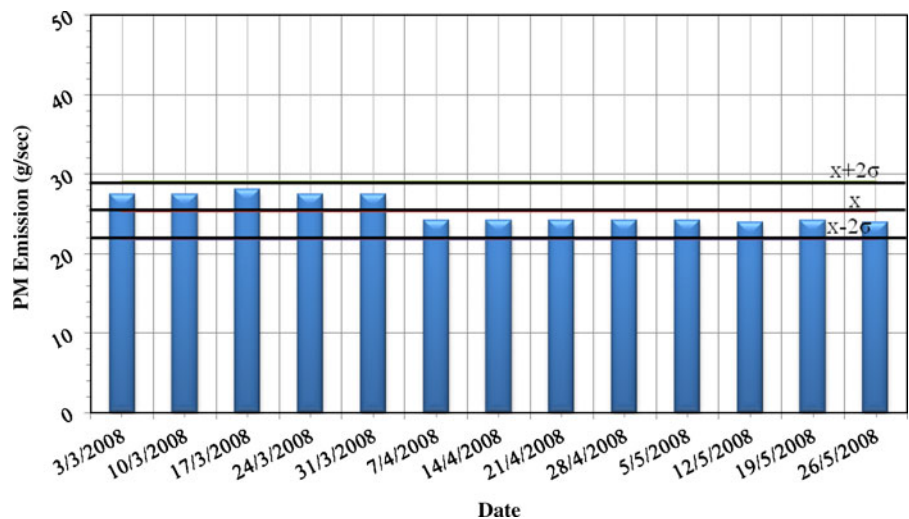
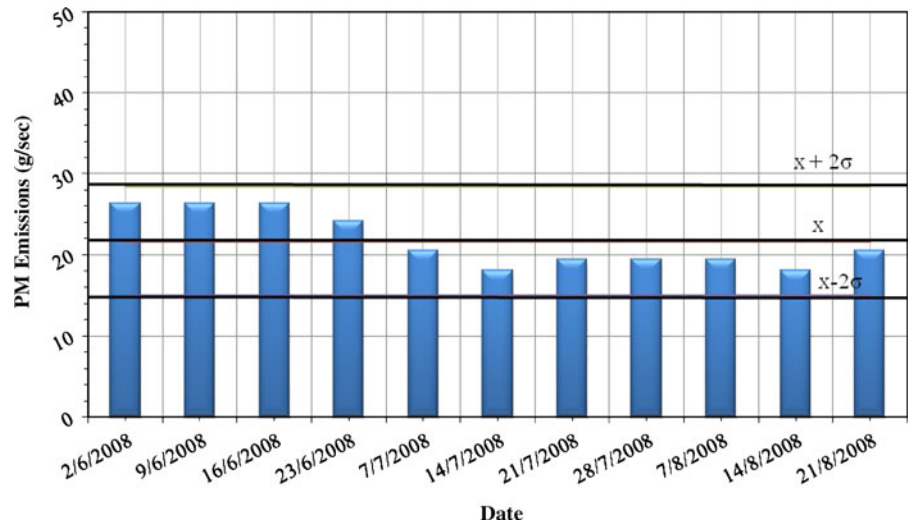


**Fig. 10** PM emissions rates (in grams per second) for summer season



2008. The emission rate for whole autumn period is  $24.68 \pm 2 \sigma$  g/s, where standard deviation is equal to 1.040 g/s. The highest PM maximum value is in the winter season and the lowest value is in the summer season, while minimum emission rate is similar to the maximum emission values, high in winter and low summer seasons.

## 5 Conclusions

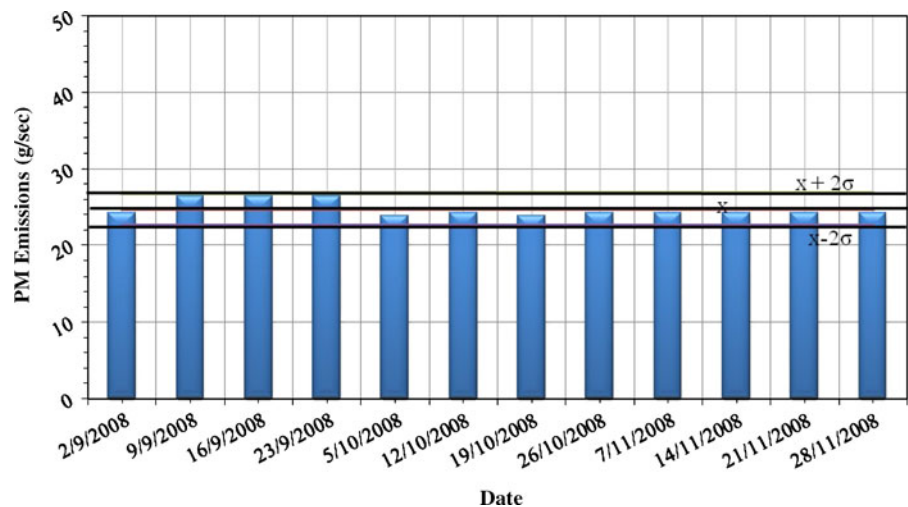
FCC unit in a refinery is a major contributor of  $\text{SO}_2$  and PM emissions, which are responsible for adverse impact on the immediate neighborhood of the refinery. A complete comprehensive emission inventories for a

yearlong period have been prepared for both  $\text{SO}_2$  and PMs. The refinery operations are not dependant on seasons but controlled by market-driven conditions to maximize the profit. The seasonal impact on refinery emissions is minimal due to its operation at optimum capacity fulfilling the international market demand.

$\text{SO}_2$  emissions are high in spring, while PM emissions are high in winter, mainly due to operational conditions that are dependent on feed rate and sulfur contents in the feed. PM emissions are mainly due to high attrition of cold makeup catalyst charge and operating conditions, vapor velocity particle velocity, particle collision, and particle degradation.

These inventories will be used in air dispersion model to thoroughly investigate the impact of FCC

**Fig. 11** PM emissions rates (in grams per second) for autumn season



# Fluid Catalytic Cracking Unit Emissions and Their Impact

Wael H. Yateem · Vahid Nassehi ·  
Abdul Rehman Khan

Received: 12 June 2010 / Accepted: 18 August 2010  
© Springer Science+Business Media B.V. 2010

**Abstract** Fluid catalytic cracking unit is of great importance in petroleum refining industries as it treats heavy fractions from various process units to produce light ends (valuable products). FCC unit feedstock consists of heavy hydrocarbon with high sulfur contents, and the catalyst in use is zeolite impregnated with rare earth metals, i.e., lanthanum and cerium. Catalytic cracking reaction takes place at elevated temperature in fluidized bed reactor generating sulfur-contaminated coke on the catalyst with large quantity of attrited catalyst fines. In the regenerator, coke is completely burnt producing SO<sub>2</sub>, PM emissions. The impact of the FCC unit is assessed in the immediate neighborhood of the refinery. Year-long emission inventories for both SO<sub>2</sub> and PM have been prepared for one of the major petroleum refining industry in Kuwait. The corresponding comprehensive meteorological data are obtained and preprocessed using Aermot (Aermod preprocessor). US EPA approved dispersion model, Aermod, is used to predict ground level concentrations of both pollutants in the selected

study area. Model output is validated with measured values at discrete receptors, and an extensive parametric study has been conducted using three scenarios, stack diameter, stack height, and emission rate. It is noticed that stack diameter has no effect on ground level concentration, as stack exit velocity is a function of stack diameter. With the increase in stack height, the predicted concentrations decrease showing an inverse relation. The influence of the emission rate is linearly related to the computed ground level concentrations.

**Keywords** Dispersion model · Aermod · Emissions · FCC · Pollutants exceedance

## 1 Introduction

Fluid catalytic cracking (FCC) of heavy ends into high value liquid fuels is a common practice in the oil refining industry. In this process the heavy feedstock containing sulfur as a major contaminant is cracked to light products. Sulfur is redistributed in the liquid and gaseous products and coke on the catalyst. In the regenerator coke with sulfur contamination is completely burnt and flue gas containing SO<sub>2</sub> is discharged. In the present work, a comprehensive emission inventories from FCC unit in an oil refinery have been prepared. These inventories are calculated based on complete combustion of sulfur and coke impregnated on the catalyst in the regenerator. Mainly

---

W. H. Yateem (✉) · V. Nassehi  
Department of Chemical Engineering,  
Loughborough University,  
Leicestershire LE11 3TU, UK  
e-mail: w.yateem@lboro.ac.uk

A. R. Khan  
Department of Environment Technology and Management,  
College for Women, Kuwait University,  
Kuwait, Kuwait



for both SO<sub>2</sub> and particulate matters (PM) emission rates are calculated accurately using material balance for a year-long period considering seasonal variations in the operation of the process unit in one of the main refining industry in Kuwait (Yateem et al. 2010). These results reflect the variation of sulfur in feedstock that comes from various refinery units. SO<sub>2</sub> and PM emission inventories are completed and used in dispersion model to assess their impact on the immediate surroundings of the refinery.

The most advanced dispersion model Aermod has been selected for prediction ground level concentration of SO<sub>2</sub> and PM based on comprehensive year-long emission inventories of FCC unit.

Aermod is a dispersion model that uses Gaussian distribution for the stable conditions and non-Gaussian probabilities density function for the unstable conditions. Aermod has two preprocessors; Aermet that provides planetary boundary layer parameters over a high altitude to yield accurate predicted concentration values for a given meteorological conditions. It can accommodate large meteorological data (multiple years). Aermap generates regular receptors over a given terrain for the evaluation of pollutants ground level concentrations.

The meteorological data for year 2008 are obtained and are used in preprocessor Aermet to generate planetary boundary layer parameters. These generated data are used in Aermod for fixed emission rate to assess the influence of prevailing meteorological conditions at this particular site. Aermod has been used for actual year-long inventories to predict ground level concentrations and validate the model by comparing the results against the recorded values from Kuwait Environmental Public Authority (K-EPA) monitoring stations.

## 2 Background

Heavy fractions from different refining units are cracked in FCC unit to useful products, generating SO<sub>2</sub> and PM emissions. SO<sub>2</sub> emission inventory is prepared from elemental sulphur balance over the unit, Yateem et al. (2010).

Whitcombe et al. (2003) showed the formation of fines in a fluidized catalytic cracker unit due to catalyst attrition and fracture as a major source of

catalyst loss. The petroleum industry employs fluid catalytic cracker units (FCCUs) as the major tool to produce gasoline from crude oil. At the center of this unit is regenerator which is used to burn coke from the surface of the spent catalyst. As the regeneration process is very turbulent, a large amount of catalyst material is discharge to the atmosphere. In addition to the fine particles present in the catalyst, the turbulent conditions inside the FCC alter the particle size distribution of the catalyst generating fine particles and significant amount of aerosols, which has been identified in the stack emission of FCCUs.

Caputo et al. (2003) conducted an inter-comparison between Gaussian, Gaussian-segmented plumes, and Lagrangian codes. Gaseous emissions are simulated under real meteorological conditions for dispersion models Aermod, HPDM, PCCOSYMA, and HYSPLIT. The Aermod and HPDM meteorological preprocessors results are analyzed, and the main differences found are in the sensible heat flux (SHTF) and  $u^*$  (friction velocity) computation, which have direct effect on the Monin–Obukov length and mixing height calculation. Gaussian models (Aermod, HPDM) computed the dispersion parameters by using the similarity relationships, whereas Gaussian-segmented model (PCCOSYMA) used P–G stability class to evaluate these parameters. Lagrangian transport model (HYSPLIT) advected the puff and calculated its growth rate with local mixing coefficients. Meteorological parameters have great effect on the performance of air dispersion models. Therefore, Aermod and HPDM have developed effective and sophisticated meteorological parameters preprocessors. It is noticed that HPDM computed the most stable condition and the lowest mixing height. The comparison also showed a significant discrepancy between HPDM and other Gaussian models. The maximum ground level concentration predicted by Aermod, HPDM, and PCCOSYMA are similar.

Rama Krishna et al. (2004) examined the assimilative capacity and the dispersion of pollutants resulted from various industrial sources in the Visakhapatnam bowl area, which is situated in coastal Andhra Pradesh, India. Two different air dispersion models (Gaussian plume model, GPM, and ISCST-3) are used to predict ground level concentrations of sulfur dioxide and oxides of nitrogen and assimilative capacity of the Visakhapatnam bowl area's atmosphere for two seasons, namely, summer and winter.

The computed 8-h-averaged concentrations of the two pollutants obtained from the GPM and ISCST-3 are compared with those monitored concentrations at different receptors in both seasons and the validation carried out through Q–Q plots. Both model outputs showed similar trend with the observed values from the monitoring stations. The GPM output showed over-prediction, whereas the ISCST-3 showed underprediction in comparison with the observed concentrations. Terrain features and land/sea breeze influences are not considered in this study, which strongly affected the models outputs.

Venkatram et al. (2004) evaluated dispersion models for estimating ground level concentrations in the vicinity of emission sources in the urban area of university of California, Riverside. Aermot-PRIME and ISC-PRIME dispersion models are used to predict SF<sub>6</sub> at different receptors, where SF<sub>6</sub> is used as tracer in a simulated non-buoyant release from a small source in urban area. Both models output are compared with hourly observed concentrations. The comparison showed that both models overestimate the highest concentrations, whereas lower range of concentrations is underestimated. It is concluded that Aermot can predict reliable concentrations if turbulent velocity measurements are used to estimate plume dispersion.

Lopez and Mandujano (2005) assessed the impact of natural gas and fuel oil consumption on the air quality in an Industrial Corridor, Mexico to determine the optimal NG and fuel oil required to reduce SO<sub>2</sub> concentration. Air dispersion model Aermot is used to compute ground level concentration of SO<sub>2</sub>. Model output is then validated against SO<sub>2</sub> field measurements. Different hypothetical emission scenarios are performed to examine the impact of NG and fuel oil mixture. The obtained results in this work indicate that dispersion model Aermot presented good correlation with the measured concentrations. It is also concluded that increasing 40% of NG consumption will reduce SO<sub>2</sub> concentration by 90%.

Kesarkar et al. (2007) studied the spatial variation of PM<sub>10</sub> concentration from various sources over Pune, India. Gaussian air pollutant dispersion model Aermot is used to predict the concentration of PM<sub>10</sub>. Weather research and forecasting model is used to furnish Aermot with planetary boundary layer and surface layer parameters required for simulation. Emission inventory has been developed and field-

monitoring campaign is conducted under Pune air quality management program of the ministry of Environment and Forests. This inventory is used in Aermot to predict PM<sub>10</sub>. A comparison between simulated and observed PM<sub>10</sub> concentration showed that the model underestimated the PM<sub>10</sub> concentration over Pune. However, this work is conducted over a short period of time, which is not sufficient to conclude on adequacy of regionally averaged meteorological parameters for driving Gaussian models such as Aermot.

Isakov et al. (2007) examined the usefulness of prognostic models output for meteorological observations. These model outputs are used for dispersion applications to construct model inputs. Dispersion model Aermot is used to simulated observed tracer concentrations from Tracer Field Study conducted in Wilmington, California in 2004. Different meteorological observation sources are used, i.e., onsite measurements, National Weather Services (NWS), forecast model output from ETA model, and readily available and more spatially resolved forecast model from MM5 prognostic model. It is noted that MM5 with higher grid resolution than ETA performed better in describing sea breeze related to flow patterns observed and provided adequate estimates of maximum mixed layer heights observed at the site. It is concluded that MM5 and ETA prognostic models provided reliable meteorological inputs for dispersion models such as Aermot because wind direction estimates from forecast models are not reliable in coastal areas and complex terrain. Therefore, comprehensive prognostic meteorological models can replace onsite observations or NWS observations.

Abdul Wahab et al. (2002) studied the impact of SO<sub>2</sub> emissions from a petroleum refinery on the ambient air quality in Mina Al-Fahal, Oman. Dispersion model ISCST is used to predict SO<sub>2</sub> ground level concentration. The study is performed over a period of 21 days. Computed SO<sub>2</sub> concentrations are compared with the measured values of SO<sub>2</sub> for maximum hourly average concentration, maximum daily concentration, and total period average concentration. It is noted that the model output under-predicted the SO<sub>2</sub> concentration for all the three cases due to unavailability of background concentrations and the presence of more dominant sources. Based on the maximum daily average concentration and the total period maximum concentration, the



model underpredicted the average measured concentration by 31.77% and 41.8%, respectively. The model performed slightly better based on maximum hourly average concentration and underpredicted by 10.5%.

Zou et al. (2010) evaluated the performance of Aermid in predicting SO<sub>2</sub> ground level concentration in Dallas and Ellis counties in Texas as these two counties are populous and air pollution has been a concern. Two emission sources are considered in this study, i.e., point sources and on-road mobile sources. Aermid is used to calculate the hourly planetary boundary layer parameters such as Monin–Obikhov length, convective scale, temperature scale, mixing height, and surface heat flux. Dispersion model Aermid is used to simulate SO<sub>2</sub> ground level concentration at different time scale, i.e., 1, 3, and 8 h, daily, monthly, and annually for both counties separately. The results are validated with the observed concentrations. The results showed that Aermid performed well at the 8 h, daily, monthly, and annual time scale when combined point, and mobile emission sources are used in the simulation as model input. It is also noticed that Aermid is performed much better in simulating the high end of the spectrum of SO<sub>2</sub> concentrations at monthly scale than at time scales of 1, 3, and 8 h and daily.

Alrashidi et al. (2005) studied the locations of K-EPA monitoring station, which measure SO<sub>2</sub> concentrations emitted from the power stations in the state of Kuwait. The major sources of SO<sub>2</sub> emissions in Kuwait are from west Doha, east Doha, Shuwaikh, Shuaiba, and Az-Zour power stations. The Industrial Source Complex Short Term dispersion model is used to predict SO<sub>2</sub> ground level concentrations over residential areas. Year-long meteorological data are obtained from Kuwait International Airport and used in the simulation of the dispersion model. Different discrete receptors in the residential areas are selected. It is observed that the weather pattern in Kuwait, specially the prevailing wind direction, has strong influence on the ground level concentration of SO<sub>2</sub> in the residential areas located downwind of the both east and west Doha stations. The comparison between the predicted and the measured concentrations of SO<sub>2</sub> from the monitoring stations located at the major populated areas showed that most of these monitoring stations locations are not adequate to measure SO<sub>2</sub> concentrations emitted from the power stations.

Therefore, relocation of the monitoring stations is highly recommended to accurately record the highest ground level concentrations of SO<sub>2</sub> emitted from the power stations in Kuwait.

### 3 Model Application

#### 3.1 Input Data

Aermid dispersion model implementation requires three main input data. These are:

1. Source information: This includes pollutant emission rate (g/s), location coordinates in Universal Transverse Mercator (UTM; m), base elevation from the sea level (m), stack height (m), exit stack inner diameter (m), exit stack gas velocity (m/s), and exit stack gas temperature (°K).
2. Meteorological information for the region of interest: This includes anemometer height (m), wind speed (m/s), wind direction (flow vector from which the wind is blowing; in degrees clockwise from the north), ambient air temperature (°C), stability class at the hour of measurement (dimensionless), and hourly mixing height (m).
3. Receptor information: This can be specified or generated by the program to predict the pollutants' concentrations at the selected receptors.

The entire required source input data are obtained from FCC unit in the refinery. A stack of 80 m height, an inner diameter of 2.3 m, with an average exit gas velocity of 20 m/s and exit gas temperature of 550°K are fed into the model. Monthly emission variation is considered with total SO<sub>2</sub> emission rate of 6,089.2 g/s and total PM emission rate of 302 g/s as presented in detail (Yateem et al. 2010).

#### 3.2 Area of Study

The area of study in this work covers portion of Ahmadi governorate in the state of Kuwait. Fahaheel area is adjacent to the petroleum refinery has one of the Kuwait EPA air quality monitoring station located at a polyclinic. Both areas Fahaheel and Ahmadi are surrounded by arid desert in the west side and bordered by the Gulf from the east.

Two different types of receptor coordinates are used as input to the Aermol model to predict the ground level concentration of SO<sub>2</sub>, these are:

1. Discrete Cartesian receptors specified at the sensitive areas viz., a school, a shopping area, and EPA monitoring stations in Fahaheel. A hospital and petroleum services companies' offices are selected in Ahmadi.
2. Uniform Cartesian grid receptors covering the entire area of study where the FCC stack (emissions source) is located almost in the center of the mesh grid.

The receptors selected are based on the actual sites in a UTM location coordinate of the area of interest map. Table 1 shows the selected discrete receptors information.

The uniform grid receptors of a total 1,764 (42×42) were divided into ( $\Delta x=300\text{ m}\times\Delta y=250\text{ m}$ ) to cover about 12×10 km area of study. The optimum selection of the mesh size is based on the computational accuracy and time.

#### 4 Results and Discussion

A year-long comprehensive meteorological data are processed by Aermol to generate boundary layer parameters and to pass all meteorological observations to Aermol.

Figure 1 shows wind direction and magnitude for a period of year 2008. It is observed that most of the time, the prevailing wind direction is from north west. There is strong influence from the neighboring Gulf as the refinery is located at the coast, resulting into strong sea breeze blowing from east direction. Wind class frequency distribution for the entire year confirming 2% calm conditions, while 39.8% is between 3.6 and 5.7 m/s. The highest wind class 8.8–11.1 m/s is less than 1%.

A model run is performed for actual monthly emission variation with total annual SO<sub>2</sub> emission rate of 6,089.2 g/s and total PM emission rate of 302 g/s independently. Monthly emission factors for both pollutants are tabulated in Tables 2 and 3, respectively.

A discrete receptor is selected at Kuwait Environmental Public Authority monitoring station located at polyclinic in Fahaheel area. Concentrations of SO<sub>2</sub>, NO<sub>x</sub>, H<sub>2</sub>S, O<sub>3</sub>, CO, CO<sub>2</sub>, methane, non-methane hydrocarbon, benzene, toluene, xylenes, ethylbenzene, total suspended particulates, and meteorological parameters are continuously recorded on hourly basis.

Hourly predicted ground level concentrations at specified discrete receptor showed large scatter due to variation in meteorological conditions and the recorded values influenced by the contribution of various emission sources, resulting into specific background concentration that has made the comparison impracticable. There is large fluctuation in the background concentration, which is difficult to quantify. Hence, zero background concentration has been assumed to resolve this uncertainty. Therefore, daily average measured concentrations of SO<sub>2</sub> were compared with the daily predicted concentrations to validate the model output.

Figure 2 shows the plot between the measured top 20 daily average values vs. the daily predicted top 20 values at the discrete receptor, Kuwait EPA monitoring station.

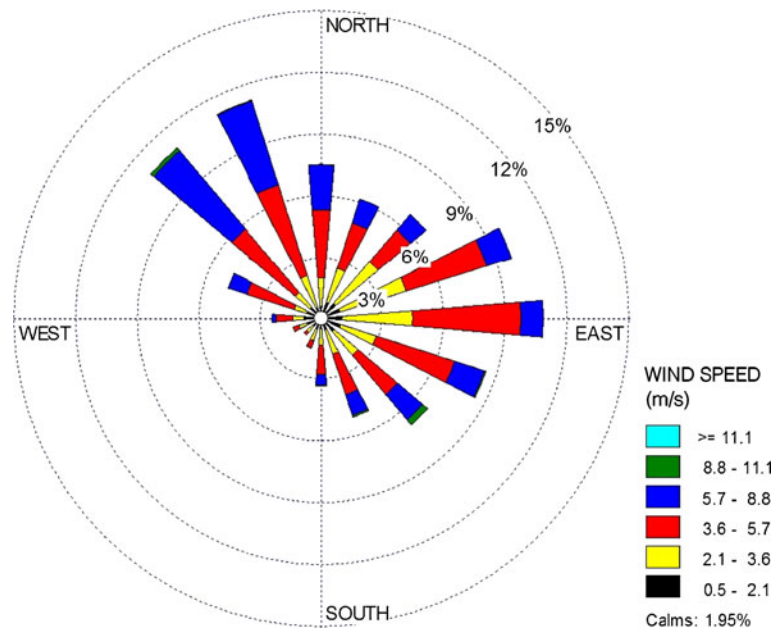
The slope is equal to 0.72, reflecting high measured values compared to predicted values, depicting the contribution of other emission sources. The correlation coefficient is equal to 0.91 reflecting an acceptable validation of the model output with measured average daily SO<sub>2</sub> concentrations.

The predicted hourly average ground level concentrations of SO<sub>2</sub> are compared with Kuwait EPA Ambient Air Quality Standards at all of the selected receptors.

**Table 1** The selected discrete receptors information

ID number	Discrete receptor identity	X coordinate	Y coordinate
1	Fahaheel Polyclinic	219,854.25	3,219,765.79
2	Petroleum Services Offices in Ahmadi	216,666.87	3,220,105.63
3	School in Fahaheel	220,300.00	3,219,820.85
4	Ahmadi Hospital	213,458.86	3,221,523.64
5	Shopping area in Fahaheel	219,274.32	3,219,554.21

**Fig. 1** Wind rose for a period of year 2008



The maximum allowable level for the hourly average concentration of  $\text{SO}_2$ , specified by Kuwait EPA, is  $444 \mu\text{g}/\text{m}^3$ . Figure 3 shows the isopleths of the predicted hourly average ground level concentration of  $\text{SO}_2$  calculated at the selected uniform grid receptors.

The isopleths indicate the predicted spatial variations of the ground level concentrations of  $\text{SO}_2$ . The maximum predicted hourly average ground level concentration of  $\text{SO}_2$  in the vicinity of the refinery exceeded by as much as  $300 \mu\text{g}/\text{m}^3$ . The highest predicted concentration is equal to  $769 \mu\text{g}/\text{m}^3$ , observed on the 8 March 2008 at 0800 hours and about 1.713 km in the NW direction from the FCC stack, and not far from the Fahaheel and Ahmadi areas at the receptor coordinates of  $X=218,557.94$ ,  $Y=3,219,169$ . This high value of the predicted  $\text{SO}_2$  concentration is expected due to the elevated  $\text{SO}_2$  emission rate, which resulted from the high sulfur content in the FCC feedstock and other operational conditions and the prevailing meteorological conditions (temperature, humidity, wind speed, wind direction, stability class, and planetary boundary layer).

A thorough inspection on Fig. 3 indicates that predicted concentrations of  $\text{SO}_2$  exceeded the allowable hourly limit at 5.3% of the study area from north west and south west direction from the stack.

Similarly, the predicted daily average ground level concentration of  $\text{SO}_2$  is compared with Kuwait EPA ambient air quality standards at all receptors. The allowable level for the daily average concentration of  $\text{SO}_2$  is  $157 \mu\text{g}/\text{m}^3$ . Figure 4 shows the isopleths of the predicted daily average ground level concentration of  $\text{SO}_2$  computed at the selected uniform grid receptors.

The isopleths indicate the daily predicted spatial variations of the ground level concentrations of  $\text{SO}_2$  in the area of study. The highest daily predicted concentration is equal to  $335 \mu\text{g}/\text{m}^3$ , observed on the 9 November 2008 and about 0.75 km in the SE direction from the stack, at a receptor coordinates of  $X=220,357.94$ ,  $Y=3,217,419$  affecting the neighboring Shuaiba industrial area, Kuwait main industrial complex. This high value of the daily predicted  $\text{SO}_2$  concentration is exceeded the allowable level by  $157 \mu\text{g}/\text{m}^3$  and obviously influenced by the prevailing

**Table 2**  $\text{SO}_2$  monthly emission factors

January	February	March	April	May	June	July	August	September	October	November	December
0.077	0.083	0.096	0.1	0.077	0.088	0.067	0.067	0.088	0.077	0.1	0.075

**Table 3** PM monthly emission factors

January	February	March	April	May	June	July	August	September	October	November	December
0.093	0.097	0.091	0.079	0.079	0.083	0.064	0.063	0.085	0.079	0.079	0.1

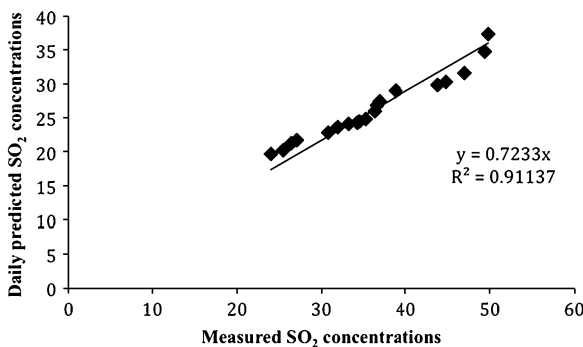
meteorological conditions, especially the predominant north west wind and other meteorological factors.

Discrete receptor 2, located at Petroleum services offices, has shown the highest SO<sub>2</sub> hourly concentration equal to 544 µg/m<sup>3</sup> on 27 February at 0800 hours. The hourly exceedance is occurred four times at this location throughout the study period. The highest daily concentration at the same receptor is equal to 39 µg/m<sup>3</sup> on 8 March.

Discrete receptor 3, located at school, has shown the highest SO<sub>2</sub> hourly concentration equal to 279 µg/m<sup>3</sup> on 2 March at 0400 hours. This concentration is below the Kuwait EPA hourly standards. The daily highest concentration is equal to 57 µg/m<sup>3</sup> on 2 March.

Discrete receptor 4, located at Ahmadi hospital, has shown the highest SO<sub>2</sub> hourly ground level concentration equal to 288 µg/m<sup>3</sup> on 27 February at 0800 hours. This value is also below the specified hourly limit set by Kuwait EPA. The daily predicted concentration is equal to 23 µg/m<sup>3</sup> on 30 April.

Discrete receptor 5, located at shopping area, has shown the highest SO<sub>2</sub> hourly ground level concentration is equal to 336 µg/m<sup>3</sup> on 23 October at 0800 hours. The daily predicted concentration is equal to 45 µg/m<sup>3</sup> on 22 April. Both hourly and daily predicted values are below Kuwait EPA hourly and daily ambient air quality standards.

**Fig. 2** Daily predicted SO<sub>2</sub> concentrations vs. measured SO<sub>2</sub> concentrations

Kulkarni et al. (2009) have reported that lanthanum and lanthanides are used as markers for particulate matters pollution as PM<sub>2.5</sub> in petroleum refineries, mainly from FCC units.

US EPA daily PM<sub>2.5</sub> standard is 35 µg/m<sup>3</sup>. In the present work, the application of Aermid to predict ground level concentration of PM is considered as PM<sub>2.5</sub> for rare earth metals, i.e., lanthanum and cerium. PM<sub>2.5</sub> is inhalable and has adverse impact on public health causing cardiovascular diseases. Kuwait EPA has no standard for PM<sub>2.5</sub> and has only specified daily and yearly standard for PM<sub>10</sub>. Figure 5 shows the isopleths of the predicted hourly average ground level concentration of PM calculated at the selected uniform grid receptors.

The isopleths indicate the hourly predicted spatial variations of the ground level concentrations of PM. The maximum hourly predicted average ground level concentration of PM is equal to 45 µg/m<sup>3</sup>, observed on the 27 February 2008 at 0800 hours and about 1.56 km in the NW direction from the FCC stack, and at receptor coordinates of X=218,557.94, Y=3,218,919.

Similarly, the predicted daily average ground level concentration of PM is compared with US EPA ambient air quality standards for PM<sub>2.5</sub> at all receptors. Figure 6 shows the isopleths of the predicted daily average ground level concentration of PM computed at the selected uniform grid receptors.

The isopleths indicate the daily average predicted spatial variations of the ground level concentrations of PM in the area of study. The highest daily predicted concentration is equal to 16 µg/m<sup>3</sup>, observed on the 29 December 2008 and about 0.75 km in the SE direction from the stack, at a receptor coordinates of X=220,657.94, Y=3,217,419 due to the influence of the prevailing meteorological conditions, especially the predominant north west wind and other meteorological factors.

To observe the computational model sensitivity, another scenario run is performed adding two finer meshes consisting of 21×21 uniform receptor points, the first one covering hourly highest ground level concentration area, the other one covering daily



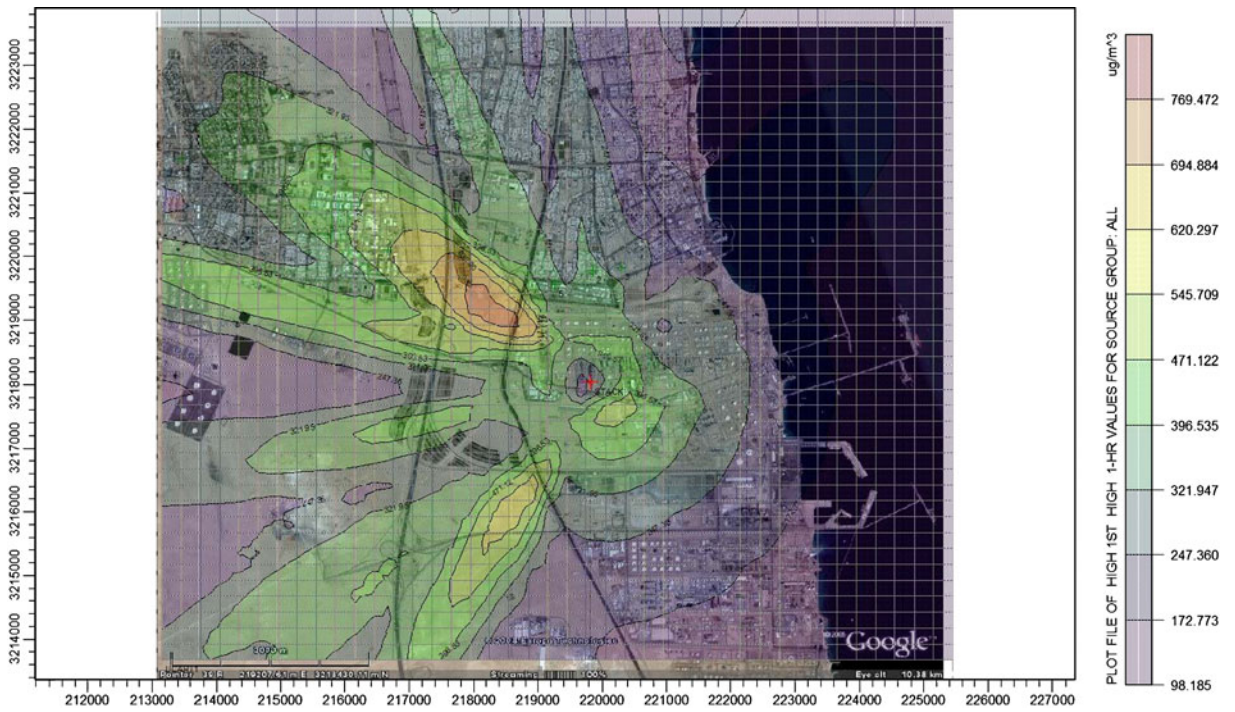


**Fig. 3** Isopleths plot of the predicted hourly average ground level concentration of SO<sub>2</sub> (Google Inc. 2010)

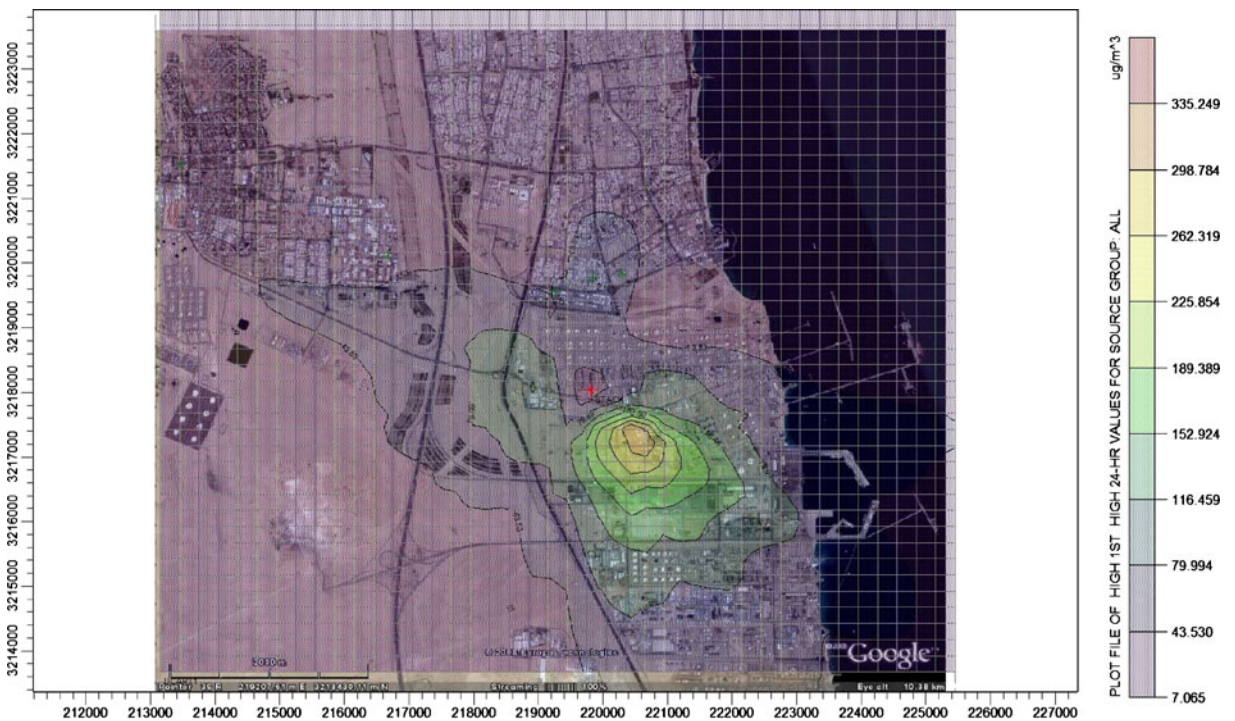


**Fig. 4** Isopleths plot of the predicted daily average ground level concentration of SO<sub>2</sub> (Google Inc. 2010)



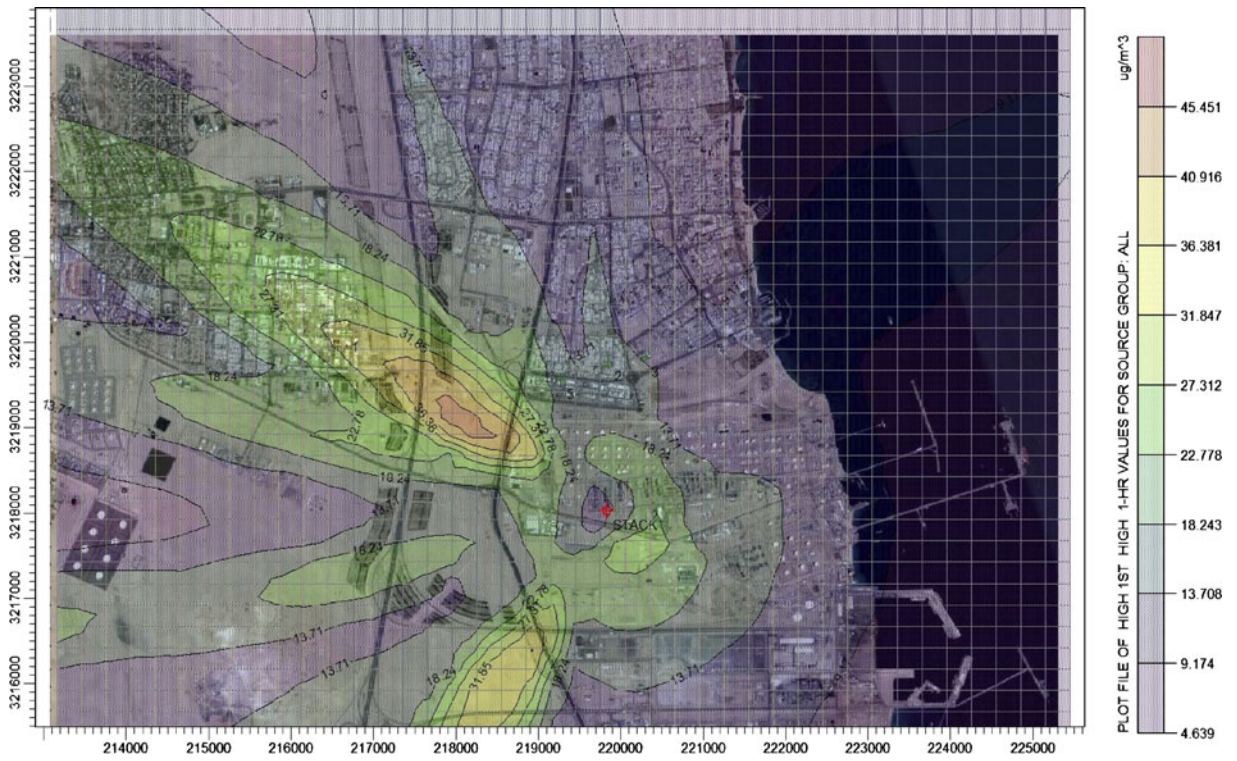


Fig. 5 Isopleths plot of the predicted hourly average ground level concentration of PM (Google Inc. 2010)

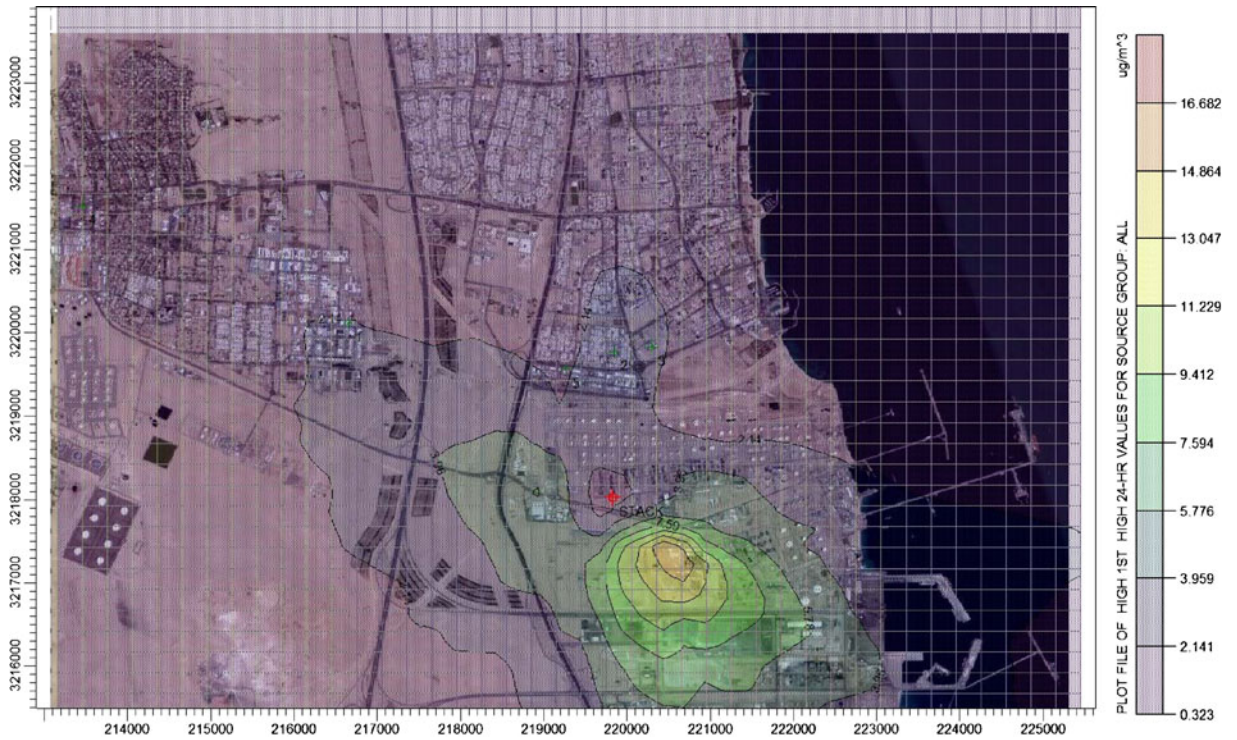


Fig. 6 Isopleths plot of the predicted daily average ground level concentration of PM (Google Inc. 2010)

highest predicted ground level concentration area. The output accuracy has improved for both pollutants due to application of interpolation using small values of  $\Delta x=150$  m,  $\Delta y=110$  m for the first mesh and  $\Delta x=100$  m,  $\Delta y=100$  m for the second mesh. There is 0.65% increase in the hourly highest ground level concentration and 2.8% increase in the daily highest ground level concentration, which are insignificant. Therefore, the only parent mesh is used in the computational process for all the other scenarios considered in the parametric studies.

FCC stack sensitivity analysis is performed on three scenarios (stack height, SO<sub>2</sub> emission rate, and stack diameter).

In scenario 1, analysis for stack heights 50, 80, 120, 160, and 200 m is conducted while keeping the emission rate, exit flue gas velocity, exit temperature, and stack diameter constant.

The influence of stack height is shown in Fig. 7. It is obvious from the figure that the highest predicted hourly and daily ground level concentrations of SO<sub>2</sub> are reduced substantially as stack height is increased. The reduction in the highest computed hourly ground level concentration of SO<sub>2</sub> is almost 50% when stack height is doubled. The decrease in evaluated hourly SO<sub>2</sub> concentration as a function of stack height is given as an exponential expression  $C(\mu\text{g}/\text{m}^3) = 1,600.7e^{-9.071 \times 10^{-3}h}$  and  $r^2$  is 0.999, where  $h$  is the stack height (m). The hourly gradient  $dC/dh = 14.52e^{-9.071 \times 10^{-3}h}$  becomes insignificant at higher stack elevations. The highest daily predicted ground level concentration as a function of stack height is given as  $C(\mu\text{g}/\text{m}^3) = 1,409.8e^{-1.732 \times 10^{-2}h}$  and  $r^2$  is 0.984. The daily highest predicted concentration

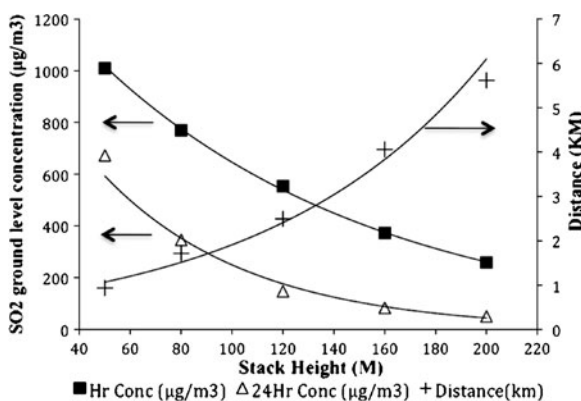


**Fig. 7** Stack height vs. hourly and daily predicted ground level concentrations of SO<sub>2</sub>

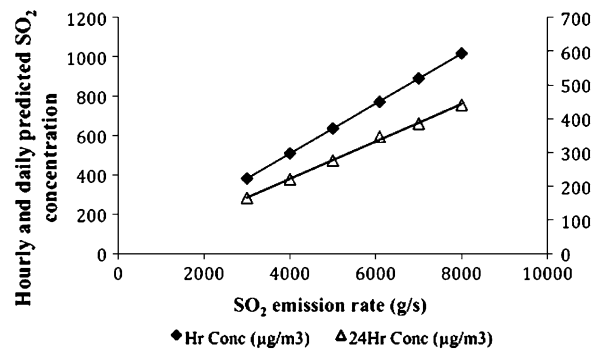


**Fig. 8** SO<sub>2</sub> emission rate vs. hourly and daily predicted SO<sub>2</sub> ground level concentrations

gradient is  $dC/dh = 24.42e^{-1.732 \times 10^{-2}h}$ . The locations of hourly highest predicted concentrations of SO<sub>2</sub> from the stack, as a function of stack height is shown in Fig. 7 and related as  $D(\text{km}) = 0.597e^{1.16 \times 10^{-2}h}$  and  $r^2$  is 0.978.

In scenario 2, SO<sub>2</sub> emission rate effect from FCC stack is tested at stack height of 80 m for different total monthly emission rates of 3,000, 4,000, 5,000, 6,000, 7,000, and 8000 g/s, taking into consideration the monthly emission variations (by using emission factors, Table 2) and fixing other stack parameters, i.e., exit temperature, exit flue gas velocity, and stack diameter.

It is noticed from Fig. 8 that the highest predicted hourly and daily ground level concentrations of SO<sub>2</sub> is substantially decreased as SO<sub>2</sub> emission rate is reduced. At 50% reduction in the emission rate, the highest hourly and daily ground level concentrations decreased by 50%.

In scenario 3, FCC stack diameter effect is examined at stack height of 80 m for different diameters of 1.5, 2.3, 3, and 4 m. The exit flue gas velocity is also changed as directly related to the square of the diameter for a fixed exit flue gas flow rate. It is observed that the dispersion and rise of the plume are not affected by diameter variation and the predicted ground level concentration of SO<sub>2</sub> remained almost unaltered. The hourly and daily predicted concentrations of SO<sub>2</sub> are almost identical for all the cases.

## 5 Conclusion

FCC unit in a refinery is the major contributor of SO<sub>2</sub>, and PM emissions are those responsible for adverse



impact on the immediate neighborhood of the refinery. A complete comprehensive emission inventories for a year-long period have been prepared for both SO<sub>2</sub> and particulate matters.

A model run performed for actual monthly emission variation with total SO<sub>2</sub> emission rate of 6,089.2 g/s and total PM emission rate of 302 g/s independently, taking into consideration monthly emission factors for both pollutants. The daily predicted ground level concentrations of SO<sub>2</sub> are compared with Kuwait EPA monitoring station daily measured SO<sub>2</sub> concentrations at the same discrete receptor and showed acceptable validation of the model output.

The highest hourly predicted concentration of SO<sub>2</sub> is equal to 769 µg/m<sup>3</sup>. It is observed on the 8 March 2008 at 0800 hours, due to elevated SO<sub>2</sub> emission rate in this month and the prevailing meteorological conditions, especially sea breeze effect in the early morning hours. The highest daily predicted concentration is equal to 335 µg/m<sup>3</sup>. It is observed on the 9 November 2008 and obviously influenced by the predominant north west wind and high SO<sub>2</sub> emission rate in the month of November.

The maximum hourly predicted average ground level concentration of PM is equal to 45 µg/m<sup>3</sup>. It is observed on the 27 February 2008 at 0800 hours. The highest daily predicted concentration is equal to 16 µg/m<sup>3</sup>, observed on the 29 December 2008.

The stack sensitivity is explored by changing stack height, total emission rate, and stack diameter independently. It is observed that the higher stack facilitated good dispersion, thus lowering the ground level average concentration of the pollutant up to 50% when the stack height doubled.

It is notice that the highest predicted hourly and daily ground level concentrations of SO<sub>2</sub> are substantially decreased as SO<sub>2</sub> emission rate is reduced. At 50% reduction in the emission rate, the highest hourly and daily ground level concentrations decreased by almost 48%.

The influence of stack diameter inherently changed the exit flue gas velocity due to invariable flue gas flow rate. The plume rise and dispersion are related to the exit flue gas velocity, which decreased with the increase of stack diameter because of

proportionality to the square of diameter. For a fixed load, there is no noticeable change in the average hourly and daily predicted ground level concentrations of SO<sub>2</sub>.

## References

- Abdul Wahab, S. A., Al-Alawi, S. M., & El-Zawahri, A. (2002). Patterns of SO<sub>2</sub> emissions: A refinery case study. *Environmental Modeling and Software*, *17*, 563–570.
- Alrashidi, M. S., Nassehi, V., & Wakeman, R. J. (2005). Investigation of the efficiency of the existing air pollution monitoring sites in the state of Kuwait. *Environmental Pollution*, *138*, 219–229.
- Caputo, M., Gimenez, M., & Schlamp, M. (2003). Inter-comparison of atmospheric dispersion models. *Atmospheric Environment*, *37*, 2435–2449.
- Google Inc. (2010). Google earth. Version 5.1, <http://www.earth.google.com>.
- Isakov, V., Venkatram, A., Touma, S. J., Koracin, D., & Otte, L. T. (2007). Evaluating the use of outputs from comprehensive meteorological models in air quality modeling applications. *Atmospheric Environment*, *41*, 1689–1705.
- Kesarkar, A. P., Dalvi, M., Kaginalkar, A., & Ojha, A. (2007). Coupling of the weather research and forecasting model with AERMOD for pollutant dispersion modeling. A case study for PM<sub>10</sub> dispersion over Pune, India. *Atmospheric Environment*, *41*, 1976–1988.
- Kulkarni, P., Chellam, S., & Fraser, M. P. (2009). Tracking petroleum refinery emission events using lanthanum and lanthanides as elemental markers for PM<sub>2.5</sub>. *Environmental Science & Technology*, *43*(8), 2990–2991.
- Lopez, J. L., & Mandujano, C. (2005). Estimation of the impact in the air quality by the use of clean fuels (fuel oil versus natural gas). *Catalysis Today*, *106*, 176–179.
- Rama Krishna, T. V. B. P. S., Reddy, M. K., Reddy, R. C., & Singh, R. N. (2004). Assimilative capacity and dispersion of pollutants due to industrial sources in Visakhapatnam bowl area. *Atmospheric Environment*, *38*, 6775–6787.
- Venkatram, A., Isakov, V., Yuana, J., & Pankratza, D. (2004). Modeling dispersion at distances of meters from urban sources. *Atmospheric Environment*, *38*, 4633–4641.
- Whitcombe, J. M., Agranovski, I. E., & Braddock, R. D. (2003). Attrition due to mixing of hot and cold FCC catalyst particles. *Powder Technology*, *137*, 120–130.
- Yateem, W., Nassehi, V., & Khan, A. R. (2010). Inventories of SO<sub>2</sub> and PM emissions from fluid catalytic cracking (FCC) units in petroleum refineries. *Water, Air, and Soil Pollution*. doi:10.1007/s11270-010-0423-z.
- Zou, B., Zhan, F. B., Wilson, J. G., & Zeng, Y. (2010). Performance of aermom at different time scales. *Simulation Modeling Practices and Theory*, *18*, 612–623.



unit emissions on the vicinity of the petroleum refinery. Different mitigation methods will be examined to abate the high concentrations of SO<sub>2</sub> and PM emissions from FCC unit.

## References

- Akeredolu, F. (1989). Atmospheric environment problems in Nigeria—an overview. *Atmospheric Environment*, 23(4), 783–792.
- Mitchell, M. M., Jr., Hoffman, J. F., & Moore, H. F. (1993). Residual feed cracking catalyst. In J. S. Magee & J. M. M. Mitchell (Eds.), *Fluid catalytic cracking: science and technology, studies in surface science and catalysis* (Vol. 76, pp. 293–338). New York: Elsevier.
- Whitcombe, J. M., Agranovski, I. E., & Braddock, R. D. (2003). Attrition due to mixing of hot and cold FCC catalyst particles. *Powder Technology*, 137, 120–130.
- Venuto, P. B., & Habib, E. T. (1978). Catalyst-feedstock-engineering interactions in fluid catalytic cracking. *Catalysis Reviews, Science and Engineering*, 18, 1–150.
- Maya-Yescasa, R., Villafuerte-Macias, E. F., Aguilarb, R., & Salazar-Sotelod, D. (2004). Sulphur oxides emission during fluidized-bed catalytic cracking. *Chemical Engineering Journal*, 106, 145–152.
- Chen, Y.-M. (2006). Recent advances in FCC technology. *Powder Technology*, 163, 2–8.

# Computer modelling of the impact of gaseous and particulate matter emissions from fluid catalytic cracking units

Wael Yateem<sup>1</sup>, Vahid Nassehi<sup>1</sup>, Bahareh Kaveh-Baghbaderani<sup>1</sup>, Abdul R. Khan<sup>2</sup>

<sup>1</sup>Chemical Engineering Department  
Loughborough University  
Loughborough LE11 3TU

Email: [v.nassehi@lboro.ac.uk](mailto:v.nassehi@lboro.ac.uk)

<sup>2</sup>Department of Environment Technology and Management  
College for Women  
Kuwait University  
Kuwait

## KEYWORDS

Dispersion model, Aermot, emissions, FCC, pollutants exceedance

## ABSTRACT

Fluid catalytic cracking unit is a major part of petroleum refineries as it treats heavy fractions from various process units to produce light ends (valuable products). FCC unit feedstock consists of heavy hydrocarbon with high sulphur contents and the catalyst used is zeolite impregnated with rare earth metals i.e. Lanthanum and Cerium. The Catalytic cracking reaction takes place at elevated temperature in fluidized bed reactor generating sulphur-contaminated coke on the catalyst with large quantity of attrited catalyst fines. In the regenerator, coke is completely burnt producing SO<sub>2</sub>, PM emissions are mainly due to high attrition of cold makeup catalyst charge and operating conditions, vapour velocity particle velocity, particle collision and particle degradation. The impact of particulate matter emission from FCC unit is assessed in the immediate neighbourhood of the refinery. Year long emission inventory of SO<sub>2</sub> and PM have been prepared. The corresponding meteorological data are obtained and fed into Aermot (Aermot pre-processor). Aermot (dispersion model) is used to predict ground level concentrations of PM SO<sub>2</sub> in the selected study area based on 2008 emission inventory (Yateem et al., 2010) for a period of one year. Model output is validated with measured values at discrete receptors and an extensive parametric study has been conducted using three scenarios, stack diameter, stack height and emission rate. It is noticed that stack diameter has no effect on ground level concentration, as stack exit velocity is a function of stack diameter. With the increase in stack height, the predicted concentrations decrease showing an inverse relation. The influence of the emission rate is linearly related to the computed ground level concentrations.

It has also observed that there is no hourly standard for PM. Therefore, daily predicted concentrations are compared with US EPA allowable standard for PM<sub>2.5</sub>. The comparison shows that there is no violation of specified

limit for daily mean predicted concentration all over in the selected study area.

## INTRODUCTION

Fluid catalytic cracking (FCC) of heavy ends into high value liquid fuels is commonly carried out in the oil refining industry. In this process the heavy feedstock containing sulphur as a major contaminant is cracked to light products. Sulphur is redistributed in the liquid and gaseous products and coke on the catalyst. In the regenerator coke with sulphur contamination is completely burnt and flue gas containing SO<sub>2</sub> is discharged with catalyst fines produced, mainly due to high attrition of cold makeup catalyst charge and operating conditions i.e. vapour velocity, particle velocity, particle collision and particle degradation (Abdul Wahab et al., 2002).

In the present work, a comprehensive emission inventories from FCC unit in an oil refinery have been prepared. These inventories are calculated based on complete combustion of sulphur and coke impregnated on the catalyst in the regenerator. Mainly for SO<sub>2</sub> and Particulate matter (PM) emission rates are calculated accurately using material balances for a yearlong period considering seasonal variations in the operation of the process unit, Yateem et al., (2010). PM emission inventory is used in dispersion model to assess its impact on the immediate surroundings of the refinery.

The most advanced dispersion model Aermot (Caputo et al., 2003; Isakov et al., 2007; Kesarkar et al., 2007) has been selected for prediction ground level concentration of PM based on comprehensive year long emission inventory of FCC unit.

Aermot is a dispersion model that uses Gaussian distribution for the stable conditions and non-Gaussian probabilities density function for the unstable conditions. Aermot (Aermot preprocessor) provides planetary boundary layer parameters over a high altitude to yield accurate predicted concentration values for a given meteorological conditions. It can accommodate large meteorological data (multiple years). Aermot (Aermot

preprocessor) generates regular receptors over a given terrain for the evaluation of pollutants ground level concentrations.

The meteorological data for year 2008 are obtained and are used in preprocessor Aermot to generate planetary boundary layers parameters. These generated data are used in Aermod for actual emission rates to predict ground level concentrations of PM and study the influence of prevailing meteorological conditions at this particular site.

## MODEL APPLICATION

### 1. Input Data

Aermod dispersion model implementation requires the following items of data:

1. Source information: including pollutant emission rate (g/s), location coordinates in Universal Transverse Mercator (UTM) (m), base elevation from the sea level (m), stack height (m), exit stack inner diameter (m), exit stack gas velocity (m/s), and exit stack gas temperature (°K).

2. Meteorological information for the region of interest: includes anemometer height (m), wind speed (m/s), wind direction (flow vector from which the wind is blowing) (in degrees clockwise from the north), ambient air temperature (°C), stability class at the hour of measurement (dimensionless) and hourly mixing height (m).

3. Receptor information: This can be specified or generated by the program to predict the pollutants' concentrations at the selected receptors.

The entire required source input data are obtained from FCC unit in the refinery. A stack of 80 m height, an inner diameter of 2.3 m, with an average exit gas velocity of 20 m/s and exit gas temperature of 550 °K are fed into the model. Monthly emission variation is considered with total SO<sub>2</sub> emission rate of 6089.2 g/s and total PM emission rate of 302 g/s as presented in detail (Yateem et al. 2010).

### 2. Area of Study

The area of study in this work covers portion of Ahmadi governorate in the state of Kuwait. Fahaheel area is adjacent to the petroleum refinery has one of the Kuwait EPA air quality monitoring station located at a polyclinic. Both areas Fahaheel and Ahmadi are surrounded by arid desert in the west side and bordered by the Gulf from the east.

Two different types of receptor coordinates are used as input to the Aermod model to predict the ground level concentration of SO<sub>2</sub> and PM, these are:

1. Discrete Cartesian receptors specified at the sensitive areas viz., a school, a shopping area and EPA monitoring stations in Fahaheel. A hospital and petroleum services companies' offices are selected in Ahmadi.

2. Uniform Cartesian Grid receptors covering the entire area of study, where the FCC stack (emissions source) is located almost in the center of the mesh grid.

The receptors selected are based on the actual sites in a UTM location coordinate of the area of interest map. Table 1 shows the selected discrete receptors information.

The uniform grid receptors of a total 1764 (42 x 42) were divided into ( $\Delta x = 300$  m and  $\Delta y = 250$  m) to cover about 12 x 10 km area of study. The optimum selection of the

mesh size is based on the computational accuracy and time.

**Table 1. The selected discrete receptors information**

ID Number	Discrete receptor identity	X-coordinate	Y-coordinate
1	Fahaheel Polyclinic	219854.25	3219765.79
2	Petroleum Services Offices in Ahmadi	216666.87	3220105.63
3	School in Fahaheel	220300.00	3219820.85
4	Ahmadi Hospital	213458.86	3221523.64
5	Shopping area in Fahaheel	219274.32	3219554.21

## RESULTS AND DISCUSSION

A year long comprehensive metrological data are processed by Aermot to generate boundary layer parameters and to pass all meteorological observations to Aermod.

Figure 1 shows wind direction and magnitude for a period of year 2008. It is observed that most of the time; the prevailing wind direction is from North West. There is strong influence from the neighboring Gulf as the refinery is located at the coast, resulting into strong sea breeze blowing from East direction. Wind class frequency distribution for the entire year confirming 2 % calm conditions, while 39.8 % is between 3.6 - 5.7 m/s. the highest wind class 8.8-11.1 m/s is less than 1%.

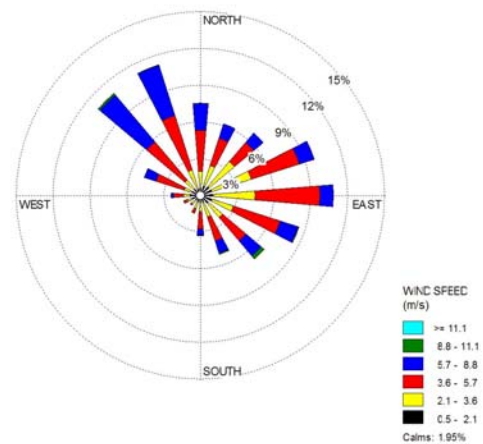


**Fig. 1 wind rose for a period of year 2008**

A model run is performed for actual monthly emission variation with total SO<sub>2</sub> emission rate of 6089.2 g/s and PM emission rate of 302 g/s. Monthly emission factors for SO<sub>2</sub> is tabulated in Table 2 and Monthly emission factors for PM is tabulated in Table 3. A discrete receptor is selected at Kuwait Environmental Public Authority monitoring station located at polyclinic in Fahaheel area. Concentrations of SO<sub>2</sub>, NO<sub>x</sub>, H<sub>2</sub>S, O<sub>3</sub>, CO, CO<sub>2</sub>, methane, non-methane hydrocarbon, Benzene, Toluene, Xylenes, ethylbenzene,

total suspended particulates and meteorological parameters are continuously recorded on hourly basis.

**Table 2 SO<sub>2</sub> monthly emission factors**

Jan	Feb	Mar	April	May	Jun
0.077	0.083	0.096	0.1	0.077	0.088
Jul	Aug	Sep	Oct	Nov	Dec
0.067	0.067	0.088	0.077	0.1	0.75

**Table 3 PM monthly emission factors**

Jan	Feb	Mar	April	May	Jun
0.093	0.097	0.091	0.079	0.079	0.083
Jul	Aug	Sep	Oct	Nov	Dec
0.064	0.063	0.085	0.079	0.079	0.1

Hourly predicted ground level concentrations at specified discrete receptor showed large scatter due to variation in meteorological conditions and the recorded values influenced by the contribution of various emission sources has made the comparison impracticable. Therefore, daily average measured concentrations of SO<sub>2</sub> were compared with the daily-predicted concentrations to validate the model output.

Figure 2 shows the plot between the measured top 20 daily average values versus the daily predicted top 20 values at the discrete receptor, Kuwait-EPA monitoring station.

The slope is equal to 0.72, reflecting high measured values compared to predicted values, depicting the contribution of other emission sources. The correlation coefficient is equal to 0.91 reflecting an acceptable validation of the model output with measured average daily SO<sub>2</sub> concentrations.

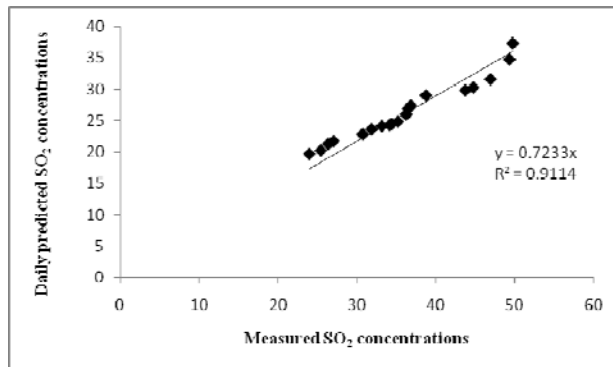


**Fig. 2 Daily predicted SO<sub>2</sub> concentrations vs. measured SO<sub>2</sub> concentrations**

The predicted hourly average ground level concentrations of SO<sub>2</sub> are compared with Kuwait-EPA Ambient Air Quality Standards (AAQS) at all of the selected receptors. The maximum allowable level for the hourly average

concentration of SO<sub>2</sub>, specified by Kuwait-EPA, is 444 µg/m<sup>3</sup>. Fig. 3 shows the isopleths of the predicted hourly average ground level concentration of SO<sub>2</sub> calculated at the selected uniform grid receptors.

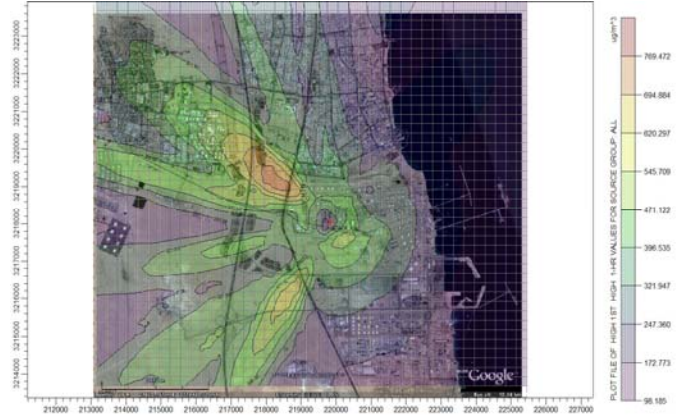


**Fig. 3 Isopleths plot of the predicted hourly average ground level concentration of SO<sub>2</sub>**

The isopleths indicate the predicted spatial variations of the ground level concentrations of SO<sub>2</sub>. The maximum predicted hourly average ground level concentration of SO<sub>2</sub> in the vicinity of the refinery exceeded by as much as 300 µg/m<sup>3</sup>. The highest predicted concentration is equal to 769 µg/m<sup>3</sup>, observed on the 8<sup>th</sup> of March 2008 at 8:00 hour and about 1.713 km in the NW direction from the FCC stack, and not far from the Fahaheel and Ahmadi areas at the receptor coordinates of X = 218557.94, Y = 3219169. This high value of the predicted SO<sub>2</sub> concentration is expected due to the elevated SO<sub>2</sub> emission rate, which resulted from the high sulphur content in the FCC feedstock and other operational conditions and the prevailing meteorological conditions (temperature, humidity, wind speed, wind direction, stability class and planetary boundary layer).

A thorough inspection on fig. 3 indicates that predicted concentrations of SO<sub>2</sub> exceed the allowable hourly limit at 5.3 % of the study area from North West and South West direction from the stack.

Similarly, the predicted daily average ground level concentration of SO<sub>2</sub> is compared with Kuwait EPA ambient air quality standards at all receptors. The allowable level for the daily average concentration of SO<sub>2</sub> is 157 µg/m<sup>3</sup>. Fig. 4 shows the isopleths of the predicted daily average ground level concentration of SO<sub>2</sub> computed at the selected uniform grid receptors.

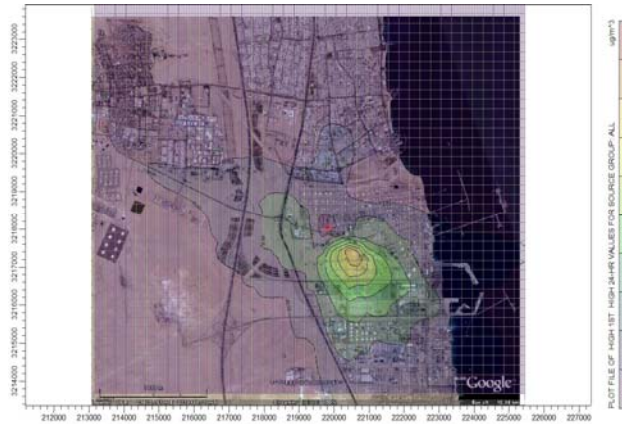


**Fig. 4 Isopleths plot of the predicted daily average ground level concentration of SO<sub>2</sub>**

The isopleths indicate the daily predicted spatial variations of the ground level concentrations of SO<sub>2</sub> in the area of study. The highest daily predicted concentration is equal to 335 µg/m<sup>3</sup>, observed on the 9<sup>th</sup> of November 2008 and about 0.75 km in the SE direction from the stack, at a receptor coordinates of X = 220357.94, Y = 3217419 affecting the neighboring Shuaiba industrial area, Kuwait main industrial complex. This high value of the daily predicted SO<sub>2</sub> concentration is exceeded the allowable level by 157 µg/m<sup>3</sup> and obviously influenced by the prevailing meteorological conditions, especially the predominant North West wind and other meteorological factors.

Discrete receptor 2, is located at Petroleum services offices, has shown the highest SO<sub>2</sub> hourly concentration equal to 544 µg/m<sup>3</sup> on 27<sup>th</sup> February at 8:00 hours. The hourly exceedance is occurred four times at this location throughout the study period. The highest daily concentration at the same receptor is equal to 39 µg/m<sup>3</sup> on 8<sup>th</sup> March.

Discrete receptor 3, is located at school, has shown the highest SO<sub>2</sub> hourly concentration equal to 279 µg/m<sup>3</sup> on 2<sup>nd</sup> March at 4:00 hours. This concentration is below the Kuwait EPA hourly standards. The daily highest concentration is equal to 57 µg/m<sup>3</sup> on 2<sup>nd</sup> March. Discrete receptor 4, is located at Ahmadi hospital, has shown the highest SO<sub>2</sub> hourly ground level concentration equal to 288 µg/m<sup>3</sup> on 27<sup>th</sup> February at 8:00 hours. This value is also below the specified hourly limit set by Kuwait EPA. The daily predicted concentration is equal to 23 µg/m<sup>3</sup> on 30<sup>th</sup> April. Discrete receptor 5, is located at shopping area, has shown the highest SO<sub>2</sub> hourly ground level concentration is equal to 336 µg/m<sup>3</sup> on 23<sup>rd</sup> October at 8:00 hours. The daily predicted concentration is equal to 45 µg/m<sup>3</sup> on 22<sup>nd</sup> April. Both hourly and daily predicted values are below Kuwait EPA hourly and daily ambient air quality standards.

### 1. Model Sensitivity

To observe the computational model sensitivity, another scenario run is performed adding two finer meshes consisting of 21 x 21 uniform receptor points, the first one covering hourly highest ground level concentration area, the other one covering daily highest predicted ground level concentration area. The output accuracy has improved for both pollutants due to application of interpolation using

small values of Δx = 150 m, Δy = 110 m for the first mesh and Δx = 100 m, Δy = 100m for the second mesh. There is 0.65% increase in the hourly highest ground level concentration and 2.8% increase in the daily highest ground level concentration, which are insignificant. Therefore, the only parent mesh is used in the computational process for all the other scenarios considered in the parametric studies.

### 2. Parametric Study

FCC stack sensitivity analysis is performed on 3 scenarios (stack height, SO<sub>2</sub> emission rate and stack diameter). In scenario 1, analysis for stack heights 50 m, 80 m, 120 m, 160 m and 200 m is conducted while keeping the emission rate, exit flue gas velocity, exit temperature and stack diameter constant. The influence of stack height is shown in fig. 5. It is obvious from the figure that the highest predicted hourly and daily ground level concentrations of SO<sub>2</sub> are reduced substantially as stack height is increased. The reduction in the highest computed hourly ground level concentration of SO<sub>2</sub> is almost 50% when stack height is doubled. The decrease in evaluated hourly SO<sub>2</sub> concentration as a function of stack height is given as an exponential expression  $C(\mu\text{g}/\text{m}^3) = 1600.7e^{-9.071 \times 10^{-3} h}$  and  $r^2$  is 0.999, where h is the stack height (m). The hourly gradient  $dC/dh = 14.52e^{-9.071 \times 10^{-3} h}$  becomes insignificant at higher stack elevations. The highest daily predicted ground level concentration as a function of stack height is given as  $C(\mu\text{g}/\text{m}^3) = 1409.8e^{-1.732 \times 10^{-2} h}$  and  $r^2$  is 0.984. The daily highest predicted concentration gradient is  $dC/dh = 24.42e^{-1.732 \times 10^{-2} h}$ . The locations of hourly highest predicted concentrations of SO<sub>2</sub> from the stack, as a function of stack height is shown in figure 7 and related as  $D(\text{km}) = 0.597e^{1.16 \times 10^{-2} h}$  and  $r^2$  is 0.9.

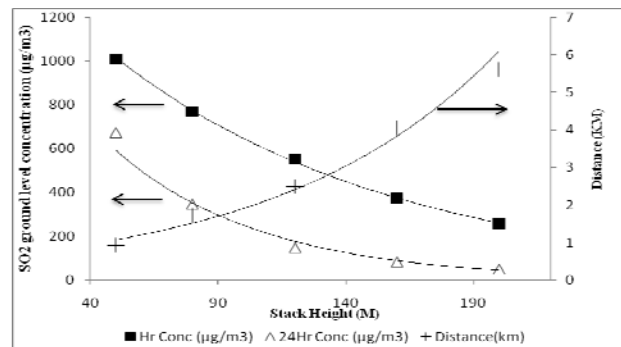


**Fig. 5 Stack height vs. hourly and daily predicted ground level concentrations of SO<sub>2</sub>**

In scenario 2, SO<sub>2</sub> emission rate effect from FCC stack is tested at stack height of 80 m for different total monthly emission rates of 3000 g/s, 4000 g/s, 5000 g/s, 6000 g/s, 7000 g/s and 8000 g/s, taking into consideration the monthly emission variations (by using emission factors, table 2) and fixing other stack parameters i.e. exit temperature, exit flue gas velocity and stack diameter. It is noticed from fig. 8 that the highest predicted hourly and daily ground level concentrations of SO<sub>2</sub> is substantially decreased as SO<sub>2</sub> emission rate is reduced. At



50% reduction in the emission rate, the highest hourly and daily ground level concentrations decreased by 50%.

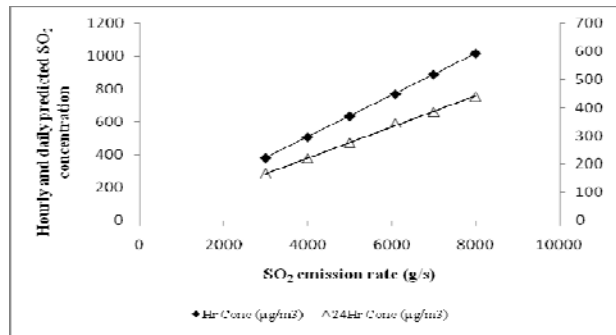


**Fig. 6 SO<sub>2</sub> emission rate vs. hourly and daily predicted SO<sub>2</sub> ground level concentrations**

In scenario 3, FCC stack diameter effect is examined at stack height of 80 m for different diameters of 1.5 m, 2.3 m, 3 m and 4 m. The exit flue gas velocity is also changed as directly related to the square of the diameter for a fixed exit flue gas flow rate. It is observed that the dispersion and rise of the plume are not affected by diameter variation and the predicted ground level concentration of SO<sub>2</sub> remained almost unaltered. The hourly and daily predicted concentrations of SO<sub>2</sub> are almost identical for all the cases. Kulkarni et al., (2009) have reported that Lanthanum and Lanthanides are used as markers for particulate matters pollution as PM<sub>2.5</sub> in petroleum refineries, mainly from FCC units. US EPA daily PM<sub>2.5</sub> standard is 35 µg/m<sup>3</sup>. In the present work, the application of Aermid to predict ground level concentration of PM is considered as PM<sub>2.5</sub> for rare earth elements i.e. Lanthanum and Cerium. PM<sub>2.5</sub> is inhalable and has adverse impact on public health causing cardiovascular diseases. Kuwait EPA has no standard for PM<sub>2.5</sub> and has only specified daily and yearly standard for PM<sub>10</sub>. Figure 5 shows the isopleths of the predicted hourly average ground level concentration of PM calculated at the selected uniform grid receptors.

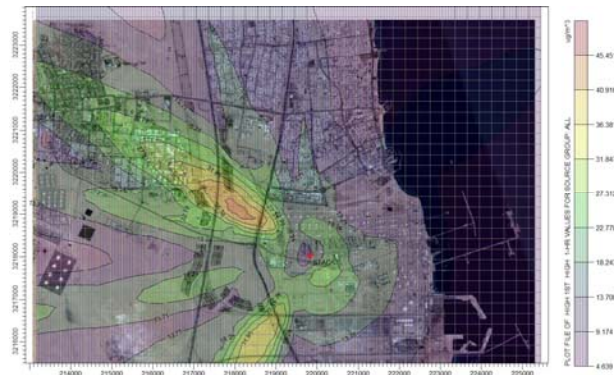


**Fig. 7 Isopleths plot of the predicted hourly average ground level concentration of PM**

The isopleths indicate the hourly predicted spatial variations of the ground level concentrations of PM. The maximum hourly predicted average ground level concentration of PM is equal to 45 µg/m<sup>3</sup>, observed on the 27<sup>th</sup> of February 2008 at 8:00 hour and about 1.56 km in the

NW direction from the FCC stack, and at receptor coordinates of X = 218557.94, Y = 3218919.

Similarly, the predicted daily average ground level concentration of PM is compared with US EPA ambient air quality standards for PM<sub>2.5</sub> at all receptors. Figure 6 shows the isopleths of the predicted daily average ground level concentration of PM computed at the selected uniform grid receptors.

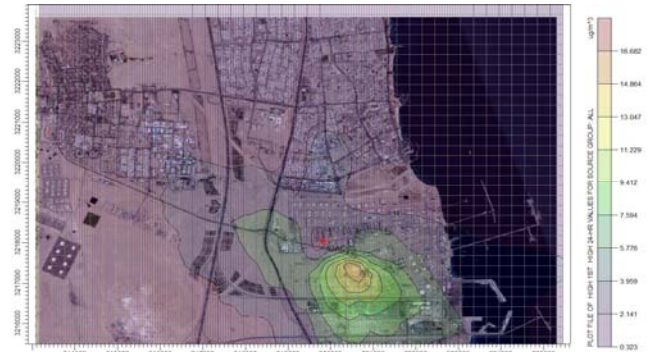


**Fig. 8 Isopleths plot of the predicted daily average ground level concentration of PM**

The isopleths indicate the daily average predicted spatial variations of the ground level concentrations of PM in the area of study. The highest daily predicted concentration is equal to 16 µg/m<sup>3</sup>, observed on the 29<sup>th</sup> of December 2008 and about 0.75 km in the SE direction from the stack, at a receptor coordinates of X = 220657.94, Y = 3217419 due to the influence of the prevailing meteorological conditions, especially the predominant North West wind and other meteorological factors.

To observe the computational model sensitivity, another scenario run is performed adding two finer meshes consisting of 21 x 21 uniform receptor points, the first one covering hourly highest ground level concentration area, the other one covering daily highest predicted ground level concentration area. The output accuracy has improved for both pollutants due to application of interpolation using small values of  $\Delta x = 150$  m,  $\Delta y = 110$  m for the first mesh and  $\Delta x = 100$  m,  $\Delta y = 100$  m for the second mesh. There is 0.65% increase in the hourly highest ground level concentration and 2.8% increase in the daily highest ground level concentration, which are insignificant. Therefore, the only parent mesh is used in the computational process for all the other scenarios considered in the parametric study.

## CONCLUSIONS

FCC unit in a refinery is major contributor of SO<sub>2</sub> and PM emissions. These gases are responsible for adverse impact on the immediate neighbourhood of the refinery. A complete emission inventory for a year long period have been prepared for SO<sub>2</sub> and PM.

A model run performed for actual monthly emission variation with total SO<sub>2</sub> emission rate of 6089.2 g/s and PM emission rate of 302 g/s, taking into consideration monthly emission factors for both SO<sub>2</sub> and PM.

The daily predicted ground level concentrations of SO<sub>2</sub> are compared with Kuwait EPA monitoring station daily measured SO<sub>2</sub> concentrations at the same discrete receptor and showed acceptable validation of the model output.

The highest hourly predicted concentration of SO<sub>2</sub> is equal to 769 µg/m<sup>3</sup>. It is observed on the 8<sup>th</sup> of March 2008 at 8:00 hour, due to elevated SO<sub>2</sub> emission rate in this month and the prevailing meteorological conditions, especially sea breeze effect in the early morning hours. The highest daily predicted concentration is equal to 335 µg/m<sup>3</sup>. It is observed on the 9<sup>th</sup> of November 2008, and obviously influenced by the predominant North West wind and high SO<sub>2</sub> emission rate in the month of November.

The maximum hourly predicted average ground level concentration of PM is equal to 45 µg/m<sup>3</sup>. It is observed on the 27<sup>th</sup> of February 2008 at 8:00 hour. The highest daily predicted concentration is equal to 16 µg/m<sup>3</sup>, observed on the 29<sup>th</sup> of December 2008.

The stack sensitivity is explored by changing stack height, total emission rate and stack diameter independently. It is observed that the higher stack facilitated good dispersion, thus lowering the ground level average concentration of the pollutant up to 50% when the stack height doubled.

It is notice that the highest predicted hourly and daily ground level concentrations of SO<sub>2</sub> are substantially decreased as SO<sub>2</sub> emission rate is reduced. At 50% reduction in the emission rate, the highest hourly and daily ground level concentrations decreased by almost 48%.

The influence of stack diameter inherently changed the exit flue gas velocity due to invariable flue gas flow-rate. The plume rise and dispersion are related to the exit flue gas velocity, which decreased with the increase of stack diameter because of proportionality to the square of diameter. For a fixed load there is no noticeable change in the average hourly and daily predicted ground level concentrations of SO<sub>2</sub>.

The model output for different scenarios has been used to mitigate the impact of sulphur dioxide and particulate emissions. Increase in stack height could reduce ground level concentration substantially. Sulphur reducing additives are used in controlling emissions to minimise the the ground level concentrations to comply with the allowable ambient air quality standards. For emission control of particulates, the application of high efficiency electrostatic precipitator is thoroughly investigated to mitigate particulates ground level concentration in the immediate neighbourhood of the refinery.

## References

- Abdul Wahab S. A., Al-Alawi S.M., El-Zawahri A. (2002), "Patterns of SO<sub>2</sub> emissions: a refinery case study" *Environmental Modeling and Software* 17 563-570
- Caputo M., Gimenez M., SchlampM. (2003), "Inter-comparison of atmospheric dispersion models" *Atmospheric Environment* 37, 2435–2449
- Isakov V., Venkatram A, Touma S. J, Koracin.D,Otte L. T. (2007) "Evaluating the use of outputs from comprehensive meteorological models in air quality modeling applications" *Atmospheric Environment* 41, 1689–1705
- Kesarkar A. P., Dalvi M., Kaginalkar A., Ojha A. (2007) "Coupling of the Weather Research and Forecasting Model with AERMOD for pollutant dispersion modeling. A case study for PM<sub>10</sub> dispersion over Pune, India" *Atmospheric Environment* 41, 1976–1988
- Kulkarni P., Chellam S., Fraser M. P. (2009) "Tracking Petroleum Refinery Emission Events Using Lanthanum and

Lanthanides as Elemental Markers for PM<sub>2.5</sub>" *Environmental Science and Technology*, 43 (8), 2990–2991, 2009.

Yateem W., Nassehi V., Khan A. R., (2010) "Inventories of SO<sub>2</sub> and PM emissions from Fluid Catalytic Cracking (FCC) units in petroleum refineries", *Water, Air & Soil pollution* ( electronic version - DOI 10.1007/s11270-010-0423-z).